NATURAL SCIENCE REVIEW 3 200604 (2026)
nsr.jinr.int

Statistical field theory of forced magnetohydrodynamic turbulence

M. Hnatič*[1,2,3], T. Lučivjanský[1], L. Mižišin[3], Yu. Molotkov[3], and A. Ovsiannikov†[3]

[1] *Institute of Physics, Faculty of Sciences, Pavol Jozef Šafárik University, Košice, Slovakia*
[2] *Institute of Experimental Physics, Slovak Academy of Sciences, Košice, Slovakia*
[3] *Joint Institute for Nuclear Research, Dubna, Russia*

Abstract

We review the results of applying the statistical field-theoretic approach to the problem of fully developed turbulence in nonrelativistic three-dimensional magnetohydrodynamics (MHD), which have been obtained over the past forty years. The review covers both general aspects of the physics of MHD turbulence and the necessary mathematical machinery of statistical field theory, including elements of renormalization theory and the renormalization-group (RG) method. The approach is illustrated using a stochastic model of stationary, locally homogeneous, fully developed three-dimensional MHD turbulence in the general case of a medium with broken spatial parity (helical MHD). In this model, RG techniques make it possible to establish the existence of several infrared-stable scaling regimes and to calculate the critical dimensions of various composite operators, the infrared asymptotics of correlation functions, and the amplitude factors in scaling laws, as well as to incorporate the effects of compressibility, anisotropy, etc.

For an important class of helical MHD systems, the field-theoretic approach provides an elegant formulation of the fundamental problem of large-scale turbulent dynamo action — namely, the generation of a large-scale magnetic field $\langle \boldsymbol{b} \rangle = \boldsymbol{B}$ (where $\boldsymbol{b}$ denotes magnetic fluctuations) at the expense of the energy of turbulent fluctuations — via the decay of the initial unstable vacuum state $\langle \boldsymbol{b} \rangle = \boldsymbol{0}$ as a result of dynamical spontaneous symmetry breaking in the spirit of the Coleman-Weinberg mechanism, followed by stabilization of the theory in the vicinity of the new ground state $\langle \boldsymbol{b} \rangle = \boldsymbol{B}$ (the dynamo regime). The field-theoretic formulation we developed, together with a generalization of the standard Feynman diagrammatic technique to the dynamo regime, not only makes it possible to treat within a unified framework the existing theoretical approaches to helical magnetohydrodynamics (kinematic MHD, large-scale dynamo theory), but also extends the RG formalism to the dynamo regime, which — unlike closure procedures still common in dynamo theory — is particularly well suited for studying statistically stationary turbulent states. The richness of MHD physics in the dynamo regime is illustrated both in the emergence of new effects (Goldstone-type corrections to Alfvén waves, anisotropic corrections associated with the transport of the large-scale field) and in the theoretically predicted strong dependence of the magnetic energy-spectrum slope on the degree of mirror-symmetry breaking.

Keywords: statistical field theory, renormalization group, stochastic helical magnetohydrodynamics, symmetry breaking, turbulent dynamo

DOI: 10.54546/NaturalSciRev.200604

*Corresponding author e-mail address: hnatic@saske.sk
†Corresponding author e-mail address: ovsiannikov@theor.jinr.ru

Received: 8 February 2026; Revised: 18 February 2026; Accepted: 25 February 2026; Published: 11 March 2026

Contents

1. Introduction

By now, the renormalization group method has become standard in turbulence theory. This, however, does not change the fact that by the term 'renormalization group', researchers in turbulence often mean a variety of rather disparate formalisms: perturbative RG as part of the toolkit of statistical field theory (SFT) [1–3], Wilson's recursive mode elimination schemes [4, 5], the Yakhot–Orszag approach [6, 7] (see also [8–10]), averaging methods over near-grid scales [11], nonperturbative (i.e., functional) RG (FRG) [12], and others. Therefore, despite the continuing intensive development of turbulence theory in many different directions, mutual understanding among specialists has not improved substantially.

The situation is even more complicated in magnetohydrodynamic turbulence: although the usefulness of RG methods is widely recognized, the considerable technical complexity of the problem has so far prevented them from attaining the same prominence as in pure hydrodynamic turbulence, and they have not yet been included in standard monographs (see, e.g., [13, 14]). Inheriting many features of purely hydrodynamic turbulence, MHD turbulence is nevertheless substantially more intricate and exhibits a wider range of interesting properties. This, together with the need to systematize recent results and the apparent lack (to the best of our knowledge) of a comparable review, motivated us to write the present review of the results of the SFT approach to the problem of fully developed MHD turbulence. However, before turning directly to magnetohydrodynamics, it would not be superfluous to say a few words about the state of the art in pure hydrodynamics.

1.1. Threshold: statistical field theory as a language of nonequilibrium physics

Statistical field theory began to take shape in the second half of the twentieth century at the interface of quantum field theory (QFT), many-body theory, and statistical physics. Initially, its main tools — Feynman diagrammatic techniques, renormalization methods, and RG — were developed in the context of problems involving interacting fields in elementary particle physics and, later, in condensed-matter theory. It soon became clear, however, that the basic objects of quantum field theory — the functional integral, the effective action, and the renormalization of parameters and observables — can be successfully carried over into a purely classical and statistical context, where randomness is due not to quantum fluctuations but to thermal noise, external stochastic forcing, or the complex dynamics of subsystems [15–18].

The key advantage of SFT is that it provides a unified, internally consistent language for describing a multitude of physical systems that at first sight appear completely unrelated. The statistical properties of systems specified by their microscopic dynamics — be it classical Hamiltonian equations of motion or ordinary/stochastic differential hydrodynamic evolution equations — are reinterpreted in terms of an equivalent Euclidean field theory formulated as a functional integral over fields corresponding to the dynamical variables and over conjugate 'response' fields [3, 19, 20] (see also [21–23]). It turns out that, for a broad class of models in classical physics, the field theories obtained in this way are multiplicatively renormalizable, allowing a controlled transition from micro to macroscopic scales (see, e.g., [3]).

From the methodological point of view, statistical field theory comprises several complementary approaches. First, there is the Martin–Siggia–Rose formalism [24] and its functional formulation in the Janssen–De Dominicis variant [25, 26] (MSRJD), which realizes expectation values of observables in a stationary state through a formal representation in the form of a path integral with the exponential of an effective action. Second, there are perturbative diagrammatic techniques and Wilsonian operator product expansion (OPE), supplemented by the powerful machinery of ultraviolet renormalization adjusted to fluctuating models [3]. Simple perturbative expansions are supplemented, on the one hand, by various functional methods adapted from QFT [3, 16, 18, 27], such as Legendre transformations, Schwinger–Dyson equations, and Ward identities, and, on the other hand, by nonperturbative methods, in particular the saddle-point method [16], lattice computations [28, 29], and so on, which together provide a substantial amount of information about the structure and properties of the theory under study. Finally, central to the framework is the use of the group of ultraviolet-finite renormalizations (the renormalization group), formulated in terms of finite renormalizations, which enables a rigorous analysis of the asymptotic behaviour of the theory — primarily in the infrared (IR) regime, in contrast to QFT, where the main emphasis is traditionally placed on ultraviolet (UV) properties [3, 17]. In contrast to Wilson's iterative coarse-graining construction, the UV-finite renormalization group can be formulated as a genuine one-parameter Lie group of transformations (see [30] for a discussion of relevant subgroups). Moreover, unlike the Yakhot–Orszag scheme, it is internally consistent — renormalizing the full set of required operators in a symmetry-preserving way — which makes practical computations beyond the lowest one-loop order feasible. The RG method provides a classification of possible scaling regimes, the calculation of critical exponents and anomalous dimensions of composite operators in the form of asymptotic expansions in some small parameter (the ε-, $1/n$-, or $1/d$-expansion; see below).

In computations at high orders of perturbation theory (in practice, beyond the second order), the resulting series are additionally resummed to obtain physical answers. The most reliable approach is generally considered to be the procedure based on knowledge of the asymptotic

behaviour of the N-th term of the perturbative series as $N \to \infty$, which is obtained nonperturbatively using instanton analysis (the Lipatov method) [31]. Anticipating later discussion, we note that for the problems of fully developed turbulence considered here, perturbative coefficients have, as a rule, been computed only up to second order, and therefore the issue of resumming the series is usually not raised. In this case, the asymptotic series itself approximates the desired quantities rather well, provided we are dealing with universal characteristics such as critical exponents or anomalous dimensions (see, e.g., the conclusions in [32]).

The collection of SFT methods has proved to be highly effective for a wide range of problems in modern statistical physics. Classic examples include the theory of phase transitions and critical phenomena, where the RG method has provided a rigorous justification of the universality hypothesis and allowed one to obtain quantitative predictions for critical exponents that agree with high accuracy with both experiment and direct numerical Monte Carlo simulations. See, for instance, the detailed discussion in [33]. Similar approaches have turned out to be very fruitful in the theory of disordered systems (spin glasses [34, 35], random media [36, 37], etc.), in polymer physics [38–42], in models of random surface growth [43–46], reaction–diffusion systems [47–59], percolation processes [60–65], and other problems in nonequilibrium dynamics where no simple variational or equilibrium description is available. Wherever multiscale behaviour, strong fluctuations, and the absence of small parameters play an essential role, statistical field theory and the RG method serve as standard tools of analysis [66, 67].

1.2. Landscape: turbulence as a statistical theory

One of the most complex and conceptually rich domains of SFT applicability is the description of the turbulent flow of a continuous medium. Being one of the oldest problems in theoretical physics, turbulence has remained the object of constant theoretical attention throughout the twentieth and twenty-first centuries. In the literature, it has by now become almost obligatory to emphasize that a theoretical understanding of this phenomenon remains, in effect, the 'last unresolved major problem of classical physics'. Moreover, the very notion of 'turbulence' has long since been not only a fundamental physical phenomenon, inherent to both inanimate and living matter and manifest over a wide range of space-time scales — 'from a cup of tea to stellar and galactic structures' [68, p. 1] — but also a part of our cultural vocabulary.

The English word *turbulent*, originating from the Latin *turbulentus* ('full of commotion', 'restless', 'disturbed'), was used to describe 'tempestuous' epochs, crises, and human characters long before it firmly entered the strictly scientific context. 'Who shall deliver me from this turbulent priest?' exclaimed Henry II Plantagenet, referring to the figure of Thomas Becket, the Archbishop of Canterbury, whose tragic death later shocked medieval Europe.[1] This example is an instructive illustration of how long and how deeply the entity under discussion has been rooted in our conception of complex, multiscale, and potentially destructive dynamics. In what follows, however, we shall consider only a certain regime of motion of a continuous medium.

Even in this substantially narrower sense, the phenomenon of turbulence pertains to an extremely wide class of physical situations, and it is hardly to be expected that a complete theory of turbulence will ever be constructed. Nevertheless, one usually singles out a canonical set of phenomena that embody and exhibit the main features of the turbulent regime. These include, in particular, the (in)stability of solutions of the hydrodynamic equations, the global

[1] Of course, like any member of the high English aristocracy of the twelfth century, King Henry did not speak English in such contexts but addressed his entourage in French or Latin. The 'classical' English wording currently quoted [69] is merely a later paraphrase, compiling several different forms, including those going back to G. Lyttelton's *History of the Life of King Henry II (1769)* [70].

problem of proving the existence and smoothness of three-dimensional solutions of the Navier–Stokes (one of Millennium Prize Problems [71]) or even Euler equations, the instability of laminar flows, various scenarios for the onset and development of turbulence, and so on.

From a theoretical standpoint, all these topics, of both practical and conceptual importance, are unified by viewing turbulence as a statistical theory. Its foundations were already laid in 1924 in the work of Friedmann[2] and Keller [72], who first applied correlation functions to turbulence and derived, directly from the Navier–Stokes (NS) equations, a hierarchy of equations for these functions, analogous to Bogoliubov–Born–Green–Kirkwood–Yvon (BBGKY) chain in statistical physics [73] and anticipating the 'closure problem' [11] that has been central to turbulence theory since the middle of the 20th century.

By the mid-20th century, as statistical physics matured, a first-principles language for turbulence theory had taken shape. It was based on hierarchies of differential equations derived essentially from Reynolds' concept of averaging for various moments of the hydrodynamic fields (correlation functions), supplemented by a range of closure hypotheses for the higher moments. This approach gave rise both to a vast family of naive zero-order closure models (Prandtl, von Kármán, Taylor) and to first- and second-order models (various l-, k-, and ν-models and their two-parameter extensions of the k–l, k–ω, k–ε type, etc.; see, e.g., reviews [74, 75]), as well as to a whole series of more self-consistent closure schemes. The latter includes, in particular, the direct-interaction approximation (DIA) closure[3] proposed by Kraichnan [77] (for more details see also [78–80]) and its further generalizations, the two-scale direct-interaction approximation (TSDIA) [81], as well as the eddy-damped quasi-normal Markovian (EDQNM) approximation introduced by Orszag [82].

At present, these theoretical approaches have, in one form or another, served as the basis for an even more 'representative' array of semi-empirical ('engineering') models for the numerical simulation of turbulence of the most diverse nature, developed over recent decades. These include, in particular, models of unresolved-scale descriptions, such as Reynolds-averaged Navier–Stokes (RANS) models and Reynolds stress models (RSM) [74, 83], large-eddy simulation (LES) and detached-eddy simulation (DES) [84, 85] as intermediate strategies, direct numerical simulation (DNS) [86] with explicit resolution of all essential scales, as well as alternative approaches, including probability density function (PDF) methods [87], lattice Boltzmann method (LBM) [88], proper orthogonal decomposition (POD) [89], dissipative particle dynamics (DPD) [90] and direct simulation Monte Carlo (DSMC) [91] methods aimed at molecular-level simulation.

All of the approaches listed above — both theoretical and numerical — suffer, however, from one crucial fundamental drawback. Although they allow one to describe very successfully various scenarios for the onset of turbulence and regimes of relatively weak turbulence in a wide class of situations, they, despite all the progress of recent decades, are poorly suited to describing a statistically stationary, fully developed turbulent state corresponding to high Reynolds number Re. Let us note that fully developed hydrodynamic turbulence is attained already at (based on outer scale) Reynolds numbers of order $\mathrm{Re} \sim 10^5 - 10^6$. For DNS simulations, practically attainable limits remain around $\mathrm{Re} \sim 10^5$; extending to significantly higher values is currently infeasible because the number of grid points and the integration time grow very rapidly (often quoted as Re^3 for the computational cost in idealized settings). By contrast, in LES/DES and other hybrid approaches, where small-scale dynamics are parametrized in advance — e.g., through wall models — rather than fully resolved (as in simulations of wing aerodynamics or

[2]Better known for his famous cosmological models.

[3]For stirred hydrodynamics [76], DIA is equivalent to the single-loop approximation to the Dyson equations.

the atmospheric boundary layer), global Reynolds numbers as large as $\mathrm{Re} \sim 10^7 - 10^8$ can be reached. Nevertheless, for obvious reasons, such computations still provide only limited additional insight into the fundamental physics of fully developed turbulence.

This problem — the theory of 'genuine' fully developed hydrodynamic turbulence — has always been one of the central topics in the study of turbulent flows. Turbulence of this type is characterized by strong fluctuations of hydrodynamic fields and pronounced multiscale behaviour, which manifests itself in the presence, in turbulent statistics, of a wide inertial interval in which the energy injected at large scales (the forcing scale) is transferred with almost no loss down to small scales where viscosity becomes important (the dissipation scale). In this inertial interval, the statistical characteristics of interest exhibit well-developed scaling properties. A detailed exposition of principal achievements of the fundamental theory of hydrodynamic turbulence, together with an extensive bibliography on this long-standing but in essence still open problem, can be found in the classical monographs [5, 92–95].

Theoretical approaches to fully developed turbulence are so far focused mainly on the concepts of (local) homogeneity and (local) isotropy, first proposed by Kolmogorov and Obukhov in the framework of their celebrated Kolmogorov 1941 (K41) theory [96–99]. This theory provides an accurate phenomenological description of fully developed turbulence, relying essentially on dimensional considerations and two axioms that determine the form of the scaling functions (see, e.g., [92, 93]). After the experimental confirmation of $-5/3$ spectra in the 1960s (see, e.g., [100]), Kolmogorov's hypotheses called for a theoretical justification; the field-theoretic RG provided a systematic derivation of K41-type scaling within stochastic Navier–Stokes (NS) models. A pioneering step was the 1977 application of RG methods to the hydrodynamics of randomly stirred (but not yet turbulent) fluids described by what later became the paradigmatic stochastic NS equation with random Gaussian forcing, as was done in the work of Forster *et al.* [101], demonstrating the enormous potential of SFT for problems of this kind. This potential was quickly realized, and by 1979, the K41 scaling exponents were recovered within the RG framework [102] (see also [103]). Subsequent work has largely aimed at a complete proof of Kolmogorov's hypotheses and the resolution of related issues — such as the 'freezing' of critical dimensions and the emergence of 'dangerous' composite fields with negative critical dimensions — as well as the study of anomalous scaling (see below), which remains an open problem.

It is worth recalling that real turbulence exhibits intermittency, i.e., the presence, at dissipative scales, of a 'bursty' space–time structure of small-scale fluctuations. In other words, instead of an approximately uniform cascade *à la* K41, energy is dissipated in rare but statistically significant events (thin vortex tubes, shear layers, etc.), and the distribution of velocity increments $\delta v(r) \coloneqq \big(\boldsymbol{v}(\boldsymbol{x}+\boldsymbol{r}) - \boldsymbol{v}(\boldsymbol{x})\big) \cdot \boldsymbol{r}/r$ becomes strongly non-Gaussian, with progressively heavier tails as the scale r decreases. In turn, this implies that the moments of the distribution of $\delta v(r)$, i.e., the Galilean-invariant correlation functions (structure functions) $S_n(r)$, are in fact characterized by an infinite set of independent (local) scaling exponents associated with different intermittent events (multifractality) [93]. The observed global exponent ζ_n, i.e., the anomalous scaling phenomenon $S_n(r) \sim r^{\zeta_n}$ with $\zeta_n \neq \zeta_n^{\mathrm{K41}} \coloneqq n/3$, arises from an optimization relation for this set of local exponents. Technically, anomalous scaling manifests itself as a singular dependence of the structure functions $S_n(r)$ on the integral scale of turbulence $l_{\max}$ as $l_{\max} \to \infty$. In the language of Wilson's operator product expansion, this is equivalent to the following asymptotic behaviour of certain coefficients, $C_F(r) \sim (r/l_{\max})^{\Delta_F}$ as $l_{\max} \to \infty$, where Δ_F is the negative critical dimension of the corresponding 'dangerous' operator F. In particular, the leading (most singular) contributions associated with the composite fields $\boldsymbol{v}^n$,

i.e., powers of the fluctuating velocity, were explicitly resummed in [104, 105]. Then, this procedure was extended to the case of a time-dependent large-scale field [106]. These results provide an adequate RG-based description of sweeping effects. For details on these issues, we refer the reader to the review [1], where one can also find the main bibliographic references tracing the main stages in the development of RG theory of turbulence, and to the monographs [2, 3], where this theory is presented in detail within the SFT framework adopted here.

For completeness, we also present here Kolmogorov's hypotheses in their refined form [107] (see also [1, 3]). Let $m := l_{\rm max}^{-1}$ and $\Lambda := l_{\rm min}^{-1}$, where $l_{\rm max}$ and $l_{\rm min}$ are characteristic macro- and microscales of the system (e.g., the system size and the dissipative length, respectively). Then, for any turbulent flow at sufficiently large Re, one has:

1. In the region $k \gg m$, $|\omega| \gg \omega_{\rm min}$, the distribution function of the spatial Fourier components $\boldsymbol{v}(\boldsymbol{k}, t)$ of the random velocity field $\boldsymbol{v}(\boldsymbol{x}, t)$, taken at coincident times, has a finite limit as $m/k \to 0$ for $m \to 0$.

2. In the region $k \ll \Lambda$, $|\omega| \ll \omega_{\rm max}$, the distribution of the Fourier components $\boldsymbol{v}(\boldsymbol{k}, \omega)$ of the random velocity field $\boldsymbol{v}(\boldsymbol{x}, t)$ does not depend on the viscosity coefficient ν_0.

Over the last three decades, since the review [1], the SFT approach to the problem of fully developed turbulence has evolved along several distinct directions: refinements of perturbative RG for the forced stochastic Navier–Stokes equation, nonperturbative RG, and extension of the class of models. Within the first paradigm, a two-loop RG analysis was performed for the simplest case of incompressible NS with a Gaussian random force having a purely power-law spectrum, $\langle \boldsymbol{f} \otimes \boldsymbol{f} \rangle \sim k^{4-d-2\epsilon}$, where ϵ is an expansion parameter analogous in spirit to Wilson's $(4-d)$-expansion but not directly related to the spatial dimension d [108]. The main outcome of this work can be viewed both as a two-loop confirmation of the stability of the Kolmogorov fixed point and as a conclusion that the ϵ-expansion becomes of limited practical use for amplitude factors already at the two-loop order (in particular, the resulting two-loop prediction for the Kolmogorov constant $\mathcal{C}_{\rm K} \simeq 3.02$ substantially exceeds the experimentally measured value). Accordingly, various 'improved' ϵ-expansions perform substantially better, including schemes that resum pole contributions of renormalization constants as $d \to 2$ [32, 109, 110] or incorporate the $d \to \infty$ asymptotics [108, 111]; with these refinements, even a one-loop estimate $\mathcal{C}_{\rm K} \simeq 1.89$ [110] comes close to modern measurements $\mathcal{C}_{\rm K} \simeq 2.21$ [112]. A broader comparison of experimental and theoretical determinations of $\mathcal{C}_{\rm K}$ is given in Table 2 of [113]. Beyond the incompressible case, the two-loop effects of compressibility [114] and parity breaking [115] on the model's universal regimes were also investigated.

An active research line seeks to go beyond the 'pure' ϵ-scheme, in which the physically relevant case $d = 3$ with realistic (infrared) power-law forcing corresponds to the rather large value $\epsilon = 2$. Early attempts to this problem borrowed tools from critical phenomena — self-consistency equations with skeleton diagrams (bootstrap) leading to a $1/n$ expansion, with n the number of order-parameter components — but in the turbulence setting, this strategy remains unsuccessful. In particular, introducing n 'replicas' of the velocity field to construct $1/n$ expansion conflicts with Galilean invariance [116].

In this respect, the $1/d$ expansion[4], which has been repeatedly proposed in the context of turbulence in a wide variety of schemes and settings [117–120], appears to be considerably more promising. Of particular interest is the limit $d \to \infty$, which provides the leading-order approximation in the $1/d$ expansion. Indeed, calculations in the limit $d \to \infty$ are greatly

[4]Note that for three-dimensional turbulence one has $1/d = 1/3$, which is a reasonably small parameter.

simplified; moreover, there is some hope that in this limit the model becomes 'exactly solvable'. At the very least, this is suggested by the fact that in the limit $d \to \infty$ the theory displays similar features to K41 (intermittency and anomalous scaling disappear or acquire a simple 'calculable' form) [118]. From the perspective of the ϵ-scheme, a crossover from Kolmogorov scaling to anomalous scaling is expected at some (as yet unknown) value of ϵ. In recent years, several very intriguing results have been obtained in this field [111, 121–123]: diagrammatic calculations carried out up to four-loop order for the only model parameter that is realistically needed — the anomalous dimension of the viscosity, $\gamma_\nu(\epsilon)$ — show that, in the limit $d \to \infty$, the coefficients of its ϵ expansion are rational numbers. This observation raises the hope that, for $d \to \infty$, the ϵ expansion has a finite radius of convergence[5] and may therefore be resummed exactly by inferring the general term of the series from its initial segment.

An alternative to the purely perturbative strategy has been the conceptual leap achieved in recent decades and associated with the FRG. Building on Wilson's idea of integrating out fluctuations scale by scale, FRG employs exact Wetterich-type flow equations for the effective action $\Gamma[\phi]$ [125].[6] In contrast to the original Wilson RG, the RG flow is formulated directly for $\Gamma[\phi]$, and practical approximations need not rely on a small parameter such as ϵ. FRG was soon applied to the forced stochastic Navier–Stokes equation in $d = 2, 3$, yielding RG fixed points associated with fully developed turbulence [128–130]. Within a simple but symmetry-consistent truncation, it produces fixed points corresponding to the direct and (in $d = 2$) inverse energy cascades and reproduces key K41 predictions in three dimensions (notably the $-5/3$ spectrum and Kolmogorov's fourth-fifths law [93]). Logarithmic deviations from pure power-law scaling in higher-order structure functions, suggestive of intermittency, also arise naturally [129]. However, capturing strong deviations from self-similarity, such as those described by models like She-Lévêque [131], likely requires more sophisticated approximations that include a richer set of (multi-local) composite operators and an expanded action space. Initial efforts towards an 'OPE within FRG' are ongoing, though precise reproduction of experimental multi-exponent scaling remains a challenge. Furthermore, FRG predicts a breakdown of simple scale invariance in time-correlations: for a fixed wavenumber k, the two-time correlation function can exhibit a crossover from Gaussian-like decay $e^{-\alpha(kv_k t)^2}$ at short times $t \ll 1/(kv_k)$ to an exponential decay $e^{-\beta\Omega_k t}$ at long times, where v_k is the characteristic velocity at scale $1/k$ and $\Omega \sim kv_k$ is a characteristic frequency [130]. This behaviour is linked to the non-local (in time) structure of the effective interactions. High-precision DNS supports these temporal features in the inertial range [132]. Notably, the FRG method has also proven capable of uncovering new fixed points inaccessible to perturbative schemes, such as a non-trivial fixed point for the inviscid Burgers equation in $d \geqslant 1$ characterized by a dynamic exponent $z = 1$ [133].

The third major block of progress in the development of RG approaches to turbulence is associated with a broad spectrum of stochastic models related to the NS equation, to which the same perturbative RG formalism, supplemented by the OPE, has been applied. Studies in this direction, while not providing a direct solution to the problem of 'pure' isotropic Navier–Stokes turbulence, have described a rather extensive class of situations in which RG yields controlled multiscaling exponents and demonstrates how turbulent fluctuations modify the universal properties of other systems [67, 134]. First and foremost, one should mention models of passively advected scalar and vector impurities, where, based on Kraichnan's ensemble with synthetic turbulence specified by the pair correlator of a random velocity field that is δ-correlated in

[5] A similar situation occurs in the $1/n$ expansion in the theory of critical phenomena, where in the limit $n \to \infty$ the critical exponents are frequently given by simple analytic functions of ϵ [124].

[6] General details on FRG can be found in reviews [126, 127] and references therein.

time and possesses a tunable spectrum in k [135, 136], systematic expansions have been obtained for anomalous dimensions of structure functions of composite operators describing the multiscaling of a passive scalar or vector [67, 137–140]. Models with power-law correlations and finite correlation time τ_c, that is, with 'coloured' noise violating Galilean invariance, have also been studied [141, 142]. Both early one-loop studies [143, 144] and subsequent systematic developments deserve attention. For the Navier–Stokes equation with coloured forcing, three IR-stable fixed points have been identified, corresponding to the regimes of 'white', 'rapid', and 'frozen' noise [145]. Subsequent work has shown that the correlation time τ_c inevitably tends to zero in the IR limit [146], so that the asymptotics in the deep IR regime coincide with those of the limiting case of white noise. A two-loop analysis of the analogous scaling behaviour for a passively advected scalar with finite τ_c has shown that intermittency is enhanced as τ_c increases and leads to a set of universal multifractal exponents [147]. A concise, up-to-date synopsis of these results is provided in [148]. Most recently, in [149], it was shown that Galilean symmetry, although explicitly broken by coloured noise, is spontaneously restored within the inertial range, so that the infrared asymptotics coincide with those of the limiting white-noise case. The RG approach has also been applied to problems of the influence of turbulent advection on critical behaviour (model A and other types of critical dynamics in the standard classification [150]), as well as to reaction-diffusion systems, which has made it possible to construct phase diagrams for the 'system plus turbulence' and to describe changes in universality classes under the action of stochastic advection [50, 53, 67, 151]. Finally, all of the above methods have, in one form or another, been extended to magnetohydrodynamic turbulence (both with preserved and with broken mirror symmetry), including models of turbulent dynamo action and passive magnetic fields. The present article is devoted to a review of the results of this kind.

2. Fundamentals of magnetohydrodynamics

This section is written primarily for specialists in quantum and classical field theory, to demonstrate that magnetohydrodynamics is not merely 'yet another hydrodynamic model,' but rather a broad and far-reaching area of science that continually confronts researchers with new and ever-emerging challenges. Without claiming completeness, we provide only the background material in the form that seems most natural to us from the perspective of a field theorist. For further details, the reader is referred to the references cited throughout the text.

Magnetohydrodynamics studies the motion of an electrically conducting continuous medium (plasma or liquid metal) in an electromagnetic field. Historically, it emerged largely from astrophysical needs.[7] The necessity of applying the theory of the interaction of a conducting medium with an electromagnetic field to astrophysical problems was first clearly formulated in Alfvén's famous article [153]. He drew attention to the following well-known facts. First, the interstellar gas, stellar atmospheres, and the matter in stellar interiors are strongly ionized and therefore are excellent electrical conductors. Second, many objects in the Universe possess magnetic fields. These circumstances, together with the fact that, despite the extremely low density, the linear dimensions of phenomena considered in astrophysics usually greatly exceed the mean free path of the particles, so that the medium can be treated as continuous, formed the basis of the modern theory of cosmic electromagnetic processes. Besides, conducting flows are widely used in large-scale technologies, including MHD generators, tokamaks and stellarators, breeder reactors with liquid-metal coolant, and metallurgical devices, etc.[7] We also note recent progress in numerical modelling of MHD systems.

[7] A list of relevant references can be found, for example, in the introduction to [152].

2.1. Background: from the conservation laws for flows or two-fluid kinetics to one-fluid MHD

First, one may view any hydrodynamics simply as a set of equations for the fluxes of conserved quantities, closed in one way or another. The theoretical basis of classical (non-relativistic) MHD[8] combines Maxwell's equations without the displacement current and the equations of motion of a continuous medium (the Euler or Navier–Stokes equations) [155–157]. These two sets of equations are coupled via induction currents produced by the motion of a conducting fluid in a magnetic field, which enter Maxwell's equations, and via the electromagnetic body force (typically the Lorentz force) exerted by the field on the medium, which enters the hydrodynamic equations. This mutual interaction between magnetic and velocity fields is essential for describing realistic flows in strongly nonlinear regimes [157–159].

Alternatively, MHD can be obtained from kinetic theory as the outcome of a systematic reduction of the two-fluid (electrons plus ions) description of fully ionized media derived from the Boltzmann equation [160, 161]. In the regime of frequent collisions, this reduction yields a single-fluid formulation in terms of mass-averaged variables [161–163]. Given the physical significance of this situation, let us examine this result in more detail. The extended single-fluid equations for three-dimensional non-relativistic conducting media (hereafter often simply 'plasma') can be written in the form

$$\mathrm{D}_t\rho_0 + \rho_0(\boldsymbol{\nabla}\cdot\boldsymbol{u}) = 0, \qquad \rho_0\mathrm{D}_t\boldsymbol{u} = -\boldsymbol{\nabla}\cdot\mathbf{P} + \boldsymbol{\nabla}\cdot\boldsymbol{\Pi} + (\boldsymbol{J}\times\boldsymbol{B})/c + \boldsymbol{F}, \tag{1}$$

$$\boldsymbol{E} + (\boldsymbol{u}\times\boldsymbol{B})/c = \boldsymbol{J}/\sigma_0 + (\boldsymbol{J}\times\boldsymbol{B})/en_ec - (\boldsymbol{\nabla}\cdot\mathbf{P}_e)/en_e + (m_e/e)\mathrm{D}_t^{(e)}\boldsymbol{u}_e. \tag{2}$$

Hereinafter, $\boldsymbol{u}$ is the single-fluid Eulerian velocity; $\boldsymbol{E}$ and $\boldsymbol{B}$ are the macroscopic electric and magnetic fields, respectively; $\boldsymbol{J}$ is the conduction current, and $\boldsymbol{F}$ represents external force (gravity, inertial forces, turbulent stirring, etc.). The total pressure tensor is $\mathbf{P} = \mathbf{P}_e + \mathbf{P}_i$, with the electron and the ion pressures $\mathbf{P}_e$ and $\mathbf{P}_i$, respectively, and $\boldsymbol{\Pi}$ is the viscous stress tensor. We denote by ρ_0 the mass density (later set to a constant), by σ_0 the (assumed constant) conductivity, and c is the speed of light. The Eq. (2) includes the electron velocity $\boldsymbol{u}_e = \boldsymbol{u} - \boldsymbol{J}/(en_e)$, where n_e is the electron number density, m_e is the electron mass, and e is the elementary charge; $\mathrm{D}_t \coloneqq \partial_t + (\boldsymbol{u}\cdot\boldsymbol{\nabla})$ is the Lagrangian (material) derivative[9], and $\mathrm{D}_t^{(e)} \coloneqq \mathrm{D}_t|_{\boldsymbol{u}=\boldsymbol{u}_e}$.[10] Throughout, all fields depend on $(\boldsymbol{x}, t)$ with d-dimensional spatial coordinates $\boldsymbol{x}$ and time t; $\boldsymbol{\nabla}$ is the d-dimensional gradient, $\partial_t \coloneqq \partial/\partial t$ is the partial time derivative, and the dot $\cdot$ denotes the standard Euclidean scalar product. Whenever we use the cross product or the curl, we implicitly specialize to three dimensions, since $\boldsymbol{\nabla}\times$ maps a vector field to a vector only in $d = 3$. However, the final equations can be formally generalized to $d \geqslant 3$; hence, we keep d symbolic for transparency.

The first and second equations in (1) describe, respectively, mass conservation for ρ_0 and the evolution of the momentum density $\rho_0\boldsymbol{u}$, while (2) is the generalized Ohm's law for a conducting fluid in a magnetic field. It contains the Ohmic (resistive) term $\boldsymbol{J}/\sigma_0$ and several contributions reflecting two-fluid physics: the Hall term $(\boldsymbol{J}\times\boldsymbol{B})/en_ec$, the electron-pressure (thermoelectric/baroclinic) term $-(\boldsymbol{\nabla}\cdot\mathbf{P}_e)/en_e$, and the electron-inertia term $(m_e/e)\mathbf{D}_t^{(e)}\boldsymbol{u}_e$. These terms are what make (2) 'generalized' compared with the simplest resistive-MHD form.

[8] As for relativistic MHD, see, for instance, the review [154] and cited literature.

[9] This derivative is a covariant time derivative in the sense that $\mathrm{D}_t\varphi$ remains a scalar density if φ is.

[10] The velocity in high collision limit $\boldsymbol{u}$ is defined as the centre-of-mass velocity, $\rho_0\boldsymbol{u} = m_in_i\boldsymbol{u}_i + m_en_e\boldsymbol{u}_e$. With $m_e \ll m_i$ and quasi-neutrality $n_e \simeq Zn_i$ (Z the ion charge number), one has $\boldsymbol{u} \approx \boldsymbol{u}_i$, and $\boldsymbol{u}_e$ is then obtained from the quasi-neutral conduction current $\boldsymbol{J} = Zen_i(\boldsymbol{u}_i - \boldsymbol{u}_e)$. See [160] for more details.

Over the past decades, such effects have attracted considerable interest in plasma physics, especially when Hall and electron-inertial scales are dynamically important.

As a single-fluid hydrodynamic theory, Eqs. (1)–(2) apply to macroscopic, low-frequency modes characterized by a minimal length scale ℓ and time scale τ (i.e., the shortest scales retained in the dynamics). Hydrodynamics requires a small Knudsen number $\mathrm{Kn} \coloneqq \lambda_{\mathrm{mfp}}/\ell \ll 1$, with $\lambda_{\mathrm{mfp}} \coloneqq \max_\alpha(\lambda_{\mathrm{mfp},\alpha})$, and slow evolution compared with collisional relaxation, $\tau \gg \tau_{\mathrm{col}}$ with $\tau_{\mathrm{col}} \coloneqq \max_\alpha(\nu_\alpha^{-1})$, $\alpha = e, i$; here $\lambda_{\mathrm{mfp},\alpha}$ and ν_α are the mean free path and collision frequency of electrons (e) and ions (i). The single-fluid approximation further assumes quasi-neutrality, which requires $\ell \gg \lambda_D$ (or $\ell \gg \lambda_{\mathrm{TF}}$ in degenerate conductors, e.g., liquid metals) and $\tau \gg 2\pi/\omega_{pe}$ (and hence $\tau \gg 2\pi/\omega_{pi}$), where λ_D and λ_{TF} are the Debye and Thomas–Fermi screening lengths, and $\omega_{p\alpha}$ are the plasma (Langmuir) frequencies. The non-relativistic MHD ordering is $\max(u, c_s, u_A) \ll c$, where u is a characteristic flow speed, c_s is the sound speed, and u_A is the Alfvén speed. Finally, treating σ_0 as a constant scalar conductivity assumes weak electron magnetisation, $\Omega_{ce}/2\pi\nu_e \ll 1$, where Ω_{ce} is the electron cyclotron (Larmor) frequency. No analogous ion condition is needed, since the ionic contribution to σ_0 is typically negligible.[11]

Pressure anisotropy and finite-Larmor-radius effects are negligible if $\Omega_{ci}/2\pi\nu_i \ll 1$ and $\ell \gg \lambda_{Li}$ with Ω_{ci} the ion cyclotron (Larmor) frequency and λ_{Li} the ion Larmor radius (ions are key for pressure). Then one may set $\mathbf{P} = P\mathbf{I}$, where $P = P_e + P_i$, with the electron P_e and ion P_i pressures, respectively and $\mathbf{I}$ is the unit tensor, and an isotropic (Newtonian) viscosity tensor $\mathbf{\Pi} = \mu_0\big[(\boldsymbol{\nabla} \otimes \boldsymbol{u}) + (\boldsymbol{\nabla} \otimes \boldsymbol{u})^{\mathrm{T}}\big] + \big(\zeta_0 - \frac{2}{3}\mu_0\big)(\boldsymbol{\nabla} \cdot \boldsymbol{u})\,\mathbf{I}$, where μ_0 and ζ_0 are the shear and bulk viscosities and symbol $\otimes$ stands throughout for the tensor product. If, furthermore, one adopts the standard incompressible approximation used in turbulence theory[12], $\rho_0 = \mathrm{const}$, then the viscous term in the momentum equation in (1) reduces simply to $\boldsymbol{\nabla} \cdot \mathbf{\Pi} = \mu_0 \Delta \boldsymbol{u}$ (with $\Delta = \boldsymbol{\nabla} \cdot \boldsymbol{\nabla}$ being the Laplace operator), the bulk-viscosity contribution drops out, and one arrives at the so-called solenoidal extended MHD with constant ν_0, σ_0, and ρ_0.

If also the relevant scales take on values well above electron and ion kinetic scales, $\ell \gg \{d_e, d_i\}$ and $\tau \gg \{2\pi/\Omega_{ce}, 2\pi/\Omega_{ci}\}$ (where d_e, d_i denote the electron and ion skin depths, and Ω_{ci} is the ion Larmor frequency), then the Hall and electron-inertia contributions in (2) can be neglected. Then, one obtains the following Ohm's law for a moving conductor,

$$\boldsymbol{J}/\sigma_0 = \boldsymbol{E} + (\boldsymbol{u} \times \boldsymbol{B})/c + (1/en_e)\boldsymbol{\nabla} P_e. \tag{3}$$

The electron-pressure term is a pure gradient and can be absorbed into the electrostatic potential. In the ideal-conductor limit $\sigma_0 \to \infty$, the right-hand side vanishes, expressing magnetic flux freezing: the field is advected with the flow, and its topology is preserved (Alfvén's theorem). For finite σ_0, flux freezing is weakened by magnetic diffusion, allowing changes of field-line connectivity (magnetic reconnection). On large scales, Ohm's law couples the plasma to the magnetic field, endowing the fluid with an effective magnetic elasticity: small perturbations excite Alfvén waves that propagate along the field lines with phase speed u_A. Besides Alfvén (incompressible) modes, the linear spectrum also contains magnetosonic waves — longitudinal perturbations whose propagation depends on c_s.[13]

[11] Note that the assumption of a constant σ_0 effectively requires that transport anisotropy is not too strong. In strongly magnetized, weakly collisional plasmas, one should instead use an anisotropic conductivity tensor and Braginskii's theory [161] (see also [164]).

[12] The standard argument is based on the typical smallness of the Mach number $\mathrm{Ma}_s \coloneqq u/c_s \ll 1$ for turbulent flows. From the continuity equation in (1), one can then infer that $\boldsymbol{\nabla} \cdot \boldsymbol{u} = \mathcal{O}(\mathrm{Ma}_s^2)$, i.e., the flow is essentially incompressible to leading order.

[13] In ideal MHD ($\nu_0 = \nu_{\mathrm{m}0} = 0$) with isotropic pressure there are three linear wave families on top of a uniform

2.2. Background: solenoidal resistive magnetohydrodynamics

Substituting $\boldsymbol{E}$ from (3) into Faraday's law, $\boldsymbol{\nabla}\times\boldsymbol{E}=-\partial_t\boldsymbol{B}/c$, and using the low-frequency form of Ampère's law (neglecting the displacement current), $\boldsymbol{\nabla}\times\boldsymbol{B}=4\pi\boldsymbol{J}/c$, one can eliminate $\boldsymbol{J}$ both from the induction equation and from the Lorentz force $(\boldsymbol{J}\times\boldsymbol{B})/c$ in the second equation of (1). This yields the classical solenoidal resistive-MHD equations,

$$\rho_0\mathrm{D}_t\boldsymbol{u}=-\boldsymbol{\nabla}\left(P+\boldsymbol{B}^2/8\pi\right)+(\boldsymbol{B}\cdot\boldsymbol{\nabla})\boldsymbol{B}/4\pi+\mu_0\Delta\boldsymbol{u}+\boldsymbol{F},\qquad \boldsymbol{\nabla}\cdot\boldsymbol{u}=0, \tag{4}$$

$$\mathrm{D}_t\boldsymbol{B}=(\boldsymbol{B}\cdot\boldsymbol{\nabla})\boldsymbol{u}+\nu_{\mathrm{m}0}\Delta\boldsymbol{B},\qquad \boldsymbol{\nabla}\cdot\boldsymbol{B}=0, \tag{5}$$

where $\nu_{\mathrm{m}0}\coloneqq c^2/(4\pi\sigma_0)$ is the magnetic diffusivity, and without loss of generality the force $\boldsymbol{F}$ is taken to be solenoidal, $\boldsymbol{\nabla}\cdot\boldsymbol{F}=0$ (the potential part can always be attributed to pressure). In the literature, Eq. (5) is called the induction equation. The electric field then follows from Eq. (3) and $\boldsymbol{\nabla}\times\boldsymbol{B}=4\pi\boldsymbol{J}/c$: $\boldsymbol{E}=(-\boldsymbol{u}\times\boldsymbol{B}+\nu_{\mathrm{m}0}\boldsymbol{\nabla}\times\boldsymbol{B})/c-(1/en_e)\boldsymbol{\nabla}P_e$. Let us emphasize once again that the equations (4)–(5) can be derived not only from some kinetics, but can also be simply understood as conservation laws for the hydrodynamic fields.

As for the pressure term in (4), it introduces no independent dynamics: in the incompressible setting, the total pressure $P+\boldsymbol{B}^2/8\pi$ is determined instantaneously by fields $\boldsymbol{u}$ and $\boldsymbol{B}$ through a Poisson-like equation. For instance, if $\boldsymbol{u}$ and $\boldsymbol{B}$ satisfy homogeneous boundary conditions on the boundary S of a d-dimensional ball of radius R at each time t, then (4) yields

$$\begin{aligned}P+\boldsymbol{B}^2/8\pi=&-\rho_0\int \mathrm{d}^dx'\,G(\boldsymbol{x},\boldsymbol{x}')\,\boldsymbol{\nabla}\cdot\boldsymbol{\nabla}\cdot\Big(\boldsymbol{u}(\boldsymbol{x}',t)\otimes\boldsymbol{u}(\boldsymbol{x}',t)-\boldsymbol{b}(\boldsymbol{x}',t)\otimes\boldsymbol{b}(\boldsymbol{x}',t)\Big)\\&+\mu_0\int_S \mathrm{d}S_{\boldsymbol{x}'}\,G(\boldsymbol{x},\boldsymbol{x}')\,\boldsymbol{n}(\boldsymbol{x}')\cdot\left(\frac{\partial^2\boldsymbol{u}(\boldsymbol{x}',t)}{\partial\boldsymbol{n}^2}-\frac{\partial^2\boldsymbol{b}(\boldsymbol{x}',t)}{\partial\boldsymbol{n}^2}\right),\end{aligned} \tag{6}$$

where the Green's function $G(\boldsymbol{x},\boldsymbol{x}')$ solves $\boldsymbol{\nabla}^2G(\boldsymbol{x},\boldsymbol{x}')=\delta(\boldsymbol{x}-\boldsymbol{x}')$ in the ball with Neumann boundary condition $\partial G/\partial\boldsymbol{n}\big|_S=-1/(S_dR^{d-1})$.[14] General form of $G(\boldsymbol{x},\boldsymbol{x}')$ was found recently in [165]. Here, in what follows, S_d denotes the surface area of the unit d-sphere, $S_d\coloneqq 2\pi^{d/2}/\Gamma(d/2)$, and Γ is the Euler gamma function. As will become explicit below, the pressure acts as a Lagrange multiplier enforcing the solenoidality constraints $\boldsymbol{\nabla}\cdot\boldsymbol{u}=0$ and $\boldsymbol{\nabla}\cdot\boldsymbol{B}=0$, respectively. Equivalently, pressure — and, more generally, any gradient contribution — can be eliminated from (4) and (5) by applying the Leray projector onto divergence-free vector fields, $\mathbb{P}\coloneqq\mathbb{I}-\boldsymbol{\nabla}\Delta^{-1}\boldsymbol{\nabla}\cdot$, where $\mathbb{I}$ is the identity operator. For the most common problem statement on $\mathbb{R}^d$ with $d\geq 3$, the action of $\mathbb{P}$ on a test field $\boldsymbol{v}(\boldsymbol{x},t)$ admits the singular-integral representation

$$(\mathbb{P}\boldsymbol{v})_i(\boldsymbol{x},t)=\frac{d-1}{d}v_i(\boldsymbol{x},t)+\mathrm{p.v.}\frac{1}{S_d}\int \mathrm{d}^dx'\left(\frac{d\,x_i'x_j'}{|\boldsymbol{x}'|^{d+2}}v_j(\boldsymbol{x}-\boldsymbol{x}',t)-\frac{v_i(\boldsymbol{x}-\boldsymbol{x}',t)}{|\boldsymbol{x}'|^d}\right), \tag{7}$$

where the abbreviation 'p.v' represents the principal value of the integral (see, e.g., [166]). Hereinafter, for repeating indices, Einstein's summation convention is adopted. The form of (4)–(5) obtained after applying $\mathbb{P}$ is referred to as the projection form of the MHD equations. Below, we present its explicit dimensionless version.

background field $\boldsymbol{B}_0$: the Alfvén wave and the two magnetoacoustic modes (fast and slow) with phase speeds $u_{f,s}^2=\left(u_A^2+c_s^2\pm\sqrt{\left(u_A^2+c_s^2\right)^2-4u_A^2c_s^2\cos^2(\theta)}\right)/2$, where θ is an angle between $\boldsymbol{B}_0$ and $\boldsymbol{k}$.

[14] We note that some textbooks impose homogeneous Neumann conditions (see, e.g., [5, §2.1]), which is inconsistent in a bounded domain. With homogeneous Neumann data the Green's function must satisfy $\Delta G(\boldsymbol{x},\boldsymbol{x}')=\delta(\boldsymbol{x}-\boldsymbol{x}')-1/V$, where V is the domain volume.

2.3. Background: control parameters and regime map of MHD flows

Flows described by Eqs. (4)–(5) are conveniently classified in terms of dimensionless numbers. Applying the Leray projector $\mathbb{P}$ and choosing characteristic scales of length ℓ, velocity u, and magnetic field B_0 (with $\rho_0 = \text{const}$), we rescale $\boldsymbol{x} \to \ell\,\boldsymbol{x}$, $\boldsymbol{u} \to u\,\boldsymbol{u}$, $t \to (\ell/u)\,t$, and $\boldsymbol{B} \to B_0\,\boldsymbol{B}$. This yields the dimensionless solenoidal MHD equations

$$\partial_t \boldsymbol{u} - \mathrm{Re}^{-1}\Delta\boldsymbol{u} = \mathbb{P}\,\boldsymbol{\nabla}\cdot\left(-\boldsymbol{u}\otimes\boldsymbol{u} + \mathrm{Ma}_A^{-2}\boldsymbol{B}\otimes\boldsymbol{B}\right), \tag{8}$$

$$\partial_t \boldsymbol{B} - \mathrm{Re}_{\mathrm{m}}^{-1}\Delta\boldsymbol{B} = \mathbb{P}\,\boldsymbol{\nabla}\cdot(\boldsymbol{B}\otimes\boldsymbol{u} - \boldsymbol{u}\otimes\boldsymbol{B}). \tag{9}$$

governed by three dimensionless parameters: the hydrodynamic Reynolds number $\mathrm{Re} := \rho_0 u\ell/\mu_0$ (characterizes the ratio of inertial forces to viscous friction), the magnetic Reynolds number $\mathrm{Re}_m := u\ell/\nu_{\mathrm{m}0}$ (compares the relative influence of magnetic induction and magnetic diffusion in a conducting medium), and the Alfvénic Mach number $\mathrm{Ma}_A := u/u_A$ with $u_A := B_0/\sqrt{4\pi\rho_0}$, defined by analogy with the sonic Mach number $\mathrm{Ma}_s = u/c_s$.

The magnetic Reynolds number quantifies magnetic flux freezing: for $\mathrm{Re}_m \gg 1$, advection dominates diffusion and the field is largely carried with the flow, whereas for $\mathrm{Re}_m \ll 1$ diffusion dominates and the field decouples from the motion. Likewise, $\mathrm{Re} \gg 1$ corresponds to an inertial, typically turbulent regime with a broad range of active scales, while $\mathrm{Re} \ll 1$ describes viscous, laminar flow. The Alfvénic Mach number Ma_A compares inertial effects to magnetic tension and thus indicates when, and to what extent, magnetic stresses control the dynamics. In the sub-Alfvénic regime $\mathrm{Ma}_A \ll 1$, perturbations are transmitted along field lines faster than the flow can distort them; in the trans-Alfvénic regime $\mathrm{Ma}_A \sim 1$, the flow distorts field lines on roughly the same timescale as Alfvén waves propagate along them, so neither effect dominates; in the super-Alfvénic regime $\mathrm{Ma}_A \gg 1$, the flow distorts the field more strongly and nonlinear effects, including sharp gradients and instabilities, become more prominent. Overall, the magnetic field fundamentally distinguishes MHD from ordinary hydrodynamics by generating scale-dependent anisotropy and enabling a strong back-reaction of the advected vector field on the flow.

In addition to the independent control parameters Re, Re_m, and Ma_A, it is instructive to introduce several derived dimensionless numbers that delineate relative dynamical regimes. The magnetic Prandtl number $\mathrm{Pr}_m := \mu_0/\rho_0\nu_{\mathrm{m}0} = \mathrm{Re}_m/\mathrm{Re}$ compares viscous and resistive (magnetic-diffusion) scales. Its magnitude varies widely: liquid-metal experiments typically have $\mathrm{Pr}_m \sim 10^{-6}$–$10^{-5}$, whereas astrophysical plasmas may realize both $\mathrm{Pr}_m \ll 1$ (e.g., convective zones, planetary cores) and $\mathrm{Pr}_m \gg 1$ (e.g., hot dilute media). The Stuart number $N := B_0^2\ell/4\pi\rho_0 u\nu_{\mathrm{m}0} = \mathrm{Re}_m/\mathrm{Ma}_A^2$ is a convenient criterion in quasi-static (inductionless) MHD, $\mathrm{Re}_m \ll 1$, where magnetic diffusion is fast, and Eq. (9) becomes quasi-instantaneous, while the flow dynamics is governed only by Eq. (8). It measures the relative importance of the Lorentz force compared with inertia so that $N \ll 1$ corresponds to essentially hydrodynamic flow, while $N \gtrsim 1$ indicates a strong magnetic back-reaction, typically associated with pronounced anisotropy and a tendency toward quasi-two-dimensional dynamics (three-dimensional perturbations elongated along the field are suppressed). For $N \gg 1$, electromagnetic braking and Joule dissipation dominate inertia, so that a quasi-stationary balance between momentum transport and Joule losses is established throughout the flow. In bounded domains, this 'laminarizing' action of the magnetic field typically promotes effectively two-dimensional dynamics and the emergence of large-scale vortical structures (see, e.g., [167]). The Lundquist number, $S := \tau_{\nu_{0\mathrm{m}}}/\tau_A = \mathrm{Re}_m/\mathrm{Ma}_A$ compares the resistive diffusion time $\tau_{\nu_{0\mathrm{m}}} := \ell^2/\nu_{0\mathrm{m}}$ to the Alfvén time $\tau_A := \ell/u_A$ and is particularly important in magnetic-reconnection problems. The plasma parameter $\beta := 8\pi p/B_0^2 = 2c_s^2/\gamma u_A^2 = (2/\gamma)\mathrm{Ma}_A^2/\mathrm{Ma}_s^2$ (where γ is the heat capacity ratio) shapes the magnetoacoustic branches and sets the kinetic-scale ordering

via $(\lambda_{Ls}/d_s)^2 \propto \beta_s$ $(s = e, i)$ determining whether Hall/inertial effects or finite-Larmor-radius corrections break the MHD approximation first at small scales. Finally, the Hartmann number $\mathrm{Ha} \coloneqq u_A \ell/\sqrt{\nu_0 \nu_{\mathrm{m}0}} = \sqrt{\mathrm{Re}\mathrm{Re}_m}/\mathrm{Ma}_A$ measures the ratio of Lorentz forces to viscous stresses. It is practically useful for wall-bounded MHD flows, where Ha controls the thickness of Hartmann boundary layers and thus the near-wall friction and overall flow profile.

The parameters introduced above provide a convenient basis for classifying flow regimes in conducting media. A coarse division is into (**I**) *laminar and quasi-laminar regimes*, (**II**) *hydrodynamic turbulence with a passive magnetic field*, and (**III**) *fully developed inertial-inductive MHD turbulence*. The latter encompasses astro- and geophysical turbulence as well as laboratory MHD experiments and is the primary focus of the present work. In this regime, induction and advection dominate diffusion, the magnetic field is dynamically active, and a strong two-way coupling between $\boldsymbol{u}$ and $\boldsymbol{B}$ is established via the Lorentz force. A turbulent cascade develops across scales (see below), and magnetic self-organization (including large-scale field generation) may occur. Each type of MHD flow, in turn, (qualitatively) admits several subregimes:

I.1 *Viscous–resistive regime* ($\mathrm{Re} \ll 1$, $\mathrm{Re}_m \ll 1$, $\forall\, \mathrm{Ma}_A$). Inertia is negligible, and the flow is laminar; magnetic diffusion dominates induction, so the field is only weakly affected by the motion, and its back-reaction is minimal.

I.2 *Viscous inductive regime* ($\mathrm{Re} \ll 1$, $\mathrm{Re}_m \gg 1$, and typically $\mathrm{Ma}_A \lesssim 1$). The flow remains laminar, but high conductivity implies efficient advection of magnetic flux: even slow ordered motion can substantially distort and transport field lines.

II.1 *Inertial resistive regime* $\mathrm{Re} \gg 1$, $\mathrm{Re}_m \ll 1$, $N < 1$. The flow is turbulent, yet induction is weak; the magnetic field does not significantly structure the motion and can often be treated as passive (it is weakly amplified or rapidly dissipated); thus, turbulence is close to hydrodynamic.

II.2 *Quasi-stationary turbulent MHD* ($\mathrm{Re} \gg 1$, $\mathrm{Re}_m \ll 1$, $N > 1$). Magnetic diffusion is fast, so the induced field adjusts quasi-instantaneously to $\boldsymbol{u}$ and the Lorentz force acts as distributed Joule braking. This suppresses velocity fluctuations along the local mean field, producing strong anisotropy and a tendency toward quasi-two-dimensionalization while preserving an inertial cascade in planes transverse to the field. See detailed analysis in [168].

III.1 *Sub-Alfvénic turbulence* ($\mathrm{Re} \gg 1$, $\mathrm{Re}_m \gg 1$, and $\mathrm{Ma}_A \ll 1$). At the injection scale, the amplitude of characteristic velocity fluctuation v is small compared with the Alfvén speed u_A, so the dynamics is strongly anisotropic with respect to the local mean field ($k_\perp \gg k_\parallel$). On large scales, this typically corresponds to weak (wave) MHD turbulence, with $\tau_A = \ell_\parallel/u_A \ll \tau_{\mathrm{nl}} = \ell_\perp/v$; the cascade proceeds mainly toward larger $k_\perp$ (with weak parallel transfer), and the perpendicular total energy spectrum may approach $E(k_\perp) \propto k_\perp^{-2}$ [169]. As the cascade reaches smaller perpendicular scales, nonlinear interactions strengthen, and below the transition scale $\ell_{\mathrm{tr}} \sim L\,\mathrm{Ma}_A^2$ (L is the system's size), the system usually enters the strong, critical-balance regime with $\tau_A \sim \tau_{\mathrm{nl}}$. There, the transfer is dominated by interactions of counterpropagating Alfvén wave packets [15], yielding perpendicular spectra close to $E(k_\perp) \sim k_\perp^{-5/3}$, as predicted by Goldreich–Sridhar theory (GS95) [170] or $k_\perp^{-3/2}$ (dynamic-alignment models *a là* Boldyrev [171]), with scale-dependent anisotropy (e.g., $k_\parallel \propto k_\perp^{2/3}$ in GS95).

III.2 *Trans-Alfvénic turbulence* ($\mathrm{Re} \gg 1$, $\mathrm{Re}_m \gg 1$, and $\mathrm{Ma}_A \simeq 1$). At the injection scale $\tau_A \sim \tau_{\mathrm{nl}}$, so the cascade is strong from the outset, and anisotropy develops dynamically with

[15] This can be seen by adding and subtracting Eqs. (8) and (9), which yields the symmetrized (Elsässer) problem formulation. In this form it is clear that the nonlinearity couples counterpropagating packets only: for instance, $\boldsymbol{u} + \boldsymbol{B}/\sqrt{4\pi\rho_0}$ interacts with $\boldsymbol{u} - \boldsymbol{B}/\sqrt{4\pi\rho_0}$ but has no self-interaction.

respect to the local mean field. Magnetic E_M and kinetic E_K energies are typically comparable, although strict equipartition need not hold due to $E_K - E_M \neq 0$. This possible imbalance is associated with nonzero cross-helicity (see the definition below).

III.3 *Super-Alfvénic turbulence* ($\mathrm{Re} \gg 1$, $\mathrm{Re}_m \gg 1$, and $\mathrm{Ma}_A \gg 1$). At the outer scale, the magnetic field is dynamically weak, and the turbulence is close to hydrodynamic (approximately Kolmogorov), but for sufficiently large Re_m a small-scale dynamo (see below) amplifies magnetic fluctuations. As the cascade proceeds to smaller scales, the velocity amplitude decreases, and at the transition scale $\ell_A \sim L\,\mathrm{Ma}_A^{-3}$ one reaches a local $\mathrm{Ma}_A \sim 1$; below ℓ_A the cascade typically becomes Alfvénic and develops the characteristic anisotropy with respect to the local field [172]. At $\mathrm{Re}_m \gg 1$ (equivalently, large local Lundquist numbers of current sheets), a reconnection-mediated subrange may appear at sufficiently small scales: turbulence generates thin current layers that become tearing-/plasmoid-unstable, and reconnection begins to affect the transfer and dissipation, potentially limiting the anisotropy. This is not a new class in Ma_A, but rather a possible small-scale modification of the inertial cascade in highly conducting MHD [173, 174].

2.4. Background: dynamos, cascades, and invariants

Even before the advent of magnetohydrodynamics, the origin and persistence of planetary, stellar, and galactic magnetism had been a longstanding challenge. With the emergence of MHD, it soon took shape as a general theory of magnetic-field generation and/or maintenance in moving conducting media — magnetic dynamo theory [158, 175–181]. Built on the equations of MHD (both non-relativistic and relativistic), dynamo theory applies to a wide range of geophysical and astrophysical phenomena (planetary and solar cycles, geomagnetic reversals, star formation, jets and protostellar disks, accretion flows, etc.) as well as to laboratory plasmas, where it addresses self-excitation and kinematic growth, nonlinear saturation via Lorentz-force back-reaction, and the dynamo electromotive force (EMF) sustaining the field.[7]

The very term 'dynamo' reflects the ability of electrically conductive fluid motions to generate and sustain magnetic fields — much like an electrical generator, but without coils and wires. The possibility of such a self-excited mechanism, first suggested in 1919 by Larmor [182], was initially met with strong skepticism[16], reinforced by a series of 'anti-dynamo' theorems that rule out steady self-sustained fields in broad classes of overly symmetric or effectively two-dimensional flows (e.g., Cowling's for axisymmetric fields [184], Zel'dovich's for planar flows [185], and Elsässer's for toroidal-velocity; see [186, 187] for review). Until the middle of the 20th century, the existence of a dynamo was considered impossible. The resolution is that successful dynamos require sufficiently three-dimensional, symmetry-breaking motions; explicit kinematic examples were subsequently constructed, such as Roberts [188] or Ponomarenko-type [189] periodic flows. See [190] for review. For large-scale (mean) magnetic field generation, the key ingredient is the emergence of an EMF containing an α-type contribution (the α-effect), possible only if parity symmetry is violated. In mirror-symmetric turbulence, by contrast, α-effect vanishes, and the dominant effect on the large-scale field is turbulent diffusion. In mean-field theory, this was formalized in classic works by Parker [191], Elsässer [192], Braginsky [193–196], and especially Steenbeck *et al* [197]. However, most observed large-scale fields typically rely on broken reflectional symmetry induced by rotation, stratification, and/or shear. Thus, modern dynamo theory focuses on the excitation and maintenance of magnetic fields by three-dimensional, symmetry-breaking motions in conducting fluids [187, 198].

[16] In particular, in 1924 Einstein proposed that the Earth's and the Sun's magnetic fields might arise from a tiny mismatch between the proton and electron charges and 'is not produced by magnetic bodies' [183].

Neglecting the displacement current in the non-relativistic MHD approximation for media with high σ_0 enables the use of the classical concept of magnetic field lines. In the ideal limit $\nu_{\mathrm{m}0} \to 0$, the magnetic flux through any material surface is conserved, so the flow advects the field and can amplify it by stretching, folding, and twisting field lines (see, e.g., [199]), thereby converting kinetic energy into magnetic energy while conserving the total energy. However, a systematic growth of a large-scale magnetic field requires a mechanism that breaks reflection symmetry, so that the mean EMF can contain an α-type contribution. A simple measure of such parity breaking is the kinetic helicity $H_k = \langle \boldsymbol{u} \cdot (\boldsymbol{\nabla} \times \boldsymbol{u}) \rangle$. Hereafter, in this section $\langle \bullet \rangle$ denotes some averaging procedure. Like any helicity, $H_k \neq 0$ (in average) only in mirror-asymmetric media, which are therefore often called helical (older literature also uses the term gyrotropic). Note that, unlike pure hydrodynamics, vorticity $\boldsymbol{\nabla} \times \boldsymbol{u}$ in MHD is not frozen into the flow, and H_k is not conserved: the magnetic field can generate and redistribute vorticity. By contrast, the ideal MHD equations (Eqs. (4) and (5) with $\nu_0 = \nu_{\mathrm{m}0} = 0$) possess genuine invariants such as the magnetic helicity $H_m := \langle \boldsymbol{A} \cdot \boldsymbol{B} \rangle$ with $\boldsymbol{B} = \boldsymbol{\nabla} \times \boldsymbol{A}$ (invariant under suitable boundary conditions), the cross-helicity $H_c := \langle \boldsymbol{u} \cdot \boldsymbol{B} \rangle$, and the total energy E. Together with other Casimir invariants (see, e.g., [200]), these constraints underlie the rich cascade phenomenology of MHD by restricting how invariants and energy can be redistributed across scales.

Let us emphasize that the existence of ideal invariants beyond the energy makes the cascade phenomenology of MHD substantially richer than that of pure hydrodynamics. Recall that a cascade (of E, H_m, etc.) is a regime in which a nearly scale-independent flux transports an invariant (or quasi-invariant) quantity across scales via nonlinear transfer. The approximate constancy of this flux is the hallmark of a cascade and the underlying reason why power-law spectra arise (e.g., K41-type scalings).[17] For example, when reflection symmetry is broken so that $H_m \neq 0$, magnetic helicity can undergo a robust inverse cascade toward small wavenumbers [206, 207]. This, in turn, promotes the growth of the part of large-scale magnetic energy[18] and hence of a mean magnetic field. Thus, while the total energy cascade remains predominantly forward, a helicity-carrying fraction of the magnetic energy is transferred upscale, leading to the emergence of large-scale fields (a large-scale dynamo). In spectral terms, this is essentially the same mechanism that underlies the well-known α-effect in dynamo theory.

Looking slightly ahead, we note that in the case where the turbulent character of the medium motion dominates, the above picture of frozen-in magnetic flux turns out to be incompatible with the notion of free motion of turbulent vortices. Indeed, in the absence of mechanisms that change the topology of the magnetic field, one would expect the formation of an extremely tangled, felt-like magnetic-field structure, which is not observed in practice. The point is that magnetic fields in turbulent fluids do not obey Alfvén's theorem and can change their topology and connectivity due to the process of magnetic reconnection [208, 209]. The discovery of this mechanism made it possible to explain rapid changes of magnetic fields in conducting media and became a key milestone in the development of modern magnetohydrodynamics [14].

The classification of dynamo mechanisms is multifaceted and partly overlapping. The references below are representative monographs and are not intended to be exhaustive. One may distinguish (i) mean-field dynamos based on the α-effect in combination with shear (e.g., $\alpha\Omega$)

[17] A cascade need not require fully developed turbulence: statistically steady spectral fluxes of invariants also arise in more organized regimes such as weak (wave) turbulence [201, 202]. For MHD, see, e.g., [169]. In that case, the dynamics is governed by kinetic (or other effective) equations rather than the hydrodynamic system (4)–(5) considered here. Nevertheless, such regimes can also be studied within statistical field theory; see, e.g., [3, 203–205] for treatments of Langmuir (wave) turbulence.

[18] One may infer that from the bound $|H_m(k)| < E_m(k)/k$ [207].

or without it (e.g., α^2) [158, 178, 210]; (ii) Lagrangian/topological scenarios of magnetic amplification associated with field-line stretching, folding, and twisting (often discussed in the context of fast dynamos) [158, 211]; (iii) regimes classified by the magnetic Reynolds number — fast versus slow dynamos in the limit $\mathrm{Re}_m \to \infty$ [158, 211]; (iv) laminar [158, 211] versus turbulent dynamos [13, 157]; (v) large-scale (mean-field) [178, 210, 212] versus small-scale (fluctuation) dynamos [13, 157, 177]; (vi) classifications by the type of forcing (convective, shear-driven, precession- or tide-driven, etc.) [210, 212, 213] and by the symmetry and temporal behaviour of the generated field (steady/oscillatory, dipolar/quadrupolar, axisymmetric/non-axisymmetric) [158, 212].

From a theoretical standpoint, dynamo theory is commonly discussed in two formulations: kinematic (linear) and nonlinear. In the kinematic formulation, the magnetic field is assumed to be dynamically passive, with magnetic energy well below kinetic energy, and one studies whether a prescribed velocity field can amplify magnetic fluctuations. In the nonlinear dynamo, the growth saturates: magnetic stresses become comparable to inertial forces, the Lorentz-force back-reaction is essential, and one must work with the fully coupled MHD system (4)–(5). The kinematic regime is thus best viewed as an initial stage, since it typically produces a field strong enough to affect the flow on astrophysically short timescales [158, 175]. Although kinematic dynamos are analytically tractable and widely studied, nonlinear dynamos are the physically relevant regime — especially in geophysical and astrophysical settings, where the driving is turbulent [158, 175, 187, 198, 214–216]. Such turbulent dynamos can be described efficiently within statistical theories, which is one of the themes of this review. It is also worth noting that substantial experimental progress has been achieved in recent decades, notably in liquid-sodium facilities (see the still-relevant review [217]) designed to probe turbulent dynamo [218–222].

2.5. Background: MHD turbulence and overview of representative systems

Observations of flows in the interstellar medium, galaxy clusters, and the solar wind indicate that turbulence in cosmic plasmas is the rule rather than the exception [223–225]. Likewise, the secular variability of planetary magnetic fields in the Solar System points to vigorous turbulent motions in liquid-metal cores [226–229]. Together, these facts make MHD turbulence a key example underpinning the view that turbulence is among the most widespread nonequilibrium states in nature. Its driving is commonly attributed to convection and compositional buoyancy, as well as to a broad range of instabilities, including the magnetorotational instability (MRI) in accretion disks, Kelvin–Helmholtz shear instabilities in jets and boundary layers, Rayleigh–Taylor modes in gravitationally stratified media, Parker instability in magnetized atmospheres, tearing in current sheets, and kink/sausage instabilities in flux ropes and pinches [13, 230].

The MHD turbulent cascade is more naturally viewed not as a vortex cascade but as interactions of counterpropagating Alfvén wave packets. In the weak-turbulence, this is literal: the cascade proceeds through resonant three-wave interactions of Alfvén waves [169, 201], whereas at sufficiently small (dissipative) scales the dynamics is increasingly dominated by intermittent current sheets and localized reconnection events [174]. In developed turbulence, the relevant 'waves' are nonlinear Alfvénic fluctuations — localized Elsässer wave packets (or Favre-weighted analogs for $\rho_0 \neq \mathrm{const}$ [231]) — that are advected and distorted by the cascade. As for theory, unlike K41, there is no single compact axiomatic system that provides a unique universal spectrum for all MHD turbulence phenomena. The underlying reason is that MHD introduces new key ingredients: Alfvén waves and the associated time scale τ_A, scale-dependent anisotropy relative to the local mean field, distinct cascade 'channels' for kinetic and magnetic energies, and additional invariants and regimes (weak/strong, balanced/imbalanced, etc.).

As for fundamental characteristics of the MHD turbulent state, the Politano–Pouquet laws [232] play a central role as the analogue of Kolmogorov's 4/5 law. Derived directly from the von Kàrmàn–Howarth equation for MHD under standard statistical assumptions, they relate third-order mixed structure functions of velocity and magnetic-field increments to the dissipation rates $\varepsilon^{\pm}$ associated with the two Elsässer 'channels'. For solenoidal, (locally) homogeneous three-dimensional MHD (without assuming local isotropy), they read

$$\boldsymbol{\nabla}_{\boldsymbol{r}} \cdot \left\langle \Big(\delta\boldsymbol{u}(\boldsymbol{r},t) \mp \delta\boldsymbol{b}(\boldsymbol{r},t) \Big) \left| \delta\boldsymbol{u}(\boldsymbol{r},t) \pm \delta\boldsymbol{b}(\boldsymbol{r},t) \right|^2 \right\rangle = -4\,\varepsilon^{\pm}, \tag{10}$$

where $\delta\boldsymbol{u}(\boldsymbol{r},t) \coloneqq \boldsymbol{u}(\boldsymbol{x}+\boldsymbol{r},t) - \boldsymbol{u}(\boldsymbol{x},t)$, $\delta\boldsymbol{b}(\boldsymbol{r},t) \coloneqq \boldsymbol{b}(\boldsymbol{x}+\boldsymbol{r},t) - \boldsymbol{b}(\boldsymbol{x},t)$, and $\boldsymbol{b} \coloneqq \boldsymbol{B}/\sqrt{4\pi\rho_0}$ is the magnetic field in Alfvénic units. These relations show that the inertial-range fluxes $\varepsilon^{\pm}$ are not merely postulated but are constrained by exact third-order laws.

For strong incompressible MHD turbulence, the most widely used 'Kolmogorov analogue' is the GS95 [170] phenomenology, which postulates critical balance, $\tau_{\rm nl}(\ell_\perp) \simeq \tau_A(\ell_\parallel)$, leading to $E(k_\perp) \propto k_\perp^{-5/3}$ and scale-dependent anisotropy $k_\parallel \propto k_\perp^{2/3}$. An alternative phenomenology due to Boldyrev [171] incorporates scale-dependent alignment of $\delta\boldsymbol{u}$ and $\delta\boldsymbol{b}$, which weakens the effective nonlinearity and yields $E(k_\perp) \propto k_\perp^{-3/2}$ while remaining consistent with the exact third-order laws. In the presence of a strong guide field and weak nonlinearity, weak (wave) MHD turbulence applies, giving a Kolmogorov–Zakharov-type spectrum $E(k_\perp) \propto k_\perp^{-2}$ and a predominantly perpendicular cascade. Finally, in imbalanced turbulence (e.g., in the solar wind), where $H_c \neq 0$, two distinct fluxes $\varepsilon^{\pm}$ appear, and additional closure assumptions are required, further weakening universality at the level of amplitudes and characteristic times.

Real systems may fall into one of the aforementioned regimes (**I.1**)–(**III.3**) or occupy transitional states between them. The Table 1 summarizes representative MHD systems in nature and in the laboratory, indicating whether turbulence is present, the degree of mirror-symmetry breaking, and the occurrence of dynamo action. It suggests that simple one-fluid, non-relativistic, three-dimensional solenoidal resistive MHD with scalar viscosity and conductivity (Eqs. (4)–(5)) is most adequate as an all-in-one model for liquid metals: planetary outer cores, laboratory sodium/gallium flows, MHD pumps and electromagnetic braking, and, to first order, liquid-metal batteries. These media are typically dense, strongly collisional, and quasi-neutral, with $u \ll c$ and often weak compressibility, so electrons and ions (or the lattice) are tightly coupled and the effective coefficients μ_0 and σ_0 (hence ν_0 and $\nu_{\rm m0}$) may be treated as scalars. The same framework is only conditionally applicable as a large-scale model — often requiring effective (turbulent) transport coefficients and/or compressible/anelastic formulations — in stellar convective zones, parts of accretion disks, and for global modes in tokamaks and spheromaks, where stratification, compressibility, anisotropic transport, and Hall/two-fluid effects limit the scalar closure; likewise, although MHD is widely used for the intracluster medium, a scalar-$\nu_0, \nu_{\rm m0}$ resistive model is often inadequate in weakly collisional, microinstability-prone regimes. Nevertheless, in these settings Eqs. (4)–(5) can still provide a useful and often quantitatively accurate description of the turbulent cascade at sufficiently large scales. By contrast, the model is generally inapplicable to weakly ionized multi-component media (molecular-cloud ISM and ionospheric–magnetospheric current systems), where ambipolar diffusion and Hall conductivity are essential, and to largely collisionless space plasmas (solar corona, solar wind, magnetosheath), as well as jets and supernova remnants with shocks and possible relativistic effects. Finally, magnetic reconnection in many natural settings requires two-fluid/Hall or kinetic physics: scalar resistive MHD with a single $\nu_{\rm m0}$ may provide a coarse macroscopic model, but often misses the mechanism of fast reconnection.

Table 1. Representative MHD systems in nature and laboratory experiments: turbulence, flow mirror symmetry, and dynamo action. Generally known information about them is provided in footnotes.

	Conducting medium	Turbulence	Developed turbulence	Mirror symmetry	Magnetic dynamo
Astrophysical and cosmic plasmas	Interstellar medium (ISM), molecular clouds[a]	✓	✓	✘(large-scale dynamo/helicity)	✓(galactic mean-field & small-scale)
	Accretion disks[b]	✓	✓(anisotropic)	Variable	✓(MRI dynamo)
	Stellar convective zones[c]	✓	✓	✘(helical convection)	✓(global $\alpha\Omega$)
	Jets and remnants of supernovae[d]	✓	Partial	✘(shocks/shear)	✓(turbulent small-scale)
	Intracluster medium (ICM) of galaxies[e]	✓	Often	Approximate	✓(turbulent small-scale)
	Solar corona, coronal loops[f]	✓	Rarely	✘(photospheric helicity injection)	✘(field supplied from below)
	Solar wind, interplanetary medium[g]	✓	✓(imbalanced)	✘(cross-helicity/imbalance)	✘(advected solar field)
	Magnetospheric magnetosheath[h]	✓	Often	✘(weakly broken)	✘
	Large-scale magnetic reconnection[i]	✓	Often	✘(guide-field or global geometry)	✘(dissipative, not generative)
Planetary media	Liquid outer cores of planets[j]	✓	✘(geostrophic constraints)	✘(helical convection)	✓(planetary dynamo)
	Ionospheric-magnetospheric current systems on planets[k]	Possible	✘	Variable	✘
Laboratory systems	Liquid metal flows (sodium/gallium)[l]	✓	Partial	✘(geometry/rotation)	✓(above critical R_m)
	Tokamaks, spheromaks[m]	✓	Partial	✘(geometry-induced helicity)	Spheromak: ✓; Tokamak: ✘
	MHD pumps, electromagnetic jet braking[n]	✘	✘	✓(engineered)	✘($R_m \ll 1$)
	Liquid metal batteries (Taylor instability)[o]	Possible	✘	✘(kink-mode chirality)	✘(TI alone not self-sustaining)

[a] In the ISM (including molecular clouds), turbulence (trans- or super-Alfvénic) is driven mainly by supernova feedback (shocks) and large-scale galactic flows; $\mathrm{Re} \gg 1$ (up to $\mathrm{Re} \gtrsim 10^6 - 10^9$), and magnetic advection dominates Ohmic diffusion on cloud/ISM scales ($\mathrm{Re}_m \gg 1$; in weakly ionised gas, ambipolar diffusion becomes important at small scales). Net kinetic helicity associated with galactic rotation enables an $\alpha\Omega$ mean-field dynamo and sustains a coherent large-scale magnetic field.

[b] In sufficiently ionised accretion discs (around stars or black holes), differential rotation renders weakly magnetised flows unstable to the magnetorotational instability (MRI), which typically drives vigorous MHD turbulence (usually considered trans-Alfvénic unless an external field is present) with $\mathrm{Re}, \mathrm{Re}_m \gg 1$. Owing to rotation and strong shear, the turbulence is intrinsically anisotropic. MRI turbulence also acts as a dynamo, sustaining magnetic energy and, in many cases, generating organized large-scale field patterns (e.g., cyclic mean fields), via mechanisms that may be helical in stratified discs or non-helical in unstratified shear flows.

[c] Stellar convective zones are highly conducting plasmas with vigorous turbulent convection spanning a wide range of scales whose characteristic amplitudes and time-scales vary with depth. Turbulence here is usually considered to be trans-Alfvénic. In a rotating, stratified envelope the Coriolis force imparts a systematic twist to convective motions, breaking mirror symmetry and enabling mean-field dynamo action: differential rotation provides the Ω-effect, while helical convection contributes an α-effect, together sustaining a large-scale magnetic field (in the Sun, associated with the ~ 11-yr activity cycle and the ~ 22-yr magnetic polarity cycle) on top of a strong small-scale turbulent field.

[d] Relativistic jets and supernova remnants are strongly inhomogeneous, with turbulence (in different regimes depending on the scale and magnetic mean field) generated only in parts of the flow: in jets, chiefly in internal/recollimation shocks, shear layers, and MHD instabilities, and in remnants, mainly in the shocked downstream region and in instability-driven mixing layers. The corresponding Reynolds numbers are typically enormous, yet the dynamics can remain dominated by bulk expansion/outflow rather than fully developed turbulence. The shock–shear–instability-driven fluctuations can power efficient small-scale (turbulent) magnetic-field amplification, whereas a global large-scale dynamo is not generally expected; in jets, the large-scale field is largely set by the central engine and is subsequently reshaped and intermittently amplified in situ.

[e] ICM is a hot, dilute, weakly collisional plasma in which mergers and sloshing drive intermittent and spatially inhomogeneous trans-Alfveńic turbulence (with effectively large Re and Re_m, though the microphysical transport coefficients are uncertain). Because clusters lack coherent global rotation, the net kinetic helicity is expected to be small (mirror symmetry approximately restored on average), so a classical large-scale $\alpha\Omega$ dynamo is not favoured; nevertheless, a small-scale turbulent dynamo can amplify seed fields to μG strengths, producing tangled magnetic structures with coherence scales of order ~ 1–$50\,\mathrm{kpc}$.

[f] The solar corona and coronal loops are hot, tenuous, magnetically dominated plasma structures above the photosphere; their dynamics is typically organized into long-lived magnetic arches, while (sub- or trans-Alfveńic) turbulence is intermittent and local (e.g., in braided fields, current sheets, and during flares). Photospheric footpoint motions inject twist/magnetic helicity and free energy into coronal fields, thereby breaking mirror symmetry. The corona is not the seat of a global dynamo: its large-scale field is generated below the surface and is mainly stored, transported, and reconfigured (and dissipated) by reconnection rather than produced anew in situ.

[g] The solar wind and interplanetary medium are open, expanding magnetised plasmas with broadband MHD turbulence (trans- or super-Alfvénic) with a well-developed cascade of velocity and magnetic fluctuations from large (hours) to small (seconds and below) time-scales, driven by solar-origin Alfvénic disturbances and by stream–stream interactions (shear/compressions). The turbulence is often strongly imbalanced (large cross helicity) because outward-propagating Alfvén waves dominate, which breaks reflection symmetry. No self-excited global dynamo is expected: the large-scale field is of solar origin, advected outward and decays with expansion, while turbulence redistributes and dissipates its energy.

[h] The planetary magnetosheath is the layer of shocked solar-wind plasma between the bow shock and the magnetopause, where strong velocity and magnetic fluctuations (waves and intermittent super- or trans-Alfveńic turbulence) are commonly generated by shock processing and downstream instabilities. The average net helicity is typically small (mirror symmetry only weakly broken), and no self-excited dynamo operates: the upstream field is mainly advected/compressed while flow energy is dissipated into heat and fluctuations.

[i] Large-scale magnetic reconnection (e.g., in the terrestrial magnetotail or solar flares) occurs where oppositely directed magnetic flux systems converge and reconnect within thin current sheets. At high conductivity ($S \gg 1$), such sheets commonly become unstable to tearing/plasmoid formation, fragmenting into plasmoids and secondary sheets and producing intermittent, trans-Alfvén turbulence-like fluctuations. Reflection symmetry may be broken by the global geometry and, when present, a guide field. Reconnection is not a dynamo: it mainly dissipates and rearranges the pre-existing field, converting magnetic energy into flows, particle acceleration, and heat.

[j] Planetary liquid-metal outer cores (e.g., Earth's) host electrically conducting, buoyancy-driven convection under rapid rotation. Although $\mathrm{Re} \gg 1$ (sub-Alfvénic turbulence), the flow is strongly rotation-constrained and far from isotropic, with quasi-geostrophic, columnar structures aligned with the rotation axis. Rotation-induced helicity breaks mirror symmetry and enables a self-sustained dynamo that generates the global planetary field, often described as an α-type dynamo with shear-assisted Ω contributions.

[k] Ionosphere–magnetosphere current systems (field-aligned currents and ionospheric electrojets) form large-scale, magnetically guided circuits that are usually organized by the background field, with sub- or trans-Alfvénic turbulence appearing only intermittently (e.g., in auroral arcs and thin current sheets during substorms). Mirror-symmetry properties are configuration-dependent and may vary in time. These currents do not generate the planet's main magnetic field (set by the internal core dynamo), but rather redistribute magnetic flux and convert electromagnetic energy into particle acceleration and Joule heating, producing time-dependent magnetic perturbations.

[l] Laboratory liquid-metal flows (Na, Ga, etc.) can become turbulent at sufficiently strong forcing, reaching large Re (up to $\mathrm{Re} \sim 10^6$) with $\mathrm{Re}_m \sim 10$–50 (sometimes $\sim 10^2$) the finite vessel size typically limits the inertial range, so the turbulence is not always fully developed. If so, then we speak of trans-Alfvén turbulence, otherwise of super-Alfvén. Mirror symmetry is often deliberately broken by the apparatus geometry and/or rotation to impose net flow helicity and facilitate dynamo onset. When Re_m exceeds a set-up-dependent threshold (in sodium experiments, $\mathrm{Re}_{m,\mathrm{crit}} \sim 10 - 50$), magnetic perturbations grow exponentially and saturate into a nonlinear self-sustained dynamo state (steady, oscillatory, or reversing, depending on the configuration).

[m] High-temperature toroidal fusion plasmas (tokamaks and spheromaks) exhibit MHD instabilities and sub-Alfvénic turbulence that are strongly anisotropic and organized by the confining magnetic geometry. In tokamaks, microturbulence (e.g., drift-wave turbulence) coexists with macroscopic MHD activity (e.g. sawteeth, fishbones, tearing modes), but the large-scale confining field is primarily imposed by external coils together with the plasma current, so no self-excited large-scale dynamo is expected in the usual operating regime. In spheromaks (compact tori with comparable poloidal and toroidal fields), the configuration is self-organized and typically formed/sustained by helicity injection; an internal relaxation-driven MHD dynamo can maintain the current and magnetic structure against resistive decay.

[n] MHD pumps and electromagnetic brakes drive or retard liquid-metal flows by Lorentz forces in an imposed magnetic field. They are typically operated in a controlled (often laminar or weakly turbulent) regime, while the magnetic Reynolds number is kept small, $\mathrm{Re}_m \ll 1$, so magnetic induction and any dynamo action are negligible. Consequently, no developed turbulent cascade is expected, and mirror symmetry is usually preserved by a symmetric channel/field design to avoid net helicity.

[o] Liquid-metal batteries can experience current-driven MHD instabilities at high current densities, most notably the Tayler instability (a kink-type mode of an axial current and its azimuthal magnetic field). This can drive spontaneous large-scale swirling motions (often columnar/vortical flow about the cell axis) and, at sufficiently strong forcing, fluctuations that may become weakly (sub-Alfvén-type) turbulent; in typical operating conditions, however, the flow is laminar or near transitional rather than fully developed turbulence. The kink mode selects a handedness and thus breaks mirror symmetry. Nevertheless, it does not constitute a self-sustained dynamo: its practical impact is mainly on mixing, current distribution, and heat/solute transport.

3. The model of MHD turbulent state: stochastic helical magnetohydrodynamics

3.1. Preparation: from deterministic MHD to a bulk stochastic model of stationary turbulence

As can be gleaned from Table 1, most natural MHD systems are turbulent. They are generally neither homogeneous nor unbounded: they have finite size, specific boundary conditions, and often exhibit strong large-scale inhomogeneity (e.g., stratification and density/temperature gradients). They also typically rotate and are anisotropic due to gravitational stratification and large-scale magnetic fields, and frequently exhibit large-scale shear (e.g., in accretion discs). On the other hand, theoretical descriptions of MHD turbulence (as of any strongly nonlinear problem) typically invoke simplifying assumptions such as statistical homogeneity and stationarity, an infinite domain, scalar transport coefficients, etc. Of these, (local) homogeneity is the most 'structure-forming' for a general theory, whereas the others can often be relaxed systematically. In particular, isotropy is usually only a crude idealization: a (local) mean magnetic field makes both the cascade and the fluctuation statistics essentially anisotropic [170].

As illustrated in section 2, when supplemented with appropriate initial and boundary conditions, the resistive-MHD equations (4)–(5) adequately describe the physics of liquid-metal conductors and a range of astrophysical situations away from boundaries (see [233]). Here, by contrast, we treat Eqs. (4)–(5) as the dynamical basis of a model theory for a fully developed turbulent state 'in the bulk' (i.e., far from boundaries), allowing, where needed, for pseudoscalar effects (e.g., helicity and/or cross-helicity). Although the model may include explicit anisotropy, we assume it to be not too strong (i.e., the large-scale mean field is small compared with the scale of the fluctuations), so that scalar viscosity and conductivity remain adequate.

In fully developed turbulence, in both MHD and purely hydrodynamic settings, solutions of Eqs. (4)–(5) have an extremely irregular spatio-temporal structure (see, e.g., DNS simulations [234]) and are conveniently viewed as realizations of a random process. Because many scales interact and the dynamics are highly sensitive to initial data, trajectory-based descriptions in phase or configuration space are of limited use, whereas statistical characteristics of the state become central and admittedly only feasible quantities from the pragmatic point of view. Formally, these statistics are defined assuming (practical) ergodicity by an ensemble of realisations (e.g., generated by varying initial conditions and/or external drives) and, in stationary settings, can be related to explicit 'equilibrium' ensemble constructions for truncated ideal systems [206, 235–237]. Accordingly, a model of fully developed MHD turbulence is naturally formulated as a theory of two vector random fluctuating fields obtained by 'stochasticization' of Eqs. (4)–(5).[19]

The explicit construction of the fluctuation (SFT) theory is deferred to the next section; here we outline the standard 'stochasticisation' procedure suitable for the subsequent SFT formulation. We begin with the Reynolds decomposition of the velocity field, $\boldsymbol{u} = \boldsymbol{U}_0 + \boldsymbol{v}$ with $\langle \boldsymbol{u} \rangle = \boldsymbol{U}_0$.[20] In a homogeneous full-space formulation, $\boldsymbol{U}_0 = \text{const}$ (or, at most, a slowly varying drift $\boldsymbol{w}(t)$), so one can remove it by an (extended) Galilean transformation,

$$\boldsymbol{v}_w(\boldsymbol{x}, t) = \boldsymbol{v}\big(\boldsymbol{x} + \boldsymbol{s}(t),\, t\big) - \boldsymbol{w}(t), \quad \boldsymbol{B}_w(\boldsymbol{x}, t) = \boldsymbol{B}\big(\boldsymbol{x} + \boldsymbol{s}(t),\, t\big), \quad \boldsymbol{s}(t) = \int_{-\infty}^{t} \mathrm{d}t'\, \boldsymbol{w}(t'), \quad (11)$$

[19] We emphasize that, unlike models of critical statics [3, 238], such 'fluctuation' theory is based on first-principles equations of motion rather than phenomenological ones.

[20] Naively, one may justify this by a hierarchy of space–time scales in fully developed MHD turbulence; however, the advection of small-scale Alfvénic wave packets by large-scale motions (an analogue of sweeping in non-MHD turbulence) complicates a purely Eulerian time-scale separation. Therefore, a separation of time scales is more consistently discussed employing quasi-Lagrangian variables or filtered equations [79, 239–241].

i.e., by passing to a frame comoving with the fluid and taking $\boldsymbol{v}$ as the dynamical variable. This highlights the difference between the SFT formulation, aimed at describing the turbulent state itself, and most turbulence models targeting concrete systems, where $\boldsymbol{U}_0$ is a spatially varying background and the dynamics hinges on its interaction with $\boldsymbol{v}$.[21] A key MHD distinction from the purely hydrodynamic case is that a uniform mean magnetic field $\boldsymbol{B}_0$ (unlike $\boldsymbol{U}_0$) cannot be eliminated by a Galilean transformation and instead sets a preferred direction, affecting spectral transfer and anisotropy [158]. In section 4.5 we set $\langle \boldsymbol{B} \rangle = \boldsymbol{0}$ and consider an isotropic model (as in early Iroshnikov–Kraichnan phenomenology) [79, 242], and in section 4.6 we take $\langle \boldsymbol{B} \rangle = \boldsymbol{B}_0$ and discuss the consequences of anisotropy.

As in hydrodynamics, turbulent MHD displays cascade transfer and scaling regimes, including an inertial range. In strongly developed MHD turbulence [13, 79, 170], one distinguishes: (i) an outer (energy-containing) scale $l_{\max}$ where energy is injected; (ii) an inertial interval $l_{\min} \ll \ell \ll l_{\max}$ where dissipation is negligible and transfer is governed by nonlinearity; and (iii) dissipative scales, l_{ν_0} and $l_{\nu_{\mathrm{m}0}}$, associated with viscous and ohmic damping, with $l_{\min} = \max(l_{\nu_0}, l_{\nu_{\mathrm{m}0}})$. The relevant time scales are the nonlinear time $\tau_{\mathrm{nl}} = \ell_\perp / v$ and the Alfvén time $\tau_A = \ell_\parallel / u_A$; their ratio controls the transition between wave (weak) and strong regimes and underlies the anisotropic cascade picture (critical balance) [170].

In practice, turbulent MHD fluctuations and their correlations are often measured by single-point techniques (e.g., a spacecraft in the solar wind), yielding one-dimensional frequency or wavenumber spectra $E(f)$ or $E(k)$. In this setting, one commonly invokes Taylor's hypothesis [13, 92, 93, 243], which relates temporal measurements at a fixed point to the spatial structure of the field by assuming that turbulent inhomogeneities 'evolve only weakly' while being advected past the sensor by the mean flow. Operationally, this implies that the measured frequency in the laboratory/spacecraft frame is related to the wavenumber in a nearly kinematic manner (see, e.g., [244]). For a sensor along the mean flow, one has $k \approx \omega / U_0 = 2\pi f / U_0$, where f is the measured frequency. At the level of theory, this amounts to postulating that for a constant $\boldsymbol{U}_0$, one approximates $\boldsymbol{v}(\boldsymbol{x} - \boldsymbol{U}_0 t, t) \approx \boldsymbol{v}(\boldsymbol{x} - \boldsymbol{U}_0 t, 0)$ and $\boldsymbol{b}(\boldsymbol{x} - \boldsymbol{U}_0 t, t) \approx \boldsymbol{b}(\boldsymbol{x} - \boldsymbol{U}_0 t, 0)$, which relates Eulerian time correlators to the corresponding static ones. In particular, $\langle \boldsymbol{v}(\boldsymbol{x}, t) \otimes \boldsymbol{v}(\boldsymbol{x} - \boldsymbol{U}_0 \Delta t, t) \rangle \approx \mathbf{D}^v_{\mathrm{st}}(\boldsymbol{U}_0 \Delta t)$, where $\mathbf{D}^v_{\mathrm{st}}(\boldsymbol{x})$ denotes the corresponding static correlator. Nevertheless, in the MHD context, the Taylor hypothesis involves additional features worth highlighting. The single-point measurements record $\omega(\boldsymbol{k}) = \omega_0(\boldsymbol{k}) + \boldsymbol{k} \cdot \boldsymbol{U}_0$, where ω_0 includes intrinsic wave and nonlinear contributions. The key contributions to it come from Alfvén waves $\omega_A \sim \pm \boldsymbol{k} \cdot \boldsymbol{u}_A$ and from the inverse nonlinear decorrelation (packet reorganization) time $\omega_{\mathrm{nl}} \sim \tau_{\mathrm{nl}}^{-1}$. Thus, Taylor's hypothesis in MHD requires $|(\boldsymbol{k} \cdot \boldsymbol{U}_0)| \gg \max\{\boldsymbol{k} \cdot \boldsymbol{u}_A, \tau_{\mathrm{nl}}^{-1}\}$. Empirically, it often holds in the inertial range of super-Alfvénic flows (e.g., the solar wind near 1 AU) and in many liquid-metal experiments. In contrast, it may fail when the geometry enforces predominantly $\boldsymbol{k} \perp \boldsymbol{U}_0$ (e.g., in tokamaks or stellarators). Finally, it is important to bear in mind that Taylor's hypothesis is tied to the assumption of a constant advection velocity $\boldsymbol{U}_0$. A more accurate modern interpretation is that Taylor's hypothesis represents a 'deterministic' limiting case of sweeping: small-scale structures are transported by a constant $\boldsymbol{U}_0$, whereas the sweeping effect corresponds to the more general and realistic situation in which small scales are advected by a random/fluctuating large-scale velocity $\boldsymbol{U}_0(\boldsymbol{x}, t)$, so that Eulerian (single-point) temporal correlations decay rapidly even if the small-scale structures themselves do not have time to evolve appreciably (see, e.g., [245]).

[21] For instance, in pipe and channel turbulence the main source of turbulent-energy production is $\boldsymbol{\nabla} \otimes \boldsymbol{U}_0$, whereas in our formulation this role is played by the random forcing.

3.2. Stochasticisation: effective equations for stationary fully developed turbulence

After transforming to the comoving coordinates $(\boldsymbol{x}, t) \to (\boldsymbol{x} + \boldsymbol{U}_0 t, t)$, we are left with the final key step: the stochasticisation of Eqs. (4)–(5). Within the SFT approach, this is implemented by introducing artificial random forces $\boldsymbol{f}^v$ and $\boldsymbol{f}^b$ with zero mean[22] and translationally invariant statistics, chosen to ensure a statistically stationary regime in an infinite domain. Of course, real media contain various sources of randomness (thermal fluctuations, microscopic noise, boundary imperfections, etc.). Here, however, $\boldsymbol{f}^v$ and $\boldsymbol{f}^b$ should be viewed as a model of large-scale energy injection: if the forcing is concentrated at the largest scales, smaller scales are fed predominantly by the cascade rather than directly from the work of forces $\boldsymbol{f}^v$ and $\boldsymbol{f}^b$, so inertial-range statistics are expected to depend only weakly on forcing details (a manifestation of universality of fully developed turbulence). For theory, stochastic forcing is also preferable to a deterministic, setup-specific drive (as in DNS), since it imposes minimal additional large-scale structure and reduces the risk of model-dependent artefacts in the fluctuation statistics. Finally, Gaussian forcing is largely a choice of convenience: it simplifies the SFT construction and, being the maximum-entropy distribution among all with fixed second moment, introduces no additional assumptions in the higher cumulants. The statistical distributions of the fields $\boldsymbol{v}$ and $\boldsymbol{b}$ of primary interest are then chiefly shaped by nonlinear dynamics and, in the stationary regime, are expected (within the inertial range) to be only weakly sensitive to the forcing, provided injection occurs at large scales, and the basic symmetries are respected.

However, it is important to emphasize that in standard stochastic MHD with additive Gaussian forcing, the forcing terms are taken to be statistically independent of $\boldsymbol{u}$ and $\boldsymbol{b}$ and are therefore not equivalent to prescribing initial or boundary conditions.[23] They play only an analogous role: they fix the statistical injection rates of energy and helicities and thereby ensure the existence of a stationary invariant measure on the space of field configurations. In this respect, they are closer to a thermostat/reservoir (or 'pump') than to a 'stirrer' that generates turbulence via specific initial and boundary conditions. Consequently, although stochastic MHD defines the full non-stationary evolution of the random process $(\boldsymbol{u}(\boldsymbol{x}, t), \boldsymbol{b}(\boldsymbol{x}, t))$, it need not provide a physically faithful model of the route to turbulence, nor does it necessarily describe particular linear or nonlinear instabilities, their saturation, mode excitation, and related transition dynamics. Its domain of applicability is therefore restricted primarily to the statistics of fully developed turbulence, as encoded by the corresponding stationary measure. This observation, in turn, implies that the stochastic MHD equations need not, in general, coincide term by term with the original deterministic equations (4) and (5) and may contain additional terms that were absent from the original deterministic equations but have evolved before achieving a stationary turbulent state (e.g. were generated in the course of coarse-graining or RG transformation) and must be included in the effective description model. For most models, this remark is essentially routine: all terms permitted by the symmetries and relevant in the infrared (recall that, in RG language, developed turbulence corresponds to a critical IR regime) are already present in the bare equations, and the transition to turbulence amounts to renormalizing the corresponding coefficients. Helical MHD is an exception: in this case, a pseudoscalar contribution linear in momentum is allowed in the induction equation, which in mean-field language leads to α-type terms. This is discussed in more detail in section 4.3.

[22] The imposed condition $\langle \boldsymbol{f}^v \rangle = \langle \boldsymbol{f}^b \rangle = \boldsymbol{0}$ precludes systematic (large-scale) acceleration, is consistent with translational invariance, and by itself does not select a preferred direction.

[23] Recall that for linear problems, under fairly general assumptions, inhomogeneous initial and boundary conditions can be recast as an effective source term in the equation.

3.3. The model: equations of stochastic helical magnetohydrodynamics and forcing

Finally, the canonical nonrelativistic, resistive, three-dimensional stochastic MHD equations for a homogeneous incompressible fluid read

$$\mathrm{D}_t \boldsymbol{v} = \nu_0 \Delta \boldsymbol{v} + (\boldsymbol{b}\cdot\boldsymbol{\nabla})\boldsymbol{b} - \boldsymbol{\nabla}\big(p + \boldsymbol{b}^2/2\big) + \boldsymbol{f}^v, \tag{12}$$

$$\mathrm{D}_t \boldsymbol{b} = \nu_{\mathrm{m}0} \Delta \boldsymbol{b} + (\boldsymbol{b}\cdot\boldsymbol{\nabla})\boldsymbol{v} + \boldsymbol{f}^b, \tag{13}$$

$$\boldsymbol{\nabla}\cdot\boldsymbol{v} = 0, \qquad \boldsymbol{\nabla}\cdot\boldsymbol{b} = 0, \qquad \boldsymbol{\nabla}\cdot\boldsymbol{f}^v = 0, \qquad \boldsymbol{\nabla}\cdot\boldsymbol{f}^b = 0. \tag{14}$$

Here $\boldsymbol{v}(\boldsymbol{x},t)$ and $\boldsymbol{b}(\boldsymbol{x},t) = \boldsymbol{B}(\boldsymbol{x},t)/(4\pi\rho_0)^{1/2}$ are the fluctuating velocity and magnetic-induction fields (with $\boldsymbol{b}$ in Alfvénic units), while $\rho_0 p$, $\rho_0 \boldsymbol{f}^v$, and $\rho_0 \boldsymbol{f}^b$ denote the pressure and external random forces sustaining turbulence. We also parameterise $\nu_{\mathrm{m}0} = \nu_0 u_0$ via the inverse magnetic Prandtl number $u_0 \coloneqq \mathrm{Pr}_m^{-1}$.

In the conventional SFT setting, the system (12)–(14) is supplemented by vanishing boundary and asymptotic initial conditions in the whole space,

$$\lim_{\|\boldsymbol{x}\|\to\infty} \boldsymbol{v}(\boldsymbol{x},t) = \boldsymbol{0}, \qquad \lim_{\|\boldsymbol{x}\|\to\infty} \boldsymbol{b}(\boldsymbol{x},t) = \boldsymbol{0}, \qquad \lim_{t\to-\infty} \boldsymbol{v}(\boldsymbol{x},t) = \boldsymbol{0}, \qquad \lim_{t\to-\infty} \boldsymbol{b}(\boldsymbol{x},t) = \boldsymbol{0}. \tag{15}$$

For the magnetic field, these conditions are far from obvious (unlike for the velocity field $\boldsymbol{v}$) and amount to assuming the absence of an imposed mean/external field; we shall relax this assumption below. In general, the outer scale of the inertial range is set by the system size and by the inhomogeneity scale of the forcing. In an unbounded domain without deterministic forces, one may formally envisage stationary turbulence with an inertial range extending to arbitrarily large scales (at the cost of an infinite mean energy density).

The force densities $\boldsymbol{f}^v(\boldsymbol{x},t)$ and $\boldsymbol{f}^b(\boldsymbol{x},t)$ are considered stationary (in the broad sense) random processes and are conventionally taken to be Gaussian random fields with zero mean (otherwise the mean flow u_0 would accelerate in time and stationary turbulence in infinite space would be impossible), with correlator[24]

$$\mathfrak{D}_{ij}^{\alpha\beta}(\boldsymbol{x}-\boldsymbol{x}',t-t') \coloneqq \langle f_i^\alpha(\boldsymbol{x},t) f_j^\beta(\boldsymbol{x}',t')\rangle_f = \delta(t-t') \int \frac{\mathrm{d}^d k}{(2\pi)^d}\, \mathbb{D}_{ij}^{\alpha\beta}(\boldsymbol{k})\, \mathrm{e}^{i\boldsymbol{k}\cdot(\boldsymbol{x}-\boldsymbol{x}')}, \tag{16}$$

where $\mathbb{D}_{ij}^{\alpha\beta}(\boldsymbol{k})$ are the pumping kernels specified below, $\alpha,\beta \in \{v,b\}$, and $\langle\bullet\rangle_f$ denotes averaging over the forcing statistics. Besides stationarity, the temporal white-noise $\delta(t-t')$ amounts to a Markov approximation, compatible with Galilean invariance and convenient for ϵ-expansions; non-Markovian (coloured) forcing can also be considered (see Refs. cited in section 1).

Due to (16), Eqs. (12)–(14) are translation-invariant, all moments of the resulting stationary measure inherit translation invariance. This contrasts with the Cauchy problem, where translation invariance is recovered only in the large-time asymptotic limit $t \to \infty$ once the system has effectively forgotten finite-time initial data. Under conditions (15), the state is determined by the long-time balance and is independent of any initial data prescribed at a finite time.

Technically, the RG treatment imposes additional constraints on the force correlator $\mathfrak{D}_{ij}^{\alpha\beta}$ such as a power-law behaviour of $\mathbb{D}_{ij}(\boldsymbol{k})$ as $|\boldsymbol{k}| \to 0$. In the SFT formulation the kernels $\mathbb{D}_{ij}(\boldsymbol{k})$ enter the Gaussian part of the action (see Sec. 4.1), and a scaling regime with dilatational symmetry can exist only if the leading terms in the action are homogeneous in $|\boldsymbol{k}| \to 0$; otherwise no closed self-similar asymptotics emerges.

[24]Since the Navier–Stokes equation has no genuine static limit, the force correlator is not uniquely fixed (unlike in critical-dynamics models [3]) and is therefore a part of the model of turbulence definition.

In this article, we focus on forced MHD turbulence in a helical medium. Helicity explicitly breaks mirror symmetry, so that the relevant symmetry group is $\mathbf{SO}(3) \simeq \mathbf{O}(3)/\mathbf{Z}_2$ rather than the full $\mathbf{O}(3)$ (in the discussion below, we restrict ourselves to $d = 3$).[25] In the full space, wall-free formulation, we take 'mirror reflection' to mean the complete inversion $P : \boldsymbol{x} \to -\boldsymbol{x}$ (the central element of $\mathbf{O}(3)$).

With all this in mind, we choose the simplest power-law pumping kernel 2×2 matrix $\mathbf{D}_{ij}(\boldsymbol{k}) \coloneqq \left[\mathbb{D}_{ij}^{\alpha\beta}(\boldsymbol{k})\right]$, $\alpha, \beta \in \{v, b\}$ as

$$\mathbf{D}_{ij}(\boldsymbol{k}) = \nu_0^3 k^{4-d} \begin{pmatrix} g_{01}\, k^{-2\epsilon}\, \mathbb{R}_{ij}^{(1)}(\boldsymbol{k}) & g_{03}\, k^{-\epsilon-a\epsilon}\, \mathbb{R}_{ij}^{(3)}(\boldsymbol{k}) \\ g_{03}\, k^{-\epsilon-a\epsilon}\, \mathbb{R}_{ij}^{(3)}(\boldsymbol{k}) & g_{02}\, k^{-2a\epsilon}\, \mathbb{R}_{ij}^{(2)}(\boldsymbol{k}) \end{pmatrix} \theta(\Lambda - k)\theta(k - m), \tag{17}$$

where $\theta(x)$ is the Heaviside step function, $k \coloneqq |\boldsymbol{k}|$, $\epsilon > 0$ is the analytic ('ϵ') regularization parameter (see Sec. 4.4), and $a > 0$ is a free model parameter. The bare couplings g_{0i} ($i = 1, 2, 3$) are constrained by the positive definiteness of the covariance matrix: $g_{01}, g_{02} \geq 0$, and $g_{01}g_{02} \geq g_{03}^2$. The specific a -dependence in (17) is chosen so that the interactions generated by the correlators $\mathfrak{D}^{vv}$, $\mathfrak{D}^{vb}$, and $\mathfrak{D}^{bb}$ become simultaneously logarithmic at $\epsilon = 0$; otherwise some contributions would be IR-irrelevant and could be consistently discarded [246, 247]. The θ-functions implement the UV and IR cutoffs and define the inertial range $m \ll k \ll \Lambda$ introduced above, with $m = l_{\mathrm{max}}^{-1}$, $k = \ell^{-1}$, and $\Lambda = l_{\mathrm{min}}^{-1}$. This sharp-cutoff regularization is convenient for multiloop calculations: in any Feynman diagram, the number of lines carrying $\mathbb{D}_{ij}^{\alpha\beta}(\boldsymbol{k})$ equals the number of loops. Unlike typical UV regularizations in relativistic field theory, these cutoffs do not violate the global symmetries of the model.

A power-law pumping $\sim k^{4-d-2\epsilon}$ in (17) is meaningful for $0 \leqslant \epsilon \leqslant 2$, with the physical value $\epsilon = 2$ corresponding to δ-like pumping function (after $m \to 0$ and $\Lambda \to \infty$). Since the (generically direct) MHD energy cascade requires IR pumping, it is natural to demand that at $\epsilon = 2$ the scalar kernels in $\mathbb{D}_{ij}^{bb}(\boldsymbol{k})$ and $\mathbb{D}_{ij}^{vb}(\boldsymbol{k})$ also reduce to δ-type IR forcing (from infinitely large-scale); within the simple ansatz (17) this is possible only for $a = 1$. Thus, for the present power-law model, the natural 'physical' choice is $\epsilon = 2$ and $a = 1$. More general constructions are possible, e.g., $\mathbb{D}_{ij}^{\alpha\beta}(\boldsymbol{k}) = k^{4-d-2f_{\alpha\beta}(a)\epsilon} H_{ij}^{\alpha\beta}(m/k)$, with $H_{ij}^{\alpha\beta}(0) = 1$, for which sufficiently large ϵ yields IR pumping for any $f_{\alpha\beta}(a) > 0$. To our knowledge, however, such generalized kernels have not been explored in stochastic MHD. For further details regarding the ϵ-expansion in turbulent models, see Refs. [1–3, 107, 108].

The tensor structures $\mathbb{R}_{ij}^{(n)}(\boldsymbol{k})$ in solenoidal MHD are the most general mixtures of the transverse projector $\mathbb{P}_{ij}(\boldsymbol{k}) \coloneqq \delta_{ij} - k_i k_j/k^2$ (the Leray projector $\mathbb{P}$ in Fourier space) and the helical pseudotensor $\mathbb{H}_{ij}(\boldsymbol{k}) \coloneqq i\,\varepsilon_{ijm}k_m/k$:

$$\mathbb{R}_{ij}^{(1,2)}(\boldsymbol{k}) = \mathbb{P}_{ij}(\boldsymbol{k}) + \rho_{1,2}\,\mathbb{H}_{ij}(\boldsymbol{k}), \qquad \mathbb{R}_{ij}^{(3)}(\boldsymbol{k}) = \mathbb{H}_{ij}(\boldsymbol{k}) + \rho_3\,\mathbb{P}_{ij}(\boldsymbol{k}). \tag{18}$$

where ε_{ijm} is the Levi–Civita symbol and the dimensionless parameters $\rho_{1,2,3}$ quantify parity breaking in the corresponding 'channels', due to the fact that in helical MHD, three independent characteristic pseudoscalars can be non-zero, and each of them defines, generally speaking, a specific measure of parity breaking. Positive definiteness of the covariance kernel (17) immediately yields $|\rho_{1,2,3}| \leq 1$ (often attributed to Bochner's theorem [178]). For simplicity, one may

[25] This means that any solenoidal vector field can be expanded in the helical basis, $\boldsymbol{f}(\boldsymbol{k}, t) = f^{+}(\boldsymbol{k}, t)\boldsymbol{h}^{+}(\boldsymbol{k}) + f^{-}(\boldsymbol{k}, t)\boldsymbol{h}^{-}(\boldsymbol{k})$, which diagonalizes tensors such as $\mathfrak{D}_{ij}^{\alpha\beta}$. Here $\boldsymbol{h}^{\pm}(\boldsymbol{k})$ are transverse eigenvectors of the operator $\boldsymbol{\nabla}\times$ in the $\boldsymbol{k}$-space, $i\boldsymbol{k} \times \boldsymbol{h}^{\pm} = \pm k\,\boldsymbol{h}^{\pm}$, with $\boldsymbol{h}^{\pm} \cdot \boldsymbol{k} = 0$ and $\boldsymbol{h}^{s} \cdot \boldsymbol{h}^{s'\,*} = \delta_{ss'}$, and may be chosen as $\boldsymbol{h}^{\pm} = (\boldsymbol{e}_1 \pm i\boldsymbol{e}_2)/\sqrt{2}$ for any $\boldsymbol{k} \neq \boldsymbol{0}$, where $\boldsymbol{e}_{1,2}$ are orthonormal unit vectors transverse to $\boldsymbol{k}$. We shall not use this decomposition explicitly, but only note its existence.

set $\rho_1 = \rho_2 = \rho_3 := \rho$. Assuming no additional dynamical suppression or spontaneous parity breaking, they may be estimated from observed steady-state correlators as

$$\rho_1 \simeq \frac{|\langle \boldsymbol{v}\cdot(\boldsymbol{\nabla}\times\boldsymbol{v})\rangle|}{\sqrt{\langle \boldsymbol{v}^2\rangle\langle(\boldsymbol{\nabla}\times\boldsymbol{v})^2\rangle}}, \qquad \rho_2 \simeq \frac{|\langle \boldsymbol{b}\cdot(\boldsymbol{\nabla}\times\boldsymbol{b})\rangle|}{\sqrt{\langle \boldsymbol{b}^2\rangle\langle(\boldsymbol{\nabla}\times\boldsymbol{b})^2\rangle}}, \qquad \rho_3 \simeq \frac{|\langle \boldsymbol{v}\cdot\boldsymbol{b}\rangle|}{\sqrt{\langle \boldsymbol{v}^2\rangle\langle\boldsymbol{b}^2\rangle}}. \tag{19}$$

3.4. Steady turbulent state: energy budget in stochastic MHD

As already noted, the only essential requirement on the random forces $\boldsymbol{f}^v$ and $\boldsymbol{f}^b$ is that their work compensates viscous and ohmic dissipation. This requirement is conveniently expressed by the exact energy-balance identities, obtained directly from Eqs. (12)–(14) as equalities between composite fields:

$$\begin{aligned} \partial_t(v^2/2) + \boldsymbol{\nabla}\cdot\big(\boldsymbol{v}(v^2/2+p) - \boldsymbol{b}(\boldsymbol{v}\cdot\boldsymbol{b})\big) &= -\boldsymbol{b}\cdot(\boldsymbol{b}\cdot\boldsymbol{\nabla})\boldsymbol{v} - \nu_0\boldsymbol{v}\cdot\Delta\boldsymbol{v} + \boldsymbol{v}\cdot\boldsymbol{f}^v, \\ \partial_t(b^2/2) + \boldsymbol{\nabla}\cdot\big(\boldsymbol{v}b^2/2\big) &= \boldsymbol{b}\cdot(\boldsymbol{b}\cdot\boldsymbol{\nabla})\boldsymbol{v} - \nu_{\mathrm{m}0}\boldsymbol{b}\cdot\Delta\boldsymbol{b} + \boldsymbol{b}\cdot\boldsymbol{f}^b. \end{aligned} \tag{20}$$

Note that (20) involve no averaging: they hold pointwise as identities for the composite fields (random variables) themselves.

Summing Eqs. (20) and averaging with $\langle\bullet\rangle_f$, the divergence (transfer) terms vanish by translation invariance, yielding the integral energy balance

$$E_{\mathrm{diss}} := \big\langle E_{\mathrm{diss}}^{[\nu_0]}\big\rangle_f + \big\langle E_{\mathrm{diss}}^{[\nu_{\mathrm{m}0}]}\big\rangle_f = E_{\mathrm{in}} := \frac{1}{2}\int \frac{\mathrm{d}^d k}{(2\pi)^d}\Big(\mathbb{D}^{vv}_{ii}(\boldsymbol{k}) + \mathbb{D}^{bb}_{ii}(\boldsymbol{k}) + 2\mathbb{D}^{vb}_{ii}(\boldsymbol{k})\Big), \tag{21}$$

where $E_{\mathrm{diss}}^{[\nu_0]} := \nu_0\big((\boldsymbol{\nabla}\otimes\boldsymbol{u}) + (\boldsymbol{\nabla}\otimes\boldsymbol{u})^{\mathrm{T}}\big)^2/2$ and $E_{\mathrm{diss}}^{[\nu_{\mathrm{m}0}]} := \nu_{\mathrm{m}0}\big((\boldsymbol{\nabla}\otimes\boldsymbol{b}) + (\boldsymbol{\nabla}\otimes\boldsymbol{b})^{\mathrm{T}}\big)^2/2$ denote the viscous and ohmic dissipation rates, respectively, and E_{in} is the mean injected power compensating dissipation. The forcing contributions $\langle\boldsymbol{v}\cdot\boldsymbol{f}^v\rangle_f$ and $\langle\boldsymbol{b}\cdot\boldsymbol{f}^b\rangle_f$ are rewritten using Furutsu–Novikov identities [248, 249], e.g.,

$$\langle v_i(\boldsymbol{x},t) f_j^v(\boldsymbol{x},t)\rangle_f = \int \mathrm{d}^d x'\mathrm{d}t'\, \mathfrak{D}^{v\beta}_{il}(\boldsymbol{x}-\boldsymbol{x}', t-t')\left\langle \frac{\delta v_j(\boldsymbol{x},t)}{\delta f_l^\beta(\boldsymbol{x}',t')}\right\rangle_f = \frac{1}{2}\sum_{\beta=v,b}\int \frac{\mathrm{d}^d k}{(2\pi)^d}\,\mathbb{D}^{v\beta}_{ij}(\boldsymbol{k}), \tag{22}$$

where the second equality follows from the symmetric extension of the definition of the response function at coincide times, $\langle\delta v_j(\boldsymbol{x},t)/\delta f_l^v(\boldsymbol{x}',t')\rangle_f\big|_{t\to t'-} = \delta_{jl}\,\delta(\boldsymbol{x}-\boldsymbol{x}')/2$, which is equivalent to the prescription $\theta(0) = 1/2$, i.e., to the use of the Stratonovich stochastic calculus.[26] While equations like (20) are often discussed for decaying turbulence or within closures such as EDQNM (see, e.g., [79]) and with specific model of force correlator, it is worth noting that for ordinary turbulence the work [250] reconstructed an effective 'physical' injection function in the pumping and inertial ranges; extending this idea to MHD remains a matter for the future.

Unlike the single-forcing case, in the general setting, the couplings g_{0i} are related to the total injection E_{in} in a more complicated way. At the leading order as $\Lambda/m \to \infty$, we have

$$E_{\mathrm{in}} \sim \frac{\nu_0^3}{C_d}\left(\frac{\Lambda^{\beta_{\mathrm{UV}}}}{\beta_{\mathrm{UV}}}\sum_{\beta_i=\beta_{\mathrm{UV}}} g_{0i} + \left(\sum_{\beta_i=0} g_{0i}\right)\ln\frac{\Lambda}{m} + \frac{m^{-|\beta_{\mathrm{IR}}|}}{|\beta_{\mathrm{IR}}|}\sum_{\beta_i=\beta_{\mathrm{IR}}} g_{0i}\right), \tag{23}$$

where $C_d := 2(2\pi)^d/[S_d(d-1)]$ (with S_d was defined above, see the discussion following Eq. (6) and then for physically realistic case we get $C_3 = 2\pi^2$) and

$$\beta_1 := 4-2\epsilon, \quad \beta_2 := 4-2a\epsilon, \quad \beta_3 := 4-(1+a)\epsilon, \quad \beta_{\mathrm{UV}} := \max_i\{\beta_i>0\}, \quad \beta_{\mathrm{IR}} := \min_i\{\beta_i<0\}.$$

[26] This is justified, since in deriving (20) we used classical differentiation according to the Leibniz rule.

For the present power-law forcing, we treat Eq. (23) as applicable up to $\epsilon = 2$, i.e., as an interpolation that allows different components of the pumping matrix to be dominated either by the infrared ($k \sim m$) or by the ultraviolet ($k \sim \Lambda$) end of the inertial interval, depending on their scaling exponents. In the simplest kinetic forcing model (no magnetic noise), where the only nonzero correlator is $\mathfrak{D}_{ij}^{vv}$, Eq. (23) reduces to

$$g_{01}\nu_0^3 \sim C_d E_{\rm in} \times \begin{cases} (2-\epsilon)\Lambda^{2\epsilon-4}, & 0 \leqslant \epsilon < 2, \\ 1/\ln(\Lambda/m), & \epsilon = 2, \\ (\epsilon-2)m^{2\epsilon-4}, & \epsilon > 2. \end{cases} \tag{24}$$

4. Statistical field theory approach in MHD turbulence

Before turning to the details of the SFT-based treatment of Eqs. (12)–(14), let us briefly recall how turbulent MHD has been studied by renormalization-group methods and, more generally, within the statistical field-theoretic framework. To the best of our knowledge, one of the earliest Wilson-style RG analyses of turbulent MHD was performed in [246] for the mirror-symmetric case. A more systematic field-theoretic formulation of the same problem was subsequently developed in [247]. In particular, it was shown that, in the isotropic setting, two infrared-stable fixed points exist — the so-called kinetic and magnetic fixed points. The former leads to Kolmogorov-type spectra. At the magnetic fixed point, the scaling is generally nonuniversal (in the sense that not all Green's functions possess well-defined critical dimensions).

Later, [251] addressed helical ('gyrotropic' in their terminology) MHD in the absence of magnetic noise. The key observation is that breaking mirror symmetry — even without magnetic fluctuations — makes the linearized MHD equations unstable; this effect, first identified in [252], can lead to the emergence of a large-scale homogeneous magnetic field. This field can, in principle, stabilize the system in its new 'vacuum state' through a dynamical, spontaneous breaking of three-dimensional rotational symmetry (the Coleman–Weinberg mechanism [253]), thereby bringing the system to a state equivalent to that produced by the dynamo mechanism. From a technical viewpoint, the instability generates new polynomially divergent tensor counterterms, analogous to mass renormalization in the $\mathbf{O}(n)$-symmetric φ^4 theory. These counterterms already arise at the one-loop level in the course of UV renormalization and can be removed by a suitably chosen shift of the magnetic field. Furthermore, [251] demonstrated that, in this dynamo regime, the Kolmogorov spectrum applies only to the velocity–velocity correlator. At the same time, the magnetic-field correlator acquires a different spectral slope, which essentially signals a fundamental violation of energy equipartition.

Subsequently, the RG methodology was extended to other models of magnetohydrodynamic turbulence, including the well-known Kraichnan–Kazantsev kinematic model [177, 254–258], the kinematic MHD model [259–261], as well as a broad class of advection–diffusion models that are MHD-like to varying degrees and involve different types of admixtures, such as passive scalar impurities [262, 263], magnetic impurities [264], and vector impurities [265–268]. Here, the Kraichnan–Kazantsev model is understood as a kinematic dynamo problem in which the magnetic field evolves according to the induction equation but is advected and stretched by a prescribed random velocity field, most commonly taken to be Gaussian, homogeneous and isotropic, with a scale-invariant spatial correlator and δ-correlation in time (the Kraichnan 'rapid-change' ensemble). The kinematic MHD model relaxes this idealization by letting the velocity be determined self-consistently (e.g., by a stochastic Navier–Stokes dynamics) while still neglecting the Lorentz-force back-reaction, so that the magnetic field remains a passive

(though stretched) vector admixture [269–272]. Advection–diffusion models further generalize the setting by replacing the magnetic field with a scalar or vector impurity transported by the flow: in passive variants, it does not affect the velocity statistics, whereas in active cases it feeds back on the flow through additional stresses or forces, with full MHD being the archetypal coupled active vector system. Within the RG/SFT approach, these simplified models serve as controlled laboratories for identifying IR scaling regimes and universality classes, as well as for analyzing anomalous scaling and intermittency via the renormalization of composite operators. For a review on these topics, see, e.g., [113, 273] and the references therein.

It is also worth mentioning the paradigmatic A-model (not to be confused with the standard Hohenberg–Halperin notation [150] for models of critical dynamics mentioned in Sec. 1) of an active vector impurity, of which helical MHD constitutes a particular case. Over the last two decades, the sustained efforts of the group of authors cited above have improved the precision of computations in this model to two loops [152].

4.1. General: functional representation of stochastic differential equations

In what follows, our main mathematical object is a class of stochastic evolution equations. Such equations arise routinely in statistical physics and related areas [274]. Since the seminal works [25, 275], it has been understood that their perturbation theory can be recast in a convenient field-theoretic form (see also [3, 22, 276] for reviews and further details). Below, we summarize the main steps of this construction.

We consider a broad class of semilinear stochastic partial differential equations (SPDEs) with additive Gaussian noise, written in differential Itô form as

$$\mathrm{d}\varphi_i(\boldsymbol{x},t) = \Big[(L\varphi)_i(\boldsymbol{x},t) + n_i(\boldsymbol{x},t;\varphi) + A_i^{\varphi'}(\boldsymbol{x},t)\Big]\,\mathrm{d}t + \sigma_{ij}(\boldsymbol{x})\,\mathrm{d}W_{t,j}, \qquad i,j = 1,\dots,N. \quad (25)$$

Here $\varphi_i(\boldsymbol{x},t)$ is a random field; in many SPDE settings, one works with $\varphi_i(\boldsymbol{x},t)$ taking values in a space of distributions, e.g. $\mathcal{D}'(\mathbb{R}^d)$, or in a suitable Sobolev space. The operator L is assumed to generate a strongly continuous semigroup e^{tL} on an appropriate Banach (or Hilbert) space; a standard dissipative example is $L = \nu_0\Delta$. The processes $\{W_{t,j}\}$ are independent one-dimensional Wiener processes (equivalently, components of a cylindrical Wiener process), and σ is independent of φ (additive noise). The nonlinearity $n_i(\boldsymbol{x},t;\varphi)$ contains no time derivatives and is assumed local in time. Finally, $A_i^{\varphi'}(\boldsymbol{x},t)$ is a deterministic forcing (probe) field introduced to generate response functions; its role will become explicit below. We restrict ourselves to additive noise, i.e. σ does not depend on φ; in this case, there is no Itô–Stratonovich correction, and the two interpretations yield indistinguishable solutions.

In the SPDE literature, (25) is typically posed as a Cauchy problem with initial data at some finite time t_0, $\varphi(\boldsymbol{x},t_0) = \varphi_0(\boldsymbol{x})$. In many stationary settings it is convenient to use the equivalent prescription obtained by sending $t_0 \to -\infty$ and imposing suitable asymptotic/boundary conditions (e.g. decay as $t \to -\infty$ and $|\boldsymbol{x}| \to \infty$ for fixed t).[27] More precisely, if the dynamics admits an invariant (stationary) measure, then taking φ_0 distributed according to this measure makes the Cauchy formulation equivalent to the $t_0 \to -\infty$ prescription at the level of finite-dimensional distributions.

Under standard assumptions, equation (25) can be written as

$$\varphi_i(\boldsymbol{x},t) = \int_{-\infty}^{t} \mathrm{d}\tau\, \big[e^{(t-\tau)L}\big(A^{\varphi'}(\cdot\,,\tau) + n(\cdot\,,\tau;\varphi)\big)\big]_i(\boldsymbol{x}) + \int_{-\infty}^{t} \big[e^{(t-\tau)L}\sigma\big]_{ij}(\boldsymbol{x})\,\mathrm{d}W_{\tau,j}. \quad (26)$$

[27] In the MSRJD representation, a finite-time initial condition is encoded by an additional boundary weight in the action. If this contribution is omitted, the resulting functional may break the supersymmetry/BRST-type structure of the bulk MSRJD action; see [16] for a detailed discussion.

Equation (26) is the standard variation-of-constants (Duhamel) representation of a mild solution of (25). Under standard assumptions on L, n, and σ (e.g. L generates a C_0-semigroup and n is locally Lipschitz with suitable growth bounds), one obtains existence and uniqueness of a (local or global) mild solution; see, e.g., [277, 278]. The deterministic integral is a Bochner (Lebesgue) integral in the chosen Banach/Hilbert space, while the stochastic term is an Itô integral. Depending on the additional regularity of L, n, and the noise, mild solutions can be upgraded to strong (or more regular) solutions. For instance, the three-dimensional stochastic Navier–Stokes equation admits global martingale solutions and (under additional assumptions) local strong solutions; see [278] and references therein.

For diagrammatic constructions, it is customary to pass to a shorthand 'physical' notation by introducing the formal white noise $\eta_i(\boldsymbol{x},t) \coloneqq \sigma_{ij}(\boldsymbol{x})\,\mathrm{d}W_{t,j}/\mathrm{d}t$ understood as a generalized (distributional) time derivative of W_t. In this notation (25) becomes

$$\partial_t\varphi(x) = L\varphi(x) + n(x;\varphi) + A^{\varphi'}(x) + \eta(x), \tag{27}$$

where $\varphi(x) \coloneqq \{\varphi_i(x)\}$ and $x \coloneqq (\boldsymbol{x},t)$. Similarly, $\eta(x) \coloneqq \{\eta_i(x)\}$, $n(x;\varphi) \coloneqq \{n_i(x;\varphi)\}$, and $A^{\varphi'}(x) \coloneqq \{A_i^{\varphi'}(x)\}$. We reserve the term 'source' for the non-random probe fields A^{φ} and $A^{\varphi'}$ introduced below; η will be referred to as the (random) noise or random forcing. By construction, η is a centered Gaussian generalized random field, white in time, with covariance

$$\langle\eta_i(x)\rangle = 0, \qquad \langle\eta_i(x)\eta_j(x')\rangle = \delta(t-t')\,\mathrm{D}_{ij}(\boldsymbol{x},\boldsymbol{x}'), \qquad \mathrm{D}_{ij}(\boldsymbol{x},\boldsymbol{x}') = \mathrm{D}_{ji}(\boldsymbol{x}',\boldsymbol{x}). \tag{28}$$

Note that symmetry and (positive) definiteness of the covariance kernel D imply the existence of a square root in the operator sense, so that one may write $\mathrm{D} = \sigma\sigma^{\mathrm{T}}$.

Let us also mention the special (near-equilibrium) case when $L\varphi + n[\varphi]$ (with $\varphi(x) \to \varphi(\boldsymbol{x})$) can be written as the variational derivative of a time-independent functional $U[\varphi]$,

$$L\varphi(\boldsymbol{x}) + n(\boldsymbol{x};\varphi) = \frac{1}{2}\int \mathrm{d}^d\boldsymbol{x}'\,\mathrm{D}(\boldsymbol{x},\boldsymbol{x}')\,\frac{\delta U(\boldsymbol{x};\varphi)}{\delta\varphi(\boldsymbol{x}')}, \tag{29}$$

then the dynamics satisfies detailed balance and is linked to a static model with stationary measure formally proportional to $\exp\{U[\varphi]\}$; see [3]. In such equilibrium-type models, the noise covariance D is fixed by the fluctuation–dissipation relation (as exemplified by Langevin-type equations [3, 19]), whereas far from equilibrium, the choice of D becomes an intrinsic part of the model definition. This situation is characteristic of, for instance, the stochastic Navier–Stokes or resistive MHD equations (12)–(14).

When analyzing specific physical models, the main goal is to compute averages of products of fields (e.g., over equilibrium fluctuations or over noise realizations), as well as the corresponding response functions. Diagrammatically, these objects can be generated from iterative (tree-level) solutions of (27) in the spirit of Wyld [76] and then averaged over the noise. If all field arguments are distinct, one obtains ordinary Green's (correlation) functions; coinciding arguments lead to Green's functions with composite-field insertions. Response functions are generated by functional derivatives of $\langle\varphi\rangle$ with respect to a deterministic probe field $A^{\varphi'}$. The MSRJD formalism provides a compact functional representation for both correlation and response functions.

On a purely formal level, the MSRJD formalism can be outlined as follows [3, 19, 27, 279].

Assuming the existence of solutions $\varphi(x;\eta,A^{\varphi'})$ of (27) for a fixed realization of the noise η, consider the generating functional of field products

$$\mathcal{G}[A^{\varphi},A^{\varphi'},\eta] \coloneqq \exp\{A^{\varphi}\varphi[\eta,A^{\varphi'}]\} = \sum_{n=0}^{\infty}\frac{1}{n!}\left\{\int \mathrm{d}x\,A^{\varphi}(x)\varphi\big(x;\eta,A^{\varphi'}\big)\right\}^n. \tag{30}$$

Henceforth, we employ a condensed notation that implies integration over space-time over the measure $\mathrm{d}x$ is defined as $\mathrm{d}x := \mathrm{d}^d\boldsymbol{x}\,\mathrm{d}t$ and summation over repeated discrete indices. For instance, the term $A^{\varphi}\varphi[\eta]$ in the exponent of $\mathcal{G}[A^{\varphi}, A^{\varphi'}, \eta]$ is shorthand for the expression:

$$A^{\varphi}\varphi[\eta, A^{\varphi'}] := \int \mathrm{d}x\, A^{\varphi}(x)\varphi\big(x;\eta, A^{\varphi'}\big) = \sum_i \int \mathrm{d}^d\boldsymbol{x}\,\mathrm{d}t\, A_i^{\varphi}(\boldsymbol{x},t)\varphi_i\big(\boldsymbol{x},t;\eta,A^{\varphi'}\big). \tag{31}$$

It can be readily seen that the derivatives of $\mathcal{G}[A^{\varphi},\eta]$ with respect to $A^{\varphi}(x)$, evaluated at $A^{\varphi}(x)=0$, yield products of the solution $\varphi(x;\eta)$ to equation (27). Hereinafter, the field $A^{\varphi}(x)$ will be referred to as the source (a non-random force), and $\eta(x)$ as the noise (a random force).

Then, using the functional δ-function (whose operational rules are analogous to those of the Dirac δ-function in finite-dimensional Euclidean space), (30) can be rewritten as:

$$\mathcal{G}[A^{\varphi}, A^{\varphi'}, \eta] = \int \mathcal{D}[\varphi]\ \delta(\varphi - \varphi[\eta])\mathrm{e}^{A^{\varphi}\varphi[\eta]} = \int \mathcal{D}[\varphi]\ \delta(\varphi-\varphi[\eta])\mathrm{e}^{A^{\varphi}\varphi}, \tag{32}$$

where, in the second integral, the argument of the exponent has been changed from $\varphi[\eta]$ to φ by virtue of the sifting property of the δ-function. Then, employing the Fourier integral representation of the functional δ-function:

$$\delta(\psi) = \prod_{(\boldsymbol{x},t)} \delta\left(\psi(\boldsymbol{x},t)\right) = \int \mathcal{D}\left[\frac{i\varphi'}{2\pi}\right]\ \exp\left\{\int \mathrm{d}t\,\mathrm{d}^d\boldsymbol{x}\,\varphi'(\boldsymbol{x},t)\psi(\boldsymbol{x},t)\right\} \tag{33}$$

and by transforming the argument of the δ-function in (32) from $\psi := (\varphi - \varphi[\eta])$ to $Q[\varphi,\eta,A^{\varphi'}] := -\partial_t\varphi + L\varphi + n[\varphi] + A^{\varphi'} + \eta$ (noting that $\{\psi:\ \psi=0\}$ coincides with the solution of the equation $Q[\varphi,\eta,A^{\varphi'}]=0$), we obtain an expression for $\mathcal{G}[A^{\varphi}, A^{\varphi'}, \eta]$ as a functional integral over two fields φ and φ':

$$\mathcal{G}[A^{\varphi}, A^{\varphi'}, \eta] = \int \mathcal{D}[\varphi]\mathcal{D}[\varphi']\left|\mathcal{J}[\varphi]\right| \exp\Big\{\varphi'\big(-\partial_t\varphi + L\varphi + n[\varphi] + \eta\big) + A^{\varphi'}\varphi' + A^{\varphi}\varphi\Big\}. \tag{34}$$

In the functional integral over φ' in (33), the imaginary unit was explicitly transferred from the exponent to the integration measure.[28] Subsequently, however, this factor will also be omitted from the measure by absorbing it into the definition of the functional space over which the φ' integration is performed. The functional determinant $\mathcal{J}[\varphi]$ in (34) (the Jacobian of the non-linear transformation from φ to $Q[\varphi,\eta]$ for a fixed η) is given by:

$$\mathcal{J}[\varphi] := \det\left\|\frac{\delta Q}{\delta\varphi}\right\| = \det\left\|\left(\frac{\partial}{\partial t} - L\right)\delta(x-x') - \frac{\delta n(x;\varphi)}{\delta\varphi(x')}\right\| \tag{35}$$

Formally, using $\det M = \exp\{\mathrm{Tr}\ln M\}$ and the retarded Green's function (propagator) $R := (\partial_t - L)^{-1}$, explicitly through $(\partial_t - L)\,R(\boldsymbol{x},t;\boldsymbol{x}',t') = \delta(\boldsymbol{x}-\boldsymbol{x}')\delta_+(t-t')$, where δ_+ is the asymmetric δ function [280] defined by $\int_{a+0}^{b}\mathrm{d}t' f(t')\delta_+(t-t') = \lim_{\varepsilon\to 0^+} f(t+\varepsilon)$ if $a \le t < b$ and zero otherwise[29], one finds that the Jacobian can be written as [3, 17]

$$\mathcal{J}[\varphi] = \det\|(\partial_t - L)\| \exp\left\{\theta(0)\int \mathrm{d}x\,\frac{\delta n(x;\varphi)}{\delta\varphi(x)}\right\}. \tag{36}$$

[28] It is also noteworthy that due to the invariance of the functional integral under transformations of the form $\varphi' \to c\varphi'$ (where $c\in\mathbb{C}$), the MSRJD auxiliary fields φ' can be interpreted as Lagrange multipliers enforcing the constraint $\psi(x)=0$ [3].

[29] The use of δ_+ is equivalent to the causality (retardation) condition $R(\boldsymbol{x},t;\boldsymbol{x}',t')=0$ for $t<t'$ complementing the corresponding linear problem in the case of using the usual δ-function.

This expression involves the product of two ill-defined quantities: $\theta(0)$ (the equal-time value of the Heaviside function) and the divergent integral of $\delta n(x;\varphi)/\delta\varphi$, which requires regularization [281, 282]. The field-independent factor $\det\|\partial_t - L\|$ is conventionally absorbed into the overall normalization of the functional integral. The problem that arises regarding the definition of $\theta(0)$ will be discussed below.

Summarizing, (34) provides a compact formal representation of the delta-functional constraint selecting solutions of the SPDE. Taken literally, this two-field functional integral is not meant to define a convergent iterated integral (in contrast to the Gaussian-noise case discussed below). Its proper meaning is a compact representation of the perturbation theory [283]: it is a generating device for the diagrammatic expansion (tree graphs for fixed η), equivalently encoded by the functional-differential (S-matrix) representation [22, 27].

Our primary interest, however, lies not in the functional $\mathcal{G}[A^{\varphi}, A^{\varphi'}, \eta]$ itself, but in its average over the probability distribution $P[\eta] \propto \exp\{-\frac{1}{2}\eta \mathrm{D}^{-1}\eta\}$ of the random noise η. This average defines the generating functional $\mathcal{G}[A^{\varphi}, A^{\varphi'}]$ of correlation functions for the field $\varphi(x)$:

$$\mathcal{G}[A^{\varphi}, A^{\varphi'}] = \big\langle \mathcal{G}[A^{\varphi}, A^{\varphi'}, \eta] \big\rangle_{\eta}, \qquad \big\langle \bullet \big\rangle_{\eta} \coloneqq \int \mathcal{D}[\eta] \ldots \exp\Big\{ \ln P[\eta] \Big\}, \tag{37}$$

where the operation $\langle \ldots \rangle_{\eta}$ denotes averaging over the statistical distribution of the random noise $\eta(x)$, characterized by the probability density functional $P[\eta]$. We write here explicitly $P[\eta]$ because, as can be seen from the given general construction, the MSRJD formalism can describe SPDE statistics driven by more than just Gaussian noise. This representation can be justified by arguments in the spirit of the Bochner-Minlos theorem, which guarantees the existence of a probability measure on a suitable topological vector space, given the characteristic functional of a random process. The characteristic functional is then the Fourier transform of this measure. These are, of course, largely heuristic arguments in the present context. A description of some *a priori* constraints that this vector space must satisfy can be found in [27].

Finally, the Gaussian integral over η in (37) can be performed explicitly, yielding

$$\mathcal{G}[A] = \int \mathcal{D}[\phi] \, \big|\mathcal{J}[\varphi]\big| \, e^{S[\phi] + A\phi}, \qquad S[\phi] \coloneqq \frac{1}{2}\varphi' \mathrm{D} \varphi' + \varphi' \big(- \partial_t \varphi + L\varphi + n[\varphi] \big). \tag{38}$$

Here, the functional $S[\phi]$ is known as the De Dominicis-Janssen action, and we have introduced the multiplet notation: $A \coloneqq (A^{\varphi}, A^{\varphi'})$, $\phi \coloneqq (\varphi, \varphi')$, and $\mathcal{D}[\phi] \coloneqq \mathcal{D}[\varphi]\mathcal{D}[\varphi']$. Note that in this notation, the linear term $A\phi$ is given by:

$$A\phi \coloneqq \int \mathrm{d}x \, [A^{\varphi}(x)\varphi(x) + A^{\varphi}(x)\varphi'(x)] \, . \tag{39}$$

It should be emphasized that the Jacobian determinant $\mathcal{J}[\varphi]$ is not a dispensable technicality. A convenient way to handle it is to represent $\mathcal{J}[\varphi]$ as a functional integral over Grassmann (ghost) fields, which makes the associated Becchi-Rouet-Stora-Tyutin (BRST)-type symmetry explicit; see, e.g., [16, 284]. This symmetry implies Ward identities, from which many important consequences can be derived, such as Liouville's theorem [285], and the proper normalization $\mathcal{G}[0] = 1$. Integrating out the auxiliary field φ' (with the Jacobian term treated consistently) leads to an Onsager–Machlup-type functional for φ alone [19].

A subtle point in (36) concerns the definition of $\theta(t)$ at $t = 0$ (equivalently, the equal-time value of the retarded propagator). A standard way to fix this ambiguity is time discretization in (34): forward (pre-point) discretization corresponds to the Itô convention $\theta(0) = 0$, while

midpoint discretization yields $\theta(0) = 1/2$ and corresponds to the Stratonovich interpretation of the original SPDE or symmetric Weyl ordering in QFT [3, 16]. Independently of the discretization choice, diagrams containing closed loops of retarded response lines are cancelled by contributions originating from the Jacobian determinant [3, 286]. Moreover, this cancellation is generally insensitive to the nature of η (whether stochastic or deterministic) and persists even in multiplicative-noise equations [286], contrary to some claims in the literature. Furthermore, if one focuses on the S-matrix perturbation theory, one can show that $\mathcal{G}[A]$ is, in fact, arbitrary with respect to the diagonal value of $R(\boldsymbol{x}, t; \boldsymbol{x}, t)$ and there is no need to involve stochastic problems here at all [22]. Therefore, physical Green's functions are independent of the chosen value of $\theta(0)$, provided the Jacobian is treated consistently. In practice, one may adopt the Itô convention $\theta(0) = 0$ and discard all diagrams containing closed response loops *ab initio*; this technically convenient convention will be used throughout this article.

The corresponding correlation and response functions, known in statistical field theory as Green's functions $G^{(m,n)}$, can be expressed using the general notation:

$$G^{(m,n)} := \frac{\delta^{m+n}\mathcal{G}[A]}{\delta A^{\varphi}(x_1)\cdots\delta A^{\varphi'}(x_n)}\bigg|_{A=0} = \left\langle \prod_{i=1}^{m}\varphi(x_i)\prod_{j=m+1}^{n}\varphi'(x_j)\right\rangle, \quad \langle\,\bullet\,\rangle := \int \mathcal{D}[\phi]\ldots \mathrm{e}^{S[\phi]}. \tag{40}$$

Decomposing the De Dominicis-Janssen action $S[\phi]$ in (38) into its free (quadratic) part $S_0[\phi]$ and interaction part $S_{\text{int}}[\phi]$, such that $S[\phi] = S_0[\phi] + S_{\text{int}}[\phi]$, with definitions:

$$S_0[\phi] = -\frac{1}{2}\begin{pmatrix}\varphi\\ \varphi'\end{pmatrix}\begin{pmatrix}0 & (\partial_t - L)^{\mathrm{T}}\\ (\partial_t - L) & -\mathrm{D}\end{pmatrix}\begin{pmatrix}\varphi\\ \varphi'\end{pmatrix}, \qquad S_{\text{int}}[\phi] = \varphi' n[\varphi], \tag{41}$$

we can express $\mathcal{G}[A]$ within the functional-differential representation (also known as S-matrix functional) for the generating functional

$$\mathcal{G}[A] = \mathrm{P}\ \exp\left\{S_{\text{int}}[\phi] + A\phi\right\}\bigg|_{\phi=0}, \quad \mathrm{P} := \exp\left\{\frac{1}{2}\int \mathrm{d}x\mathrm{d}x'\,\frac{\delta}{\delta\phi_i(x)}\,G^{\phi_i\phi_k}(x,x')\,\frac{\delta}{\delta\phi_k(x')}\right\}, \tag{42}$$

where P is the reduction operator (see, [22, 27, 287] for details), $\phi_1 = \varphi$ and $\phi_2 = \varphi'$, and the transpose $^{\mathrm{T}}$ operation applies to both continuous and discrete variables.

Naturally, the decomposition of an action into free and interaction parts is somewhat ambiguous; here, we adopt the most conventional choice. Here, $G := \left[G_{\phi_i\phi_k}(x,x')\right]_{i,k} = \langle\phi_i(x)\phi_k(x')\rangle_0$ $(i,k = 1,2)$ is the propagator matrix comprising the complete set of bare propagators. Its blocks are defined as follows:

$$G = \begin{pmatrix}(\partial_t - L)^{-1}\,\mathrm{D}\,(\partial_t - L)^{-1\mathrm{T}} & (\partial_t - L)^{-1}\\ (\partial_t - L)^{-1\mathrm{T}} & 0\end{pmatrix}. \tag{43}$$

Henceforth, $\langle\bullet\rangle_0$ denotes averaging of the same type as in (40), but performed with the free action $S_0[\phi]$ instead of the full action $S[\phi]$. The propagator $G_{12} = R$ is retarded, consequently, $G_{21} = G_{12}^{\mathrm{T}}$ is advanced. The symmetric propagator G_{11} contains both retarded and advanced contributions.

Expanding the exponentials in (42) as functional Taylor series yields the desired perturbation theory. In diagrammatic terms, the free part $S_0[\phi]$ is associated with lines (propagators), while the interaction part $S_{\text{int}}[\phi]$ generates vertices. These vertices typically involve one φ' field and two or more φ fields, their specific structure being determined by the form of $n[\varphi]$. Given that G_{12} is retarded, that $G_{22} = 0$, and that the correlator $\langle\varphi\varphi'\rangle$ is interpreted as a (linear) response

function $R(x,x') = \delta\langle\varphi(x)\rangle_\eta/\delta A^{\varphi'}(x')\big|_{A^{\varphi'}=0}$, the resulting Feynman diagrammatic technique coincides with the Wyld diagrams for the SPDE [76].

Equation (42) provides a compact functional restatement of Wick's theorem [3, 16, 18], which was originally formulated in operator QFT [288]. Expansion of both exponents in (42) leads to the standard Feynman diagrammatic technique for Green's functions. This diagrammatic technique plays a primary role in our constructive approach, serving to legitimize every manipulation of the functional integral. In this sense, the path-integral formulation (38) for $\mathcal{G}[A]$ is indeed an equivalent compact representation of perturbation theory: the formal expansion of the exponential in powers of $S_{\rm int}[\phi]$, combined with averaging $\langle\bullet\rangle_0$, yields the same diagrammatic series as that derived from (42). The formal correspondence between the path-integral definition (38) and expression (42) is established by the following operator relation:

$$\mathrm{P}\, F[\phi]\Big|_{\phi=0} = \langle F[\phi]\rangle_0 = \int \mathcal{D}[\phi]\, F[\phi] e^{S_0[\phi]}, \tag{44}$$

where the operator P is defined in (42). For internal self-consistency, it is assumed that the integration space is determined by the unperturbed problem (specifically, by the free action $S_0[\phi]$ when developing perturbation theory in $S_{\rm int}[\phi]$), rather than by the exact problem. This assumption is justified as long as one remains within the framework of perturbation theory [3, 27]. All relevant boundary or asymptotic conditions for φ, along with conditions ensuring the selection of the desired (retarded) Green's function R, are assumed to be implicitly incorporated into this functional integration space.

Finally, let us list a few standard consequences of causality in the MSRJD diagrammatics [3]: (i) any 1PI diagram with external legs consisting solely of φ fields vanishes (it necessarily contains a closed cycle of retarded G_{12} lines); (ii) any connected diagram with external legs consisting solely of φ' fields vanishes; in particular, all vacuum diagrams vanish, consistently with $\mathcal{G}[0] = 1$, (iii) All non-trivial (i.e., excluding bare or tree-level) diagrams for *equal-time* 1PI functions that include at least one external φ line, or for functions that include at least one φ' field, provide zero contribution.

As has been noted, from a statistical physics perspective, $\mathcal{G}[A]$ represents the partition function in an external field. On the other hand, physical significance often resides not in the partition function itself but in its logarithm, i.e., the Massieu-Planck potential in statistical mechanics terminology. Therefore, the generating functional of connected Green's functions, $W[A]$, is introduced as:

$$W[A] \coloneqq \ln \mathcal{G}[A]. \tag{45}$$

According to the (first) Mayer cluster theorem, this functional represents the sum of all connected Feynman diagrams (see, for instance, [27]). Then, the corresponding Green's functions W_n are obtained by the following functional differentiation:

$$W_n(x_1,\ldots,x_n) = \frac{\delta^n W[A]}{\delta A(x_1)\cdots\delta A(x_n)}\bigg|_{A=0}. \tag{46}$$

These $W_n(x_1,\ldots,x_n)$ represent the n-point connected Green's functions of the system.

For completeness, we also consider another important functional, which is particularly useful when studying the stability of field-theoretic models. In nontrivial models, the connected functions generated by $W[A]$ may develop non-analyticities as parameters (or sources) are varied. A familiar example is spontaneous symmetry breaking in a ferromagnet, where the one-point function $W_1(x) = \langle\varphi(x)\rangle$ becomes non-unique at zero external field in the ordered

phase. A convenient way to handle such situations is to switch to the Legendre-transformed effective action $\Gamma[\alpha]$, which is typically better behaved (e.g. convex) as a functional of the mean field[30]

$$\Gamma[\alpha] = \sup_A\{W[A] - \alpha A\}, \tag{47}$$

where A is determined by the 'equation of state': $\alpha(x) \coloneqq W_1(x) = \delta W[A]/\delta A(x)$.

The functional $\Gamma[\alpha]$ defined in (47) is known as the effective action in QFT, the Gibbs free energy in equilibrium statistical physics, and the rate function in large deviation theory. Its diagrammatic representation can be derived from the loop expansion of $W[A] = \sum_{l=0}^{\infty} W^{(l)}[A]$, where $W^{(l)}[A]$ is the sum of all connected diagrams with l loops. The corresponding loop expansion for the effective action, $\Gamma[\alpha] = \sum_{l=0}^{\infty}\Gamma^{(l)}[\alpha]$, is then given by the formulas [3]:

$$\Gamma^{(0)}[\alpha] = S_0[\alpha] + 1\mathrm{PI}\left[W^{(0)}[A] - \frac{AGA}{2}\right]\Bigg|_{A=G^{-1}\alpha},\ \Gamma^{(l)}[\alpha] = 1\mathrm{PI}\Big[W^{(l)}[A]\Big]\Big|_{A=G^{-1}\alpha} \tag{48}$$

where $S_0[\alpha] = -\alpha G^{-1}\alpha/2$ is precisely the free action of the model, the operation $1\mathrm{PI}[\mathcal{F}]$ denotes the sum of all one-particle irreducible (1PI) diagrams contributing to the functional $\mathcal{F}$, and $l \geqslant 1$. Recall that a diagram is termed one-particle irreducible if it remains connected after any single internal line is cut. In quantum field theory terminology, this is known as strong connectivity. Analogous to (46), 1PI vertex functions (or proper vertices) Γ_n are defined as:

$$\Gamma_n(x_1,\dots,x_n) = \frac{\delta^n\Gamma[\alpha]}{\delta\alpha(x_1)\cdots\delta\alpha(x_n)}\bigg|_{\alpha=0}. \tag{49}$$

Finally, we add a remark on the functional space underlying the formal 'integration' used in hydrodynamic field theories. The identity $\mathcal{G}[A] = \langle e^{A\phi}\rangle$, with $\langle\cdot\rangle$ defined by a functional integral, provides a compact representation of the corresponding perturbation theory. At the same time, the functional integral is often interpreted more broadly than as a purely perturbative device, in particular when discussing nonperturbative phenomena. With this in mind, we briefly comment on spontaneous symmetry breaking for generating functionals of the type $\mathcal{G}[A]$ in field-theoretic approaches to stochastic Navier–Stokes and MHD turbulence.

Owing to the δ-correlated pumping, the action (50) is quasi-invariant[31] under the generalized Galilean transformations $\{\boldsymbol{v}, \boldsymbol{v}'\} \to \{\boldsymbol{v}_w, \boldsymbol{v}'_w\}$, accompanied by the coordinate shift $x \mapsto x_w$. The transformation law for $\boldsymbol{v}$ is given in (11), while the response field transforms by pullback, $\boldsymbol{v}'_w(x) = \boldsymbol{v}'(x_w)$, with $x_w \coloneqq (\boldsymbol{x}+\boldsymbol{s}(t), t)$ and $\boldsymbol{s}(t)$ from (11). For $\boldsymbol{w}(t) = \mathrm{const}$, this reduces to the usual Galilean symmetry and the action becomes strictly invariant, $\mathcal{S}_0[\Phi] = \mathcal{S}_0[\Phi_w]$. However, as emphasized in [290], this symmetry is spontaneously broken in the velocity sector. The breaking is induced by the boundary/initial conditions that specify the functional integration domain in (38) (e.g., in the present stochastic MHD setting, by the conditions in (15)). Although the action (50) is invariant under (11) for $\boldsymbol{w}(t) = \mathrm{const}$, the functional integration domain (equivalently, the measure defined by the boundary conditions) need not be. Imposing, for instance, $\boldsymbol{v}(t \to -\infty) = \boldsymbol{v}_0$ selects a particular 'ground state' (reference frame), which can nevertheless be mapped to other equivalent states by (11).

[30] When traversing the model's parameter space and intersecting corresponding critical manifold, non-analyticities (colloquially, "fractures") can appear on the surface defined by $W[A]$. In contrast, for $\Gamma[\alpha]$, these correspond to regions where its convexity becomes non-strict (forming flat sections).

[31] That is, it is invariant up to a linear term of the form $\mathcal{S}_0 \to \mathcal{S}_0 - (\partial_t\boldsymbol{v}')\cdot\boldsymbol{w}$. This quasi-invariance and its implications (in particular, for renormalizability) are discussed in [289].

It is also useful to note that the transformations (11) share certain structural features with gauge symmetries: they relate physically equivalent descriptions corresponding to different choices of a reference frame. Accordingly, one may fix this freedom by adding a 'gauge-fixing' term that constrains the zero mode of the velocity field, for instance $\mathcal{S}_0 \to \mathcal{S}_0 + \frac{1}{2\xi}\int \mathrm{d}t\, \boldsymbol{u}^2(t)$, $\boldsymbol{u}(t) \propto \int \mathrm{d}^d\boldsymbol{x}\, \boldsymbol{v}(\boldsymbol{x},t)$, with a gauge parameter ξ. This term fixes only the spatially uniform mode and does not affect finite-k fluctuations. The resulting gauge-fixed theory possesses a BRST symmetry associated with the corresponding Faddeev–Popov determinant (rather than with the MSRJD Jacobian of stochastic quantization); see [16] for general background. Such gauge-like treatments are standard for the stochastic Navier–Stokes problem [291–293] and carry over to MHD without essential modifications.

In MHD, spontaneous symmetry breaking may also occur in the magnetic sector: in dynamo-type regimes, a spontaneously generated mean magnetic field selects a preferred direction and thereby breaks the rotational symmetry $\mathbf{SO}(3)$ down to an axial subgroup. Unlike a constant mean velocity, such a mean magnetic field cannot be removed by a Galilean transformation. We return to this issue in Sec. 4.3.

4.2. Core: stochastic MHD as a field theory

For Eqs. (12)–(14), the (bare) De Dominicis–Janssen [25, 26] action functional can be written in terms of the classical stochastic fields $\boldsymbol{v}$ and $\boldsymbol{b}$ together with the auxiliary transverse fields $\boldsymbol{v}'$ and $\boldsymbol{b}'$ [251]:

$$\begin{aligned}\mathcal{S}_0 = \frac{1}{2}\boldsymbol{v}'\mathfrak{D}^{vv}\boldsymbol{v}' + \frac{1}{2}\boldsymbol{b}'\mathfrak{D}^{bb}\boldsymbol{b}' + \boldsymbol{v}'\mathfrak{D}^{vb}\boldsymbol{b}' + \boldsymbol{v}'\cdot\left[-\mathrm{D}_t\boldsymbol{v} + \nu_0\Delta\boldsymbol{v} + (\boldsymbol{b}\cdot\boldsymbol{\nabla})\boldsymbol{b}\right] \\ + \boldsymbol{b}'\cdot\left[-\mathrm{D}_t\boldsymbol{b} + u_0\nu_0\Delta\boldsymbol{b} + (\boldsymbol{b}\cdot\boldsymbol{\nabla})\boldsymbol{v}\right],\end{aligned} \tag{50}$$

where $\mathfrak{D}^{vv}$, $\mathfrak{D}^{bb}$, and $\mathfrak{D}^{vb}$ are the elements of the forcing correlator matrix introduced in Eq. (16). Here and throughout, we employ a condensed notation in which integration over space–time in the action and in similar functionals is left implicit.

Within the standard perturbative framework, the action (50) can be written in the form [3]

$$\mathcal{S}_0 = -\frac{1}{2}\boldsymbol{\Phi}\mathbf{K}\boldsymbol{\Phi} + \mathcal{S}_{\mathrm{int}}, \tag{51}$$

where the field multiplet $\boldsymbol{\Phi} \coloneqq (\boldsymbol{v}, \boldsymbol{b}, \boldsymbol{v}', \boldsymbol{b}')$ collects all dynamical and auxiliary variables of the model, $\mathbf{K}$ is the 4×4 matrix specifying the quadratic form that follows from (50), and $\mathcal{S}_{\mathrm{int}}$ contains the interaction contributions.

The independent elements of the propagator matrix $\mathbf{G} \coloneqq \mathbf{K}^{-1}$ are displayed at the bottom of Fig. In the momentum–frequency representation $(\boldsymbol{k},\omega)$, these propagators take the form

$$G_{ij}^{v'v} = \frac{\mathbb{P}_{ij}(\boldsymbol{k})}{\alpha(k,\omega)},\ G_{ij}^{b'b} = \frac{\mathbb{P}_{ij}(\boldsymbol{k})}{\beta(k,\omega)},\ G_{ij}^{vv} = \frac{\mathbb{D}_{ij}^{vv}(\boldsymbol{k})}{|\alpha(k,\omega)|^2},\ G_{ij}^{bb} = \frac{\mathbb{D}_{ij}^{bb}(\boldsymbol{k})}{|\beta(k,\omega)|^2},\ G_{ij}^{bv} = \frac{\mathbb{D}_{ij}^{bv}(\boldsymbol{k})}{\alpha(k,\omega)\beta^*(k,\omega)}, \tag{52}$$

where we introduce the abbreviations $\alpha(k,\omega) \coloneqq i\omega + \nu_0 k^2$ and $\beta(k,\omega) \coloneqq i\omega + u_0\nu_0 k^2$. All remaining components of matrix $\mathbf{G}$ are fixed by the relation $G_{ij}^{ab}(\boldsymbol{k},\omega) = G_{ji}^{ba}(-\boldsymbol{k},-\omega)$ with $a,b \in \boldsymbol{\Phi}$, which encodes the Hermitian symmetry the propagator matrix. Using the transversality of all fields, the interaction $\mathcal{S}_{\mathrm{int}}$ in Eq. (51) can be recast as

$$\mathcal{S}_{\mathrm{int}} = \frac{1}{2}v_i'\mathbb{U}_{ijl}b_jb_l + \frac{1}{2}v_i'\mathbb{W}_{ijl}v_jv_l + b_i'\mathbb{V}_{ijl}v_jb_l, \tag{53}$$

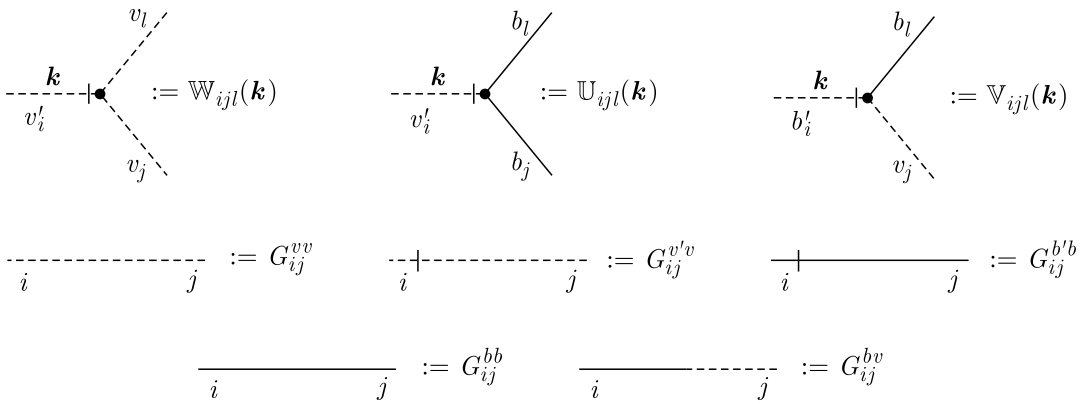

Figure 1. Graphical representation of the diagrammatic technique elements in the model (50).

with the vertex tensors defined in momentum space by

$$\mathbb{W}_{ijl}(\boldsymbol{k}) = i(k_j\delta_{il} + k_l\delta_{ij}), \qquad \mathbb{U}_{ijl}(\boldsymbol{k}) = -\mathbb{W}_{ijl}(\boldsymbol{k}), \qquad \mathbb{V}_{ijl}(\boldsymbol{k}) = i(k_j\delta_{il} - k_l\delta_{ij}). \tag{54}$$

The vertex $\mathbb{W}$ corresponds to the standard Navier–Stokes nonlinearity, $\mathbb{U}$ governs the renormalization of the Lorentz-force term, and $\mathbb{V}$ is commonly referred to as the Ohm's law vertex. For clarity, the vertex structures are shown schematically on top of Fig. 1. In Eq. (54), the momentum $\boldsymbol{k}$ is always taken to enter the vertex through the corresponding auxiliary leg: $\boldsymbol{b'}$ for $\mathbb{U}$ and $\boldsymbol{v'}$ for $\mathbb{W}$ and $\mathbb{V}$. Combinatorial factors of $1/2$ in Eq. (53) reflect the symmetry of the vertices $\mathbb{W}$ and $\mathbb{U}$ under permutations of the associated fields.

4.3. Long wavelength instability in helical MHD: kinematic and dynamo stable regimes

A convenient entry point into the physics encoded in the model (50) is its stability analysis. Recall that a necessary stability requirement in stochastic dynamics reads [3]

$$\Big\{\langle \boldsymbol{v}\otimes\boldsymbol{v'}\rangle,\, \langle \boldsymbol{b}\otimes\boldsymbol{b'}\rangle,\, G^{vv'},\, G^{bb'}\Big\} \in \mathcal{A}(\mathbb{C}_+), \tag{55}$$

where $\mathcal{A}(\mathbb{C}_+)$ denotes the class of functions analytic in the upper half-plane $\mathbb{C}_+$ of the complex frequency variable ω. The bare response propagators $G^{vv'}$ and $G^{bb'}$ are given in (52), whereas the exact (dressed) response functions can be expressed via the corresponding 1PI functions as $\langle \boldsymbol{v}\otimes\boldsymbol{v'}\rangle = -\big[\Gamma^{v'v}\big]^{-1}$ and $\langle \boldsymbol{b}\otimes\boldsymbol{b'}\rangle = -\big[\Gamma^{b'b}\big]^{-1}$, with $\Gamma^{v'v}$ and $\Gamma^{b'b}$ satisfying the Dyson equations

$$\Gamma_{ij}^{v'v}(\boldsymbol{k},\omega) = -\alpha(k,\omega)\mathbb{P}_{ij}(\boldsymbol{k}) + \Sigma_{ij}^{v'v}(\boldsymbol{k},\omega), \qquad \Gamma_{ij}^{b'b}(\boldsymbol{k},\omega) = -\beta(k,\omega)\mathbb{P}_{ij}(\boldsymbol{k}) + \Sigma_{ij}^{b'b}(\boldsymbol{k},\omega). \tag{56}$$

Here $\Sigma_{ij}^{v'v}$ and $\Sigma_{ij}^{b'b}$ are the self-energy parts that incorporate all loop corrections to the 1PI functions $\Gamma_{ij}^{v'v}$ and $\Gamma_{ij}^{b'b}$, respectively. Let us emphasize that, throughout this subsection, 'stability' is understood in the local (linear) sense. A genuinely global stability statement appears to be out of reach, at least within the present model.

The bare response propagators $G^{vv'}$ and $G^{bb'}$ have no singularities in the upper half of the complex ω-plane. By contrast, the exact response functions may develop poles whose positions are determined by the zeros of the corresponding 1PI functions. At first glance, since $\Sigma^{v'v}$ and $\Sigma^{b'b}$ start at $\mathcal{O}(g_{0i})$, one might expect them to be small compared with the viscous contributions in $\alpha(k,\omega)$ and $\beta(k,\omega)$ and therefore unable to violate (55). However, the perturbative expansion of $\Sigma_{ij}^{b'b}$ in the vicinity of $\omega = 0$ and $\boldsymbol{k} = \boldsymbol{0}$ contains a parity-odd contribution linear in $\boldsymbol{k}$. In the power-law model this term has the form $\nu_0\, h_0\, \big[i\,\varepsilon_{ijl}k_l\big]\Lambda$, where

$h_0 = h_0(\rho_s, g_{0s}, \epsilon, u_0)$ is a dimensionless coefficient; this is precisely the curl-type contribution in the terminology of [294].[32] Keeping only the terms linear in $\boldsymbol{k}$ at $\omega = 0$ in the expansion of $\Sigma_{ij}^{b'b}$, one finds that the corresponding response function, with the curl contribution resummed, takes the form

$$\langle b'_i b_j \rangle = \frac{\beta(k,\omega)\mathbb{P}_{ij}(\boldsymbol{k}) - \nu_0 h_0 k \mathbb{H}_{ij}(\boldsymbol{k})}{\beta^2(k,\omega) - \nu_0^2 h_0^2 k^2} + \mathcal{O}(k^2;\omega^1), \tag{57}$$

where the function $\beta(k,\omega)$ is defined after Eq. (52). The denominator on the right-hand side of (57) yields a pole with $\mathrm{Im}\,\omega > 0$, which violates the local stability criterion (55). In QFT language, this corresponds to a tachyonic (unstable) mode in $\langle \boldsymbol{b}' \otimes \boldsymbol{b} \rangle$, indicating that fluctuations destabilize the trivial ground state.

In the SFT parlance, this instability is nothing but the destruction of the 'naive' magnetic ground state $\langle \boldsymbol{b} \rangle = \boldsymbol{0}$ under the influence of arbitrarily small fluctuations. From a physical standpoint, we are dealing here with an instability similar to that found in the mean-field theory of the magnetic dynamo (see, e.g., [158, 175, 178]) in the description of the α-effect. This analogy, as well as further details of the instability mechanism, was discussed in [294]. Here we briefly summarize the conclusions of that article.

To reach a steady turbulent state, a helical MHD system must eliminate this instability. In [294], two such stabilization scenarios were identified: the *kinematic* regime and the *dynamo* regime of the model $\mathcal{S}_0$ in (50). Both scenarios amount to incorporating into $\mathcal{S}_0$ the curl term generated by loop diagrams, i.e., $\nu_0 h_0\, \boldsymbol{b}' \cdot (\boldsymbol{\nabla} \times \boldsymbol{b})$. In the kinematic regime, one assumes that $\mathcal{S}_0$ already contains a bare curl term whose coefficient is tuned so as to cancel, order by order, the loop-generated contribution. As a result, the effective action in this regime is precisely $\mathcal{S}_0$.

A more physically motivated option is to include the loop-generated curl contribution from $\Sigma^{b'b}$ into the action without any fine-tuned counterterm and to interpret the ensuing instability as a signal that the $\mathbf{SO}(3)$-symmetric vacuum is not the true stable state. One then assumes that turbulent fluctuations drive the system into an 'energetically favourable' $\mathbf{SO}(2)$-symmetric vacuum with $\langle \boldsymbol{b} \rangle = \boldsymbol{B}_0 \neq \boldsymbol{0}$, where $\boldsymbol{B}_0$ is a large-scale magnetic field.[33] Accordingly, the theory re-expanded in the neighbourhood of $\langle \boldsymbol{b} \rangle = \boldsymbol{B}_0$ must be stable. Within the SFT approximations adopted here (statistical homogeneity, translational invariance, etc.), $\boldsymbol{B}_0$ is simply a constant uniform field, and its emergence can be interpreted as the outcome of a large-scale turbulent dynamo mechanism. This is precisely why this regime is called the dynamo regime.

Formally, the re-expansion of $\mathcal{S}_0$ about $\langle \boldsymbol{b} \rangle = \boldsymbol{B}_0$ is implemented by the shift $\boldsymbol{b} \to \boldsymbol{b} + \boldsymbol{B}_0$. This shift modifies only the quadratic part of the action, yielding the dynamo-regime action

$$\mathcal{S}_{\boldsymbol{B}_0} = \mathcal{S}_0 + \boldsymbol{v}' \cdot (\boldsymbol{B}_0 \cdot \boldsymbol{\nabla})\boldsymbol{b} + \boldsymbol{b}' \cdot (\boldsymbol{B}_0 \cdot \boldsymbol{\nabla})\boldsymbol{v}. \tag{58}$$

Thus, among all structures in (50), only the propagator matrix $\mathbf{G}$ is modified. In $(\boldsymbol{k},\omega)$-representation, it is given by the following matrix

$$\mathbf{G}_{ij}^{[\boldsymbol{B}_0]} = \frac{1}{|\xi|^2} \begin{pmatrix} -\mathfrak{G}_{ij} & \begin{matrix} \beta^* \xi \mathbb{P}_{ij} & i\gamma\xi\mathbb{P}_{ij} \\ i\gamma\xi\mathbb{P}_{ij} & \alpha^*\xi\mathbb{P}_{ij} \end{matrix} \\ \begin{matrix} \beta\xi^*\mathbb{P}_{ij} & -i\gamma\xi^*\mathbb{P}_{ij} \\ -i\gamma\xi^*\mathbb{P}_{ij} & \alpha\xi^*\mathbb{P}_{ij} \end{matrix} & 0 \end{pmatrix}. \tag{59}$$

[32] The expansion of $\Sigma_{ij}^{v'v}$ cannot contain such a term due to the $i \leftrightarrow j$ symmetry of the NS vertex $\mathbb{W}_{ijl}$ [294].

[33] In the language of quantum field theory, this means that the system enters this state through spontaneous symmetry breaking caused by radiative corrections, known in the literature also as the Coleman-Weinberg mechanism [253, 295].

Here $\xi(\boldsymbol{k},\omega) \coloneqq \gamma^2+\alpha(k,\omega)\beta(k,\omega)$ and $\gamma \coloneqq (\boldsymbol{B}_0\cdot\boldsymbol{k})$. An asterisk * denotes complex conjugation, and ω and $\boldsymbol{k}$ are implicit arguments of all functions and tensor operators. The 2×2 matrix $\mathfrak{G}$ is given by

$$\mathfrak{G}_{ij} \coloneqq \begin{pmatrix} \beta^*(i\gamma\mathbb{D}_{ij}^{vb}-\beta\mathbb{D}_{ij}^{vv})+i\gamma(i\gamma\mathbb{D}_{ij}^{bb}-\beta\mathbb{D}_{ij}^{vb}) & \beta^*(i\gamma\mathbb{D}_{ij}^{vv}-\alpha\mathbb{D}_{ij}^{vb})+i\gamma(i\gamma\mathbb{D}_{ij}^{vb}-\alpha\mathbb{D}_{ij}^{bb}) \\ i\gamma(i\gamma\mathbb{D}_{ij}^{vb}-\beta\mathbb{D}_{ij}^{vv})+\alpha^*(i\gamma\mathbb{D}_{ij}^{bb}-\beta\mathbb{D}_{ij}^{vb}) & i\gamma(i\gamma\mathbb{D}_{ij}^{vv}-\alpha\mathbb{D}_{ij}^{vb})+\alpha^*(i\gamma\mathbb{D}_{ij}^{vb}-\alpha\mathbb{D}_{ij}^{bb}) \end{pmatrix}. \quad (60)$$

Within this symmetry-breaking picture, the kinematic regime also admits a transparent interpretation. Formally, it corresponds to assuming an external mechanism that suppresses the instability, or equivalently to working in the limit of a sufficiently weak uniform field, $\boldsymbol{B}_0 \approx \boldsymbol{0}$. This is precisely the logic adopted in the standard kinematic dynamo theory. Also note that the stabilized vacuum is analogous to an absorbing state in nonequilibrium statistical mechanics (see, e.g., [60, 62]) or to the ground state in quantum mechanics: once the system settles into it, small perturbations do not trigger further runaway instabilities. The key here is that no other instabilities arise, even in the presence of a large-scale field $\boldsymbol{B}_0$ [294].

At the level of the equations of motion, adding such a term to the action is equivalent to the appearance of an extra contribution $\nu_0 h_0 \boldsymbol{\nabla}\times\boldsymbol{b}$ on the right-hand side of the induction equation (13). Phenomenologically, one may view it as assuming a parity-odd contribution to the current density in Ohm's law (3), of the form $\xi_0\boldsymbol{B}$ with an effective pseudoscalar conductivity coefficient ξ_0. Inserted into the standard derivation of resistive MHD, this term generates the required curl contribution in (13). We emphasize that although the curl term is often discussed from the viewpoint of renormalization (in power-law pumped models (17) one has $h_0 \sim \Lambda$, i.e., a linear UV divergence), its appearance is not intrinsically tied to renormalization. Rather, it is dictated by parity breaking (the absence of mirror symmetry). For illustration, consider a model free of IR and UV divergences with a realistic energy-injection kernel $\mathbb{D}_{ij}^{\alpha\beta}(\boldsymbol{k})$, concentrated at $k \sim 1/l_{\max}$ and rapidly decaying both as $k\to 0$ and as $k\to\infty$. In such a setting, the coefficient of the curl term is finite already at the perturbative level and is not associated with renormalization, while the need to eliminate it persists because it still generates an instability.

The emergence of curl-type terms in the magnetic response function $\langle \boldsymbol{b}'\otimes\boldsymbol{b}\rangle$ (and hence in the induction equation (13)), together with their absence (at one loop) in the velocity equation (12), was first pointed out in [252]. In that work, the resulting instability was taken as an indication that a straightforward RG treatment is problematic in helical MHD. In a more systematic field-theoretic approach [251], the issue was addressed by invoking dynamical spontaneous symmetry breaking and the emergence of a large-scale field $\boldsymbol{B}_0$; however, the one-loop estimate of the resulting stabilizing field magnitude B_0 turned out to be inconsistent. Indeed, for fixed Λ and ϵ and without additional regularization, the one-loop cancellation condition for the curl term admits an exact solution only in the formal limit $B_0\to\infty$, as noted in [294]. If, however, one allows for a bare curl term in (50) with a finite coefficient $h_{00} \sim \xi_0 \propto g_{0i}$ (as permitted by a general Ohm's law in the absence of mirror symmetry), then the cancellation of the curl contribution occurs already at finite B_0 for arbitrarily small h_{00}. Moreover, even for very small $|h_{00}|$, the resulting magnitude B_0 can remain parametrically small. As argued in [294], the one-point average $\langle\boldsymbol{b}\rangle$ plays a role analogous to the ground-state energy in quantum mechanics in that it may require additional regularization to become finite.

4.4. Ultraviolet renormalization in space dimensions $d > 2$: linear and logarithmic divergences

For $d > 2$, which is the case of interest here, the renormalizability of the general model (50) follows from Refs. [247, 251, 294, 296]. The borderline case $d\to 2^+$ is discussed in [296]; see

Table 2. Canonical (engineering) dimensions of the bare fields and parameters in the action (50).

Quantity	$\boldsymbol{v}, \boldsymbol{b}$	$\boldsymbol{v'}, \boldsymbol{b'}$	ν_0	u_0, ρ	g_{01}	g_{02}	g_{03}	m, Λ
d_Q^p	-1	$d+1$	-2	0	2ϵ	$2a\epsilon$	$\epsilon(1+a)$	1
d_Q^ω	1	-1	1	0	0	0	0	0
d_Q	1	$d-1$	0	0	2ϵ	$2a\epsilon$	$\epsilon(1+a)$	1

also [2, 3, 297–299]. When $d > 2$, all superficial UV divergences occur only in the 1PI functions $\Gamma^{v'v}$, $\Gamma^{b'b}$, and $\Gamma^{v'bb}$. These divergences are identified by assigning canonical dimensions so that each term in the action (50) is dimensionless with respect to the diffusive scaling $\omega \sim k^2$, while treating momentum and frequency dimensions independently. The resulting canonical (engineering) dimensions — the momentum dimensions d_Q^p, the frequency dimensions d_Q^ω, and the total dimensions $d_Q = d_Q^p + 2d_Q^\omega$ — for all quantities Q entering (50) are collected in Table 2. Consequently, a complete UV renormalization reduces to removing the divergences in these three 1PI functions: $\Gamma^{v'v}$, $\Gamma^{b'b}$, and $\Gamma^{v'bb}$.

A careful renormalization procedure consists of two stages. First, one isolates and subtracts power divergences in the UV scale Λ (polynomial in Λ). Second, one removes the remaining logarithmic UV divergences; within analytic regularization, these manifest themselves, after the formal limit $\Lambda \to \infty$, as poles $1/\epsilon^p$, $p = 1, 2, \ldots$. Technically, analytic regularization [3, 300] is closely related to dimensional regularization, but here the parameter ϵ is *not* tied to the space dimension d and enters through the choice of the pumping function (17). For details in the MHD context, we refer to [294]; a general discussion can be found in [3].

For a strictly multiplicatively renormalizable theory, power divergences can be absorbed by renormalizing parameters already present in the action, and they do not require introducing new operators. In that sense, the standard RG machinery is most straightforwardly applicable to multiplicatively renormalizable models. In helical MHD described by (50), the situation is different. The model is pseudo-multiplicatively renormalizable: loop corrections generate a divergence (the curl term) that renormalizes an operator absent from the original action but allowed by the symmetries. Once this operator is included from the outset, the set of counterterms closes, and the renormalization of the extended model becomes multiplicative. The nontrivial two-loop analysis of the linear Λ divergence associated with the curl term, as well as its elimination, was carried out in [294] for the simplified model with $\mathfrak{D}^{bb} = \mathfrak{D}^{vb} = 0$, in both the kinematic and turbulent-dynamo regimes. As also shown in [294], there are no other power divergences in Λ in that model. Including magnetic noise does not change this conclusion qualitatively and only produces additional contributions to the coefficient of the curl term. For the resulting multiplicatively renormalizable model the counterterm functional $\Delta\mathcal{S}$ contains only a finite set of operators with the same algebraic structure as in the original action $\mathcal{S}_0$, and the renormalized action can be written as $\mathcal{S}_R = \mathcal{S}_0|_{e_0 \to e} + \Delta\mathcal{S}$ [3]. Here e_0 and e are bare and renormalized action parameters, respectively.

After the Λ-renormalization, the remaining ϵ-renormalization (with the formal limit $\Lambda \to \infty$) proceeds in the standard way in both regimes (kinematic and dynamo) [294] and reduces to computing three independent renormalization constants. In the dynamo regime, the large-scale field produces additional contributions, but they are renormalized by the same constants as in the kinematic regime. Notably, the curl term can be technically eliminated both at the stage of Λ-renormalization and after ϵ-renormalization [294]. As a result, expressing bare parameters

e_0 in (50) through the renormalized ones e according to

$$\nu_0 \to \nu, \quad u_0 \to u, \quad g_{01} \to g_1\mu^{2\epsilon}, \quad g_{02} \to g_2\mu^{2a\epsilon}, \quad g_{03} \to g_3\mu^{\epsilon(1+a)}, \quad (B_0 \to B), \tag{61}$$

while keeping the helicity parameters ρ_s ($s = 1, 2, 3$) unrenormalized [251], and adding the necessary counterterms is equivalent to introducing three independent renormalization constants Z_1, Z_2, and Z_3 that absorb all logarithmic UV divergences, irrespective of the regime.[34] The prescription (61) involves the renormalization mass (mass scale) μ [17], an auxiliary momentum scale typically chosen of the order of the ultraviolet scale, $\mu \sim 1/l_{\min}$.

In practical calculations, the renormalization constants Z_i are conveniently evaluated in the Minimal Subtraction (MS) scheme, where they are determined solely by the pole parts of their Laurent expansions in ϵ. Accordingly, their general structure can be written as

$$Z_i = 1 + \sum_{n=1}^{\infty} \sum_{m=1}^{n} \frac{1}{\epsilon^m} \sum_{s=0}^{n} z^{(i)}_{m,\,s\,n-s}(\rho, u) g_1^s g_2^{n-s}, \qquad i = 1, \ldots, 3. \tag{62}$$

One useful feature of MS-like schemes is that the renormalization of the curl operator does not affect the constants $Z_{1,2,3}$ computed in the curl-free sector: in particular, $Z_{1,2,3}$ cannot depend on IR scales (such as m) or on IR-relevant external parameters. The sum in (62) involves only the two independent couplings g_1 and g_2. Indeed, Ref. [247] implies $g_3 = \kappa\,(g_1 g_2)^{1/2}$, where κ is an arbitrary parameter constrained by $|\kappa| \leqslant 1$ (from the positivity of the correlator matrix), playing a role analogous to a gauge parameter in quantum electrodynamics.

Thus, if we factor out the independent renormalization (and subsequent cancellation) of the curl term — which, in the MS scheme, does not affect the renormalization of the remaining parameters — the key points of the logarithmic renormalization can be illustrated already in the kinematic regime. The multiplicative ϵ-renormalization in this regime has the form

$$\mathcal{S}_R\left[\mathbf{\Phi}; \nu_0, u_0, g_{01}, g_{02}, g_{03}\right] = \mathcal{S}_0\left[\boldsymbol{v},\, \boldsymbol{b}Z_b,\, \boldsymbol{v}',\, \boldsymbol{b}'Z_b;\, \nu Z_\nu,\, uZ_u,\, g_1\mu^{2\epsilon}Z_{g_1},\, g_2\mu^{2a\epsilon}Z_{g_2},\, g_3\mu^{\epsilon(1+a)}\right], \tag{63}$$

from which all the relationships between the renormalized and bare fields and parameters can be explicitly inferred

$$\begin{gathered} \boldsymbol{b} \to \boldsymbol{b}\,Z_b, \qquad \boldsymbol{b}' \to \boldsymbol{b}'\,Z_{b'}, \qquad \boldsymbol{v} \to \boldsymbol{v}, \qquad \boldsymbol{v}' \to \boldsymbol{v}', \\ \nu_0 = \nu Z_\nu, \qquad u_0 = uZ_u, \qquad g_{01} = g_1\mu^{2\epsilon}Z_{g_1}, \qquad g_{02} = g_2\mu^{2a\epsilon}Z_{g_2}, \qquad g_{03} = g_3\mu^{\epsilon(1+a)}. \end{gathered} \tag{64}$$

Diagrammatically, one determines the constants Z_1, Z_2, and Z_3 by imposing UV finiteness of the corresponding 1PI functions $\Gamma^{v'v}$, $\Gamma^{b'b}$, and $\Gamma^{v'bb}$; equivalently, these constants multiply the operators associated with the structures renormalized in the action:

$$\begin{aligned} \mathcal{S}_R = \frac{1}{2}\boldsymbol{v}'\,\mathfrak{D}_R^{vv}\,\boldsymbol{v}' + \frac{1}{2}\boldsymbol{b}'\mathfrak{D}_R^{bb}\boldsymbol{b}' + \boldsymbol{v}'\mathfrak{D}_R^{vb}\boldsymbol{b}' + \boldsymbol{v}'\cdot\Big[-\mathrm{D}_t\boldsymbol{v} + \nu Z_1\Delta\boldsymbol{v} + Z_3(\boldsymbol{b}\cdot\boldsymbol{\nabla})\boldsymbol{b}\Big] \\ + \boldsymbol{b}'\cdot\Big[-\mathrm{D}_t\boldsymbol{b} + u\nu Z_2\Delta\boldsymbol{b} + (\boldsymbol{b}\cdot\boldsymbol{\nabla})\boldsymbol{v}\Big]. \end{aligned} \tag{65}$$

Here $\mathfrak{D}_R^{\alpha\beta}$ denotes the renormalized noise correlator (16). For $d > 2$, it differs from the bare one only by the replacement of bare parameters with renormalized ones according to (61); no additional renormalization constants are required for $\mathfrak{D}_R^{vv}$ and $\mathfrak{D}_R^{bb}$ [247]. Three renormalization

[34] A fourth constant Z_4 may be introduced for the curl operator if its cancellation is postponed until the ϵ-renormalization stage; this option was also analysed in [294].

constants Z_i needed for renormalization are evaluated in the MS scheme. For $d > 2$ no counterterm is needed for $\mathfrak{D}_R^{\alpha\beta}$, so that $g_{01}\nu_0^3 \equiv g_1\nu^3\mu^{2\epsilon}$, $g_{02}\nu_0^3 \equiv g_2\nu^3\mu^{2a\epsilon}$, and $g_{03}\nu_0^3 \equiv g_3\nu^3\mu^{\epsilon(1+a)}$. Another hallmark of the RG approach to turbulence is that the fields $\boldsymbol{v}$ and $\boldsymbol{v'}$ are not renormalized (see [1, 3, 296]). From the renormalized action (65), one immediately reads off the full set of renormalization constants for the model parameters and fields via

$$Z_v = Z_{v'} = 1, \quad Z_b = Z_{b'}^{-1} = Z_3^{1/2}, \quad Z_\nu = Z_1, \quad Z_u = Z_2 Z_1^{-1}, \quad Z_{g_1} = Z_1^{-3}, \quad Z_{g_2} = Z_1^{-3} Z_3. \tag{66}$$

Thus, the objects that are actually subject to computation are the renormalization constants Z_1, Z_2, and Z_3. They are fixed by imposing ultraviolet finiteness of the corresponding 1PI functions $\Gamma^{v'v}$, $\Gamma^{b'b}$, and $\Gamma^{v'bb}$. Within the framework of the MS scheme and under analytical regularization, they contain only logarithmic divergences (in the form of poles in ϵ) and are the only parameters that completely determine the characteristics of the model's universal behaviour. These characteristics are studied using the RG method and are discussed in the two subsequent sections 4.5 and 4.6, respectively.

In the general model (65) with a mixed correlator $\mathfrak{D}_R^{\alpha\beta}$, the renormalization constants Z_i were calculated at the one-loop level [247] (see also [301]). Importantly, at that order all Z_i turned out to be independent of ρ_s (since the corresponding diagrams in the one-loop approximation do not contain pseudotensor lines G^{bv}), which allowed the results of [247] to be used in the one-loop study of the model with only non-zero $\mathfrak{D}_R^{vv}$ reported in [251].

Further progress in the calculation focused on this simplified model with energy injection only by means of kinetic helicity, i.e., with only nonzero force $\boldsymbol{f}^v$ and $\mathfrak{D}_R^{vb} = \mathfrak{D}_R^{bb} = 0$. The renormalization constants Z_i were practically extracted from reduced auxiliary models that retain only the vertices and propagators required to construct the relevant 1PI function from the set $\Gamma^{v'v}$, $\Gamma^{b'b}$, and $\Gamma^{v'bb}$. In these simplified models, many authors have worked out the two-loop parts of Z_i in a systematic way, including both parity-even (mirror-symmetric) and helical contributions, and up to now all Z_i have been brought to two-loop accuracy. For the reader's convenience, we have rewritten from [294] the summary Table 3 of results with all found and corrected typos and misprints for the physically relevant case $d = 3$.

Regarding the dynamo regime, once the uniform field $\boldsymbol{B}_0$ is fixed so as to cancel the curl term (either at the Λ-renormalization stage or at the ϵ-renormalization stage; both options are analysed in [294]), the remaining 1PI Green's functions of the shifted theory can be obtained by the field shift $\boldsymbol{b} \to \boldsymbol{b} + \boldsymbol{B}_0$ in the renormalized generating functional of 1PI Green's functions of the unshifted theory. Since shifting the argument of a UV-finite functional by a UV-finite quantity preserves UV finiteness, the parameter $\boldsymbol{B}_0$ must be renormalized with the same constant as the field $\boldsymbol{b}$:

$$\boldsymbol{B}_0 \to \boldsymbol{B} Z_b. \tag{67}$$

This statement was also explicitly verified in [294] in a two-loop calculation of B_0 itself in the simplified model with only forcing $\boldsymbol{f}^v$. From these considerations, it follows that the fully renormalized action of the dynamo regime (58) takes the form

$$\mathcal{S}_{\boldsymbol{B}R} = \mathcal{S}_R + Z_3 \boldsymbol{v'} \cdot (\boldsymbol{B} \cdot \boldsymbol{\nabla}) \boldsymbol{b} + \boldsymbol{b'} \cdot (\boldsymbol{B} \cdot \boldsymbol{\nabla}) \boldsymbol{v}. \tag{68}$$

4.5. MHD in the kinematic regime: fixed points, inclusion of anisotropy, energy equipartition

In this section, we recapitulate the main results of the SFT/RG analysis of the model in the kinematic regime defined by the renormalized action (65). The central objective of this

Table 3. All two-loop coefficients in ϵ-poles of the renormalization constants Z_i in the simplified model (65) with $\mathfrak{D}_R^{vb} = \mathfrak{D}_R^{bb} = 0$. All data are taken from the work [294].

$z^{(i)}_{m,s\,0}(u,\rho)$	$Z_1(g_2=0)$	Ref. year	$Z_2(g_2=0)$	Ref. year	$Z_3(g_2=0)$	Refs. years
$z^{(i)}_{1,10}(u)$	$-1/40\pi^2$	[302] 1984	$-1/12\pi^2 u(1+u)$	[302] 1984	$-1/60\pi^2 u$	[247] 1985
$z^{(i)}_{1,20}(u_\star,\rho)\times 10^5$	-1.05868	[108, 115] 2003, 2009	$-2.25613 + 0.0340506\,\rho^2$	[264, 267] 2016, 2016	$0.430812 + 0.617026\,\rho^2$	[152] 2024
$z^{(i)}_{2,20}(u)$	$-(z^{(1)}_{11})^2$	[108] 2003	$-\frac{z^{(2)}_{11}}{2(1+u)}\left(uz^{(2)}_{11} + (2+u)z^{(1)}_{11}\right)$	[32] 2005	$-\frac{z^{(3)}_{11}}{2}\left(z^{(3)}_{11} - 2z^{(1)}_{11} - z^{(2)}_{11}\right)$	[152] 2024

Note. The year of publication is indicated in small numbers under each article in the 'Source' column.

approach is to extract the infrared (large-scale) asymptotic behaviour and the associated universal scaling laws within the renormalization group framework. A convenient way to study these asymptotics is to work with the generating functional of renormalized connected Green's functions, $\mathcal{W}_R(A) \coloneqq \ln \mathcal{G}_R(A)$, where $\mathcal{G}_R(A)$ is defined as in (45) with the bare action (50) replaced by its renormalized form (65). For $\mathcal{W}_R(A)$, one can write the standard Euler homogeneity relations (separately for momentum and frequency dimensions, $s \in \{k, \omega\}$)

$$\left[\mathrm{D}_\mu + \sum_{\alpha\in\mathfrak{g}} d^s_\alpha \mathrm{D}_\alpha + d^s_\nu \mathrm{D}_\nu + \sum_{\varphi\in\mathbf{\Phi}} \int \mathrm{d}x\, A^\varphi(x)\left(d^s_{A^\varphi} - \mathrm{D}^{[s]}\right)\frac{\delta}{\delta A^\varphi(x)}\right]\mathcal{W}_R(A) = 0, \tag{69}$$

together with the main RG equation, which follows from the μ-independence of the bare (unnormalized) functional $\mathcal{W}(A)$ at fixed bare parameters (see [3]):

$$\left[\mathrm{D}_\mu + \sum_{\alpha\in\mathfrak{g}} \beta_\alpha \partial_\alpha - \gamma_\nu \mathrm{D}_\nu + \sum_{\varphi=b,b'} \gamma_\varphi \int \mathrm{d}x\, A^\varphi(x)\frac{\delta}{\delta A^\varphi(x)}\right]\mathcal{W}_R(A) = 0. \tag{70}$$

In both equations, the summations run over the variables explicitly indicated under the corresponding summation signs. Hereafter, we denote the set of couplings as $\mathfrak{g} \coloneqq (g_1, g_2, u)$. From the RG viewpoint, u plays the role of a coupling because it enters the renormalization constants Z_i; in contrast, g_3 is omitted here since it does not appear in the expressions for Z_i. The operators $\mathrm{D}_e \coloneqq e\,\partial_e$ are the usual logarithmic derivatives with respect to the corresponding renormalized parameter $e \coloneqq (\mathfrak{g}, \nu)$. The canonical dimensions of the sources are $d^\omega_{A^\varphi} = 1 - d^\omega_\varphi$ and $d^k_{A^\varphi} = d - d^k_\varphi$, where $d^{\omega,k}_\varphi$ are the canonical dimensions of the fields $\mathbf{\Phi} = (\boldsymbol{v}, \boldsymbol{b}, \boldsymbol{v'}, \boldsymbol{b'})$ listed in Table 2.

Eqs. (69) express the usual scale invariances with respect to spatial coordinates $\boldsymbol{x}$ and time t of the functional $\mathcal{W}_R(A)$. Depending on the index s, the operator $\mathrm{D}^{[s]}$ denotes the spatial $\mathrm{D}^{[k]} \coloneqq \boldsymbol{x}\cdot\boldsymbol{\nabla}$ or temporal $\mathrm{D}^{[\omega]} \coloneqq t\,\partial_t$ logarithmic derivatives, respectively. Eq. (70) expresses the fact that $\mathcal{W}_R(A)$ does not depend on the renormalization mass μ provided the sources A and the bare parameters are held fixed. The functional operators $\mathrm{D}^\varphi \coloneqq \int \mathrm{d}x\, A^\varphi(x)\,\delta/\delta A^\varphi(x)$, with $\varphi \in \{\boldsymbol{b}, \boldsymbol{b'}\}$, act on a given connected correlator (i.e. on a coefficient of $\mathcal{W}_R$ in its expansion in A) and simply return the number of external legs: $\mathrm{D}^{\boldsymbol{b}} \to n_{\boldsymbol{b}}$ and $\mathrm{D}^{\boldsymbol{b'}} \to n_{\boldsymbol{b'}}$. Here the sum over φ is taken only for $\boldsymbol{b}$ and $\boldsymbol{b'}$, since $Z_v = Z_{v'} = 1$ implies $\gamma_v = \gamma_{v'} = 0$ (see below).

The coefficients in (70) are the RG functions: the β functions, which quantify the departure from scale invariance, and the anomalous dimensions γ_ν, γ_b, and $\gamma_{b'}$, which determine the exponents governing power-law asymptotics of correlation functions and parameters. These RG functions are expressible through the renormalization constants Z_i. Specifically, we define

$$\gamma_i \coloneqq \overline{\mathrm{D}}_\mu \ln Z_i, \qquad \beta_{\mathfrak{g}} \coloneqq \overline{\mathrm{D}}_\mu \mathfrak{g}, \tag{71}$$

where $\overline{\mathrm{D}}_\mu \coloneqq \mathrm{D}_\mu\big|_{e_0}$ differentiates with respect to μ at fixed bare parameters $e_0 \coloneqq (g_{01}, g_{02}, u_0, \nu_0)$. It then follows that, for any function $F(\mathfrak{g})$,

$$\overline{\mathrm{D}}_\mu F(\mathfrak{g}) = \beta_{\mathfrak{g}}\partial_{\mathfrak{g}} F(\mathfrak{g}) \coloneqq \big[\beta_{g_1}\partial_{g_1} + \beta_{g_2}\partial_{g_2} + \beta_u\partial_u\big]F(\mathfrak{g}). \tag{72}$$

Using (63), (66), and (71), one arrives at

$$\begin{gathered}\gamma_{g_1} = -3\gamma_1, \quad \gamma_{g_2} = \gamma_3 - 3\gamma_1, \quad \gamma_\nu = \gamma_1, \quad \gamma_u = \gamma_2 - \gamma_1, \quad \gamma_b = -\gamma_{b'} = \gamma_3/2, \quad \gamma_v = \gamma_{v'} = 0,\\ \beta_{g_1} = g_1(-2\epsilon - \gamma_{g_1}), \qquad \beta_{g_2} = g_2(-2a\epsilon - \gamma_{g_2}), \qquad \beta_u = -u\gamma_u.\end{gathered} \tag{73}$$

Since γ_i, $i = 1, 2, 3$, are UV-finite [3], in the MS scheme each of them can be expressed through the coefficient of the first ϵ pole in the expansion (62) of the corresponding Z_i. Using Eqs. (71) and (72) and keeping terms up to two-loop order, we obtain

$$\gamma_i = -2\Big(z^{(i)}_{1,10}g_1 + az^{(i)}_{1,01}g_2 + (1+a)z^{(i)}_{1,11}g_1g_2 + 2\big(z^{(i)}_{1,20}g_1^2 + az^{(i)}_{1,02}g_2^2\big)\Big) + \mathcal{O}(g_1^3; g_2^3). \tag{74}$$

To characterize inertial-range IR asymptotics of correlation functions, one must determine the IR-attractive fixed point $\mathfrak{g}_\star \coloneqq (g_{1\star}, g_{2\star}, u_\star)$ at which all beta-functions vanish, i.e., $\beta_{g_1}(\mathfrak{g}_\star) = \beta_{g_2}(\mathfrak{g}_\star) = \beta_u(\mathfrak{g}_\star) = 0$. The stability of the found fixed point is governed by the requirement that the real parts of the eigenvalues of the matrix $\mathbf{\Omega} \coloneqq (\partial\beta_\alpha/\partial\alpha)\big|_{\mathfrak{g}_\star}$, with $\alpha \in \{g_1, g_2, u\}$, be positive in the vicinity of $\epsilon = 0$.

In the presence of a stable fixed point, one can further write representations for various Green's functions as solutions of the RG equation, i.e., functions of its first integrals (RG representations). In the model (65), of greatest interest are pair correlation functions

$$W^v_{ij}(\boldsymbol{k}, t) \coloneqq \int \mathrm{d}^d x \langle v_i v_j\rangle_{\mathrm{c}}(\boldsymbol{x}, t)\, \mathrm{e}^{-i\boldsymbol{k}\cdot\boldsymbol{x}}, \quad W^b_{ij}(\boldsymbol{k}, t) \coloneqq \int \mathrm{d}^d x \langle b_i b_j\rangle_{\mathrm{c}}(\boldsymbol{x}, t)\, \mathrm{e}^{-i\boldsymbol{k}\cdot\boldsymbol{x}}. \tag{75}$$

Here, we assumed statistical homogeneity and stationarity, so the correlators depend only on the separations; the subscript 'c' denotes the only connected diagrams selection. The equal-time (static) correlators $W^{v,b}_{ij}(\boldsymbol{k}, 0)$ determine the kinetic and magnetic energy spectra, $E^v(k)$ and $E^b(k)$. It is convenient to distinguish between the full (possibly anisotropic) three-dimensional spectrum and the isotropic one-dimensional spectrum obtained after angular integration:

$$\text{3D:} \quad E^{v,b}(\boldsymbol{k}) \coloneqq \frac{1}{2}W^{v,b}_{ii}(\boldsymbol{k}, 0), \qquad \text{1D:} \quad E^{v,b}(k) \coloneqq \frac{1}{2}\frac{S_d}{(2\pi)^d}\, k^{d-1} W^{v,b}_{ii}(k, 0) \tag{76}$$

Note that the energy spectra are traditionally defined through unrenormalized correlation functions. Such spectra were studied, in particular, in [301], where a mirror-symmetric anisotropic generalization of the model (65) was studied at the one-loop level.

To obtain RG representations of the correlators W^v_{ij} and W^b_{ij} it is convenient to express W^v_{Rij} and W^b_{Rij} through dimensionless scaling functions using

$$F_R = k^{d_F}\nu^{d^\omega_F} R^F\left(tk^2\nu, s, g_1, g_2, u, B/(\nu k)\ldots\right), \tag{77}$$

where $s \coloneqq k/\mu$, R^F is a dimensionless scaling function associated with F, and d_F and d^ω_F are the total canonical and frequency dimensions of F. The last argument, $B/(\nu k)$, is relevant only in the dynamo regime. Thus, extracting from general functional relation (70) the RG equations for W^α_{Rij} in the form

$$\left[\mathrm{D}_\mu + \sum_{\mathfrak{g}}\beta_\alpha\partial_\alpha - \gamma_\nu \mathrm{D}_\nu\right] W^v_{Rij} = 0, \qquad \left[\mathrm{D}_\mu + \sum_{\mathfrak{g}}\beta_\alpha\partial_\alpha - \gamma_\nu\mathrm{D}_\nu + 2\gamma_b\right] W^b_{Rij} = 0, \tag{78}$$

and introducing the dimensionless functions R^v_{ij} and R^b_{ij} according to (77), one can use the method of characteristics to represent the functions W^v_{Rij} and W^b_{Rij} as solutions of the corresponding equations

$$W^v_{Rij}(\boldsymbol{k},t)=\bar\nu^2 R^v_{ij}\big(tk^2\bar\nu,1;\,\bar{\mathfrak{g}}\big),\quad W^b_{Rij}(\boldsymbol{k},t)=\bar\nu^2 R^b_{ij}\big(tk^2\bar\nu,1;\,\bar{\mathfrak{g}}\big)\,\exp\left(2\int_1^s\frac{\mathrm{d}s'}{s'}\gamma_b\big(\bar{\mathfrak{g}}(s')\big)\right), \tag{79}$$

where the first integrals $\bar{\mathfrak{g}}$ are solutions of the following Gell-Mann-Low type equations

$$\begin{aligned}&\mathrm{D}_s\bar g_1(s)=\beta_{g_1}(\bar{\mathfrak{g}}(s)),\quad &&\mathrm{D}_s\bar g_2(s)=\beta_{g_2}(\bar{\mathfrak{g}}(s)),\quad &&\mathrm{D}_s\bar u(s)=\beta_u(\bar{\mathfrak{g}}(s)),\\ &\bar g_1(s)|_{s=1}=g_1,\quad &&\bar g_2(s)|_{s=1}=g_2,\quad &&\bar u(s)|_{s=1}=u,\end{aligned} \tag{80}$$

and for the invariant kinematic viscosity $\bar\nu$ one obtains the exact relation

$$\frac{\bar\nu}{\nu}=\exp\left(-\int_1^s\frac{\mathrm{d}s'}{s'}\gamma_\nu\big(\bar{\mathfrak{g}}(s')\big)\right)=\exp\left(\int_{\bar g_1}^{g_1}\mathrm{d}x\,\frac{\gamma_\nu(x,g_2(x),u(x))}{\beta_{g_1}(x,g_2(x),u(x))}\right)=\left(\frac{g_1\mu^{2\epsilon}}{\bar g_1}\right)^{1/3}k^{-2\epsilon/3}. \tag{81}$$

The last equality holds because of the identity $\beta_{g_1}(\mathfrak{g})\equiv g_1(-2\epsilon+3\gamma_\nu(\mathfrak{g}))$ in (73), which follows from the absence of renormalization of correlator $\mathfrak{D}^{\alpha\beta}$.

Typically, in MHD, one is interested in the one-dimensional (isotropic) spectrum of the total energy $E(k)=E^v(k)+E^b(k)$ (often discussed in terms of Elsässer variables, see e.g. [13]). Equivalently, it can be defined via the equal-point correlators as $W^v_{Rii}(\boldsymbol{x},t;\boldsymbol{x},t)+W^b_{Rii}(\boldsymbol{x},t;\boldsymbol{x},t)=2\int_0^\infty\mathrm{d}k\,E(k)$. From here, using (75) and (79), we obtain a representation for the spectrum in terms of scaling functions [296]

$$E(k)=\frac{k^{1-4\epsilon/3}}{(4\pi)^{d/2}\Gamma(d/2)}\left(\frac{g_{10}\nu_0^3}{\bar g_1}\right)^{2/3}\left[R^v_{ii}\big(0,1;\,\bar{\mathfrak{g}}\big)+Z_3\,R^b_{ii}\big(0,1;\,\bar{\mathfrak{g}}\big)\,\exp\left(2\int_1^s\frac{\mathrm{d}s'}{s'}\gamma_b\big(\bar{\mathfrak{g}}(s')\big)\right)\right], \tag{82}$$

where for the invariant kinematic viscosity $\bar\nu$ we used the representation $\bar\nu=(g_{10}\nu_0^3/\bar g_1k^{2\epsilon})^{1/3}$, which can be derived from (81) and $g_{10}\nu_0^3\equiv g_1\nu^3\mu^{2\epsilon}$.

Calculations in the model (65) show that for $d=3$ and $\rho_{1,2,3}=0$, there are two IR-attractive fixed points: the kinetic one, $\mathfrak{g}^{\mathrm{k}}_\star\coloneqq(g^{\mathrm{k}}_{1\star},\,g^{\mathrm{k}}_{2\star}=0,\,u^{\mathrm{k}}_\star)$, and an additional ('magnetic') one, $\mathfrak{g}^{\mathrm{m}}_\star\coloneqq(g^{\mathrm{m}}_{1\star}=0,\,g^{\mathrm{m}}_{2\star},\,u^{\mathrm{m}}_\star=0)$. The kinetic fixed point corresponds to the Kolmogorov (K41) regime. Their one-loop coordinates in mirror-symmetric (nonhelical) MHD were first obtained in [246] and later refined in [247] (see also [301]). At one-loop order, the magnetic fixed point is IR stable for $a>0.25$, whereas the kinetic fixed point is stable for $a\lesssim1.16$; hence, in the overlap region $0.25<a\lesssim1.16$ both fixed points are IR attractive, and the RG flow depends on the initial values of the couplings. In particular, this interval includes the physically relevant value $a=1$ for magnetic forcing (see Sec. 3.3), implying that the critical behaviour of three-dimensional nonhelical MHD is not fully universal [3]. It was subsequently shown that the kinetic fixed point (unlike the magnetic one) remains stable for $d\geqslant2$ [296]; it also persists and is stable in helical MHD with $\rho_{1,2,3}\neq0$ (at least for $d=3$). These results have recently been extended to two-loop order; see the references collected in Table 3. To the best of our knowledge, an analogous analysis of the magnetic fixed point in a helical medium has not yet been performed.

Let us now briefly discuss the problem of anomalous dimensions in MHD. This issue for the kinematic regime has been discussed in detail in monographs [2, 3], and therefore, we will limit ourselves to the main conclusions. Within the inertial range $l_{\min}\ll\ell\ll l_{\max}$, any

quantity Q is characterized, in addition to its canonical dimension d_Q, by a critical dimension Δ_Q that governs its power-law dependence on $k \propto \ell^{-1}$ (at fixed ν and fixed large-scale forcing parameters). Determining these universal characteristics is a standard task of the RG method. At an IR-stable fixed point $\mathfrak{g}_\star$, the critical dimensions of (renormalized) composite operators $F_R = \{F_{R\alpha}\}$ are usually obtained from (see [3])

$$\Delta_F = d_F^k + \Delta_\omega(\mathfrak{g}_\star) d_F^\omega + \gamma_F(\mathfrak{g}_\star) = d_F + \gamma_\nu(\mathfrak{g}_\star) d_F^\omega + \gamma_F(\mathfrak{g}_\star), \qquad \big[\Delta_\omega(\mathfrak{g}_\star) = 2 - \gamma_\nu(\mathfrak{g}_\star)\big], \quad (83)$$

where the matrix of anomalous dimensions γ_F is determined by operator mixing within the family F. This standard derivation implicitly assumes that the corresponding scaling functions approach finite, nonzero limits as $s = k/\mu \to 0$. In MHD this assumption may fail because some stable fixed points lie on the boundary of the coupling-constant space (i.e. some coordinates of $\mathfrak{g}_\star$ vanish), so that certain scaling functions develop zeros at $\mathfrak{g}_\star$ (the 'zeros in R-functions' problem). At the kinetic fixed point, this leads to a nontrivial modification of the naive scaling in the magnetic sector (see below). As for the magnetic fixed point, at $d = 3$ and $\rho_{1,2,3} = 0$ one can show (see [3]) that dynamic Green functions with an even total number of magnetic legs, $n_b + n_{b'} = 2k$ ($k \in \mathbb{Z}$), obey IR scaling with definite critical dimensions. The same holds for the corresponding static correlators provided they are well-defined in the limiting theory with $u = g_1 = 0$ (i.e., the frequency integrals converge), which yields

$$\begin{aligned} \Delta_\omega^{\rm m} = -\Delta_t^{\rm m} = 2 - \gamma_{2\star}^{\rm m}, \qquad & \Delta_{\boldsymbol{v}}^{\rm m} = 1 - \gamma_{2\star}^{\rm m}, \qquad \Delta_{v'}^{\rm m} = 2 + \gamma_{1\star}^{\rm m} \\ \Delta_{b'}^{\rm m} = 3 - \Delta_b^{\rm m}, \qquad & \Delta_b^{\rm m} = 1 - 2a\epsilon + \gamma_{2\star}^{\rm m}/2, \end{aligned} \quad (84)$$

where the one-loop values of $\gamma_{i\star}^{\rm m}$ are $\gamma_{1\star}^{\rm m} = 4a\epsilon$, $\gamma_{2\star}^{\rm m} = 0$, and $\gamma_{3\star}^{\rm m} = 4a\epsilon$ [3]. In contrast, for $n_b + n_{b'} = 2k + 1$ and for static correlators that are ill-defined at $u = g_1 = 0$, no universal IR scaling with fixed field/parameter dimensions exists [3].

To close this section, we briefly consider the recently obtained two-loop RG predictions in the simplified model with a single non-zero correlator $\mathfrak{D}_R^{vv} \neq 0$, i.e., at $g_2 = 0$. For such a magnetic-noise-free model, the only possibility is the kinetic (Kolmogorov) fixed point. At the two-loop level, its coordinates can be parametrized as[35]

$$g_{1\star}^{\rm k} = g_{1\star}^{(1)}\epsilon + g_{1\star}^{(2)}\epsilon^2 + \mathcal{O}(\epsilon^3), \qquad u_\star^{\rm k} = u_\star^{(1)} + u_\star^{(2)}\epsilon + \mathcal{O}(\epsilon^2), \quad (85)$$

$$u_\star^{(1)} = \big(\sqrt{43/3} - 1\big)/2, \quad u_\star^{(2)} = 0.0138 + 0.0312\rho_1^2, \quad g_{1\star}^{(1)} = 40\pi^2/3, \quad g_{1\star}^{(2)} = -1.0994 g_{1\star}^{(1)}. \quad (86)$$

The first relation in (85) coincides with the familiar fixed point of ordinary Navier–Stokes turbulence. Its stability has long been established (see [108, 115]). Moreover, [264] presented a numerical study of the kinematic fixed point's stability, showing that finite helicity further enhances its stability.

Our model also possesses two exact identities, i.e. relations without ϵ^2 (or higher) corrections:

$$\gamma_{1\star}^{\rm k} := \gamma_1(g_{1\star}^{\rm k}) = 2\epsilon/3, \qquad \gamma_{2\star}^{\rm k} := \gamma_2(g_{1\star}^{\rm k}, u_\star^{\rm k}) = \gamma_{1\star}^{\rm k}. \quad (87)$$

The first identity is a standard result in the RG theory of turbulence, while the second follows from the first together with $\beta_u(g_{1\star}^{\rm k}, 0, u_\star^{\rm k}) = u_\star^{\rm k}(\gamma_{2\star}^{\rm k} - \gamma_{1\star}^{\rm k}) = 0$. Beyond (87), the anomalous dimension $\gamma_{3\star}$ is accessible perturbatively. Its two-loop estimate was obtained in [152] and reads

$$\gamma_{3\star}^{\rm k} = -0.319\,\epsilon + \big(0.0556 - 0.4202\,\rho_1^2\big)\,\epsilon^2 + \mathcal{O}(\epsilon^3). \quad (88)$$

[35] References for the coefficients in (86) are given in Table 3.

Another quantity of interest in the kinematic regime is whether the kinetic and magnetic sectors are in (spectral) equipartition, i.e. whether $E^v(k)$ and $E^b(k)$ have the same inertial-range scaling. It is instructive to recall the analysis of [301] performed for the model (50) with the simplification $g_{03} = 0$. As already noted, this simplification affects only non-universal scaling functions and does not change universal characteristics such as the spectral slopes. Since the exact identity $\gamma_{1\star} = 2\epsilon/3$ holds in helical MHD as well, the conclusions below apply to both mirror-symmetric and helical cases. In [301], the following IR asymptotics for the magnetic and kinetic spectra were obtained

$$E^v(k) \sim \frac{k^{1-2\gamma_{1\star}}}{(4\pi)^{\frac{d}{2}}\Gamma\left(\frac{d}{2}\right)} \left(\frac{g_{10}\nu_0^3}{g^{\rm k}_{1\star}}\right)^{2/3} R^v_{ii}\left(0,1;\, g^{\rm k}_{1\star}, 0, u^{\rm k}_\star\right), \tag{89}$$

$$E^b(k) \sim \frac{k^{1-2\gamma_{1\star}+\gamma_{3\star}}}{(4\pi)^{\frac{d}{2}}\Gamma\left(\frac{d}{2}\right)} \left(\frac{g_{10}\nu_0^3}{g^{\rm k}_{1\star}}\right)^{2/3} s^{\omega_2} \widetilde{R}^b_{ii}\left(0,1;\, g^{\rm k}_{1\star}, 0, u^{\rm k}_\star\right) \exp\left(\int_0^1 \frac{{\rm d}s'}{s'}\left[\gamma_3\big(\bar g(s')\big) - \gamma_{3\star}\right]\right), \tag{90}$$

where $\gamma^{\rm k}_{1\star}$ is given by Eq. (87), $\gamma^{\rm k}_{3\star}$ by (88), and in the magnetic spectrum, it was taken into account that $R^b_{ii}\left(0,1;\, \mathfrak{g}^{\rm k}_\star\right) \simeq g^{\rm k}_{2\star} = 0$ at lowest order. Accordingly, Ref. [301] factorized the scaling function as $R^b_{ii}\left(0,1;\bar{\mathfrak{g}}\right) = \bar g_2\, \widetilde{R}^b_{ii}\left(0,1;\bar{\mathfrak{g}}\right)$, so that, as $\bar{\mathfrak{g}}(s) \to \mathfrak{g}^{\rm k}_\star$ for $s \to 0$, one has $R^b_{ii} \sim s^{\omega_2}\widetilde{R}^b_{ii}\left(0,1;g^{\rm k}_{1\star},0,u^{\rm k}_\star\right)$, where $\omega_2 = 2\epsilon - 2a\epsilon - \gamma^{\rm k}_{3\star}$ is the correction exponent extracted from β_{g_2} at the fixed point. From Eqs. (89) and (90) it is clear that the "zeros in R-functions" problem amounts to an additional IR scaling factor in the magnetic sector: for Green functions with $n_b > n_{b'}$ the corresponding scaling functions carry an extra factor $s^{(n_b - n_{b'})\omega_2/2}$. In particular, this compensates for the vanishing of R^b_{ii} at $\mathfrak{g}^{\rm k}_\star$ and restores the Kolmogorov slope of the energy spectra in the kinematic regime. For $d = 3$, $\epsilon = 2$, and $a = 1$, Eqs. (89) and (90) reduce to the classical Kolmogorov law $E^{v,b}(k) \propto k^{-5/3}$. Possible deviations from equipartition at the kinetic fixed point are controlled by the forcing exponent a: for $a \neq 1$, one finds $E^b(k) \propto k^{1-4\epsilon/3+2\epsilon(1-a)}$.

Intermittency corrections are not expected for the two-point functions discussed here, but they may arise in higher-order correlators/structure functions through anomalous dimensions of composite operators; this mechanism is especially transparent in Kraichnan's rapid-change models, where anomalous exponents can be obtained analytically [134, 135, 255]. For intermittency in MHD turbulence (e.g., in Elsässer-field structure functions) see, for instance, [232, 303].

Summarizing Ref. [301] (see also [3]), in the kinematic regime at $\mathfrak{g} = \mathfrak{g}^{\rm k}_\star$ all Green functions in helical MHD exhibit IR scaling with the usual (Kolmogorov) critical dimensions for t, $\boldsymbol{v}$, and $\boldsymbol{v'}$, whereas the magnetic fields $\boldsymbol{b}$ and $\boldsymbol{b'}$ recover the Kolmogorov scaling only at $a = 1$. The complete set of critical dimensions at the kinetic fixed point for $d = 3$ is given by

$$\begin{aligned} &\Delta^{\rm k}_\omega = -\Delta^{\rm k}_t = 2 - \gamma^{\rm k}_{1\star}, \qquad && \Delta^{\rm k}_{\boldsymbol{b}} = 1 - \gamma^{\rm k}_{1\star} + (\gamma^{\rm k}_{3\star} + \omega_2)/2 = 1 - 2\epsilon/3 + \epsilon(1-a), \\ &\Delta^{\rm k}_{\boldsymbol{v}} = 1 - \gamma^{\rm k}_{1\star}, && \Delta^{\rm k}_{v'} = 3 - \Delta^{\rm k}_v, \qquad && \Delta^{\rm k}_{\boldsymbol{b'}} = 3 - \Delta^{\rm k}_{\boldsymbol{b}}. \end{aligned} \tag{91}$$

Finally, note that even in nonhelical MHD, an anisotropy can qualitatively change the RG scenario. In the isotropic case, the magnetic field does not feed back on the inertial-range velocity dynamics at the kinetic fixed point and thus behaves as a passive field. In the anisotropic case, the Lorentz force becomes IR relevant and destabilizes this fixed point [301].

The main message of the kinematic regime is that, for nontrivial stochastic MHD models such as (65), the RG analysis may yield not only standard universal IR scaling with finite scaling functions, but also more subtle behaviour when scaling functions vanish at a stable fixed point (the 'zeros in R-functions' scenario). In this sense, the RG approach is richer than a naive picture based solely on critical dimensions.

4.6. MHD in the dynamo regime: large-scale B_0, anisotropic transport, equipartition violation

The turbulent dynamo regime of stochastic helical MHD, described by the shifted action (58), is technically a much more involved sector of the SFT/RG description of MHD turbulence. For a long time, it was addressed mainly through partial one-loop calculations and qualitative arguments (see the discussion at the beginning of Sec. 4), because the spontaneously generated large-scale magnetic field introduces anisotropy and requires a nonstandard diagrammatic treatment. A systematic investigation of this regime started with the two-loop analysis [294] in a simplified stochastic MHD model (12)–(14) driven by kinetic forcing $\boldsymbol{f}^v$ only (i.e., with $\boldsymbol{f}^b = \boldsymbol{0}$). Physically, this restriction is mainly technical: if $\boldsymbol{f}^b = \boldsymbol{0}$, then one has $\langle \boldsymbol{b} \rangle = \boldsymbol{0}$ and, correspondingly, all correlators built solely from $\boldsymbol{b}$ vanish because there are no diagrams that generate them. This 'normal' solution is, however, unstable; the system stabilizes by generating a uniform mean field $\langle \boldsymbol{b} \rangle = \boldsymbol{B}_0$, and higher-order correlators of $\boldsymbol{b}$ become nonzero in the broken-symmetry state. If magnetic noise is present, $\boldsymbol{f}^b \neq \boldsymbol{0}$, then higher-order $\boldsymbol{b}$-correlators are nonzero from the beginning, but $\langle \boldsymbol{b} \rangle = \boldsymbol{0}$, and the dynamo transition corresponds to the appearance of a nonzero mean field, $\langle \boldsymbol{b} \rangle \neq \boldsymbol{0}$.

In this section, we briefly summarize the main results of [294] for the dynamo regime. For completeness, we first recall the basic logic of the transition to this regime (see also Sec. 4.3). The starting point is solenoidal resistive MHD with a helical random force $\boldsymbol{f}^v$ in the velocity equation and no magnetic forcing $\boldsymbol{f}^b$. The helical part of the velocity forcing generates, already in perturbation theory, a parity-odd contribution to the magnetic self-energy, i.e., a linear-in-k ('curl') term in the 1PI function $\Gamma^{b'b}$ whose long-wavelength form is equivalent to the α-term of mean-field dynamo theory. This term renders the initially statistically isotropic state $\langle \boldsymbol{b} \rangle = \boldsymbol{0}$ infrared-unstable in the same sense as the kinematic dynamo instability: one magnetic mode grows at sufficiently long wavelengths. See [294] for a more detailed discussion.

Within the SFT formulation, the dynamo regime is realized by expanding around a broken-symmetry state with a uniform mean magnetic field, implemented via the formal shift $\boldsymbol{b}(\boldsymbol{x}, t) \to \boldsymbol{b}(\boldsymbol{x}, t) + \boldsymbol{B}_0$ with $\boldsymbol{B}_0 = \text{const}$ in the bare action $\mathcal{S}_0$ of Eq. (50). This shift modifies only the quadratic part of $\mathcal{S}_0$, producing additional bilinear terms and yielding the shifted action $\mathcal{S}_{\boldsymbol{B}_0}$ in Eq. (58). The dynamo regime is thus a nonequilibrium analogue of an ordered phase: rotational symmetry $\mathbf{SO}(3)$ is spontaneously broken down to the subgroup $\mathbf{SO}(2)$ of rotations about the axis $\boldsymbol{B}_0$. The magnitude B_0 is fixed dynamically by requiring that the curl term be canceled order by order in the dressed magnetic response, while the direction of $\boldsymbol{B}_0$ remains undetermined, in direct analogy with an order parameter in systems with a continuous symmetry.

In the model (58), the linear in the external momentum $\boldsymbol{k}$ (curl) part of the magnetic 1PI function $\Gamma^{b'b}$ has the form

$$\Gamma^{b'b}_{ij}\Big|_{\text{curl}} = \rho_1 \, \nu_0 \, (h_0 + j_0) \, k \, \mathbb{H}_{ij}(\boldsymbol{k}) + \mathcal{O}(k^2), \tag{92}$$

where $j_0 = j_0(B_0)$ is the loop-induced curl-type contribution arising from the new $\mathbf{SO}(2)$-symmetric vacuum state. The stability of the dynamo vacuum $\langle \boldsymbol{b} \rangle = \boldsymbol{B}_0$ is therefore defined by the condition

$$h_0 + j_0(B_0) = 0, \tag{93}$$

which is an implicit equation for its magnitude B_0. A few remarks are essential here.

First, Eqs. (92) and (93) are valid both for non-renormalized $\Gamma^{b'b}$, then (suitably regularized) B_0 is found at the stage of Λ-renormalization for fixed Λ, and for renormalized $\Gamma^{b'b}_R$, then all bare indices '0' in (92) and (93) are 'suppressed' and the UV-finite B found after this from (93)

is connected with B_0, found at the stage of Λ-renormalization by some fixed transformation of the UV-finite renormalization. In renormalized variables, the UV-finite two-loop result [294] can be expressed as

$$B = \nu A(u)\frac{|h|}{g_1}\left[1 - A(u)c_2^{[B]}(u)g_1 - \left(\frac{1}{2} - 2\ln\left(\frac{A(u)|h|}{\mu g_1\sqrt{u}}\right)\right)\epsilon + g_1\mathcal{C}_{\rm add}^{[h]}(u)\right]. \tag{94}$$

Here $A(u) \coloneqq 16\pi\sqrt{u}\,(1+u)$. The renormalized curl coefficient h (proportional to the helical coupling) is assumed to have the same sign as the bare one, $h_0 < 0$. The finite term $\mathcal{C}_{\rm add}^{[h]}(u)$ parametrizes the expected non-universality (subtraction-scheme dependence) of the amplitude B. This result reveals a pronounced sensitivity to the inverse magnetic Prandtl number at small u: the genuine two-loop coefficient $c_2^{[B]}(u)$ is obtained numerically and grows rapidly as $u \to 0$ (large magnetic Prandtl number), with an apparent asymptotic behaviour $c_2^{[B]}(u) \sim u^{-3/2}$, while remaining tiny for very large u. This suggests that, at very large magnetic Prandtl numbers, the naive perturbative estimate of B may receive sizable higher-loop corrections and would likely benefit from resummation or from an alternative expansion scheme.

We also stress that the explicit helicity dependence of B is weak in this setup. At one-loop order, B is independent of the helicity parameter ρ_1, and the two-loop ρ_1-dependent contribution identified in [294] is numerically tiny. This supports the interpretation that helicity is essential to trigger the curl instability and thereby to access the dynamo regime, whereas once the broken-symmetry phase is formed, the amplitude B is dominated by nonhelical loop structures. Whether a stable $\langle \boldsymbol{b}\rangle \neq \boldsymbol{0}$ phase can be realized dynamically in a strictly mirror-symmetric system remains an open question, discussed further below.

Second, we stress that helicity, not magnetic noise, triggers the dynamo: the instability mechanism and its stabilization demonstrate directly that parity breaking in the kinetic sector is sufficient to generate a nonzero mean field. Adding magnetic noise would not change the conceptual picture, but would dramatically enlarge the diagrammatics. Third, the obtained mean field B_0 or B is homogeneous within the model. This is ideal for a clean RG analysis, but also highlights a modelling limitation: realistic astrophysical and geophysical dynamos typically produce structured large-scale fields (dipolar, multipolar), which likely requires extending the stochastic setup beyond homogeneous isotropic forcing and/or including additional slow fields (rotation, stratification, boundaries).

A distinctive hallmark of the dynamo regime is that the model (58) allows additional anisotropic tensor structures to appear already in the linear-in-$\boldsymbol{k}$ asymptotics of the unrenormalized 1PI functions $\Gamma_{ij}^{v'v}$, $\Gamma_{ij}^{v'b}$, $\Gamma_{ij}^{b'v}$, and $\Gamma_{ij}^{b'b}$. The complete basis of such structures for $\Gamma_{ij}^{\alpha\beta}(\boldsymbol{k},0)\Big|_{k\to 0}$ in $d=3$ takes the form

$$\Gamma_{ij}^{\alpha\beta} \sim i\rho_1\nu_0\Big[\delta_{b'}^{\alpha}\chi_{vb}^{\beta}h_0\epsilon_{ijs}k_s + c_{01}\big[\boldsymbol{k}\times\hat{\boldsymbol{B}}_0\big]_i\hat{B}_{0j} + c_{02}\big[\boldsymbol{k}\times\hat{\boldsymbol{B}}_0\big]_j\hat{B}_{0i} + c_{03}(\boldsymbol{k}\cdot\hat{\boldsymbol{B}}_0)\epsilon_{ijs}\hat{B}_{0s}\Big]. \tag{95}$$

Here $\hat{\boldsymbol{B}}_0 \coloneqq \boldsymbol{B}_0/B_0$. The indicator $\chi_{\mu\nu}^{\beta}$ is defined as $\chi_{\mu\nu}^{\beta} \coloneqq \delta_{\mu}^{\beta} + \delta_{\nu}^{\beta} - \delta_{\mu}^{\beta}\delta_{\nu}^{\beta}$, so that $\chi_{\mu\nu}^{\beta} = 1$ if $\beta = \mu$ or $\beta = \nu$, and $\chi_{\mu\nu}^{\beta} = 0$ otherwise. The coefficients c_{0n} encode anisotropic transport effects associated with the dynamo regime; in the terminology adopted in [294], c_{01} is the exotic term, c_{02} is bizarre, and c_{03} is a drift-type structure.

The analysis [294] provides an explicit stable closed-form solution of the resistive linearized system and frames the inclusion of two-loop structures (c_{02}, c_{03}, and off-diagonal self-energies) as a controlled perturbation of the same matrix form. At the one-loop level, only the exotic term survives in the relevant linear matrix for the wave problem, with c_{01} known explicitly

from [251]. At the two-loop level additional structures enter: the two-loop correction to the exotic term, the new bizarre and drift terms (c_{02}, c_{03}), and all one-loop off-diagonal terms in the coupled $(\boldsymbol{v}, \boldsymbol{b})$ sector. The crucial stability fact proved in [294] is that only the curl structure in $\Gamma_{ij}^{b'b}$ is 'dangerous'. Any analogous curl-type contribution in $\Gamma_{ij}^{b'v}$ is IR-subleading (it appears at a higher order in the long-wavelength expansion) and therefore does not produce an exponential long-wave growth by itself. The other linear terms do not generate exponential long-wave growth by themselves. The form of the effective linear operator of the linearized system remains stable under higher-loop corrections: higher loops renormalize coefficients but do not generate new functional dependence beyond the established tensor basis. This makes the dynamo vacuum feasible: one cancels only the curl contribution via (93), while retaining $c_{01,02,03}$ as physical anisotropic transport coefficients in the linearized dynamics.

The presence of a spontaneous mean field $\boldsymbol{B}_0$ leads to Alfvén-type excitations with the familiar dispersion modified by viscosity ν_0 and resistivity $u_0\nu_0$; in the dynamo state, the propagator denominators in Eq. (59) contain functions $\xi(\boldsymbol{k}, \omega)$ explicitly defined as

$$\xi(\boldsymbol{k}, \omega) = -\omega^2 - i\omega(1+u)\nu_0 k^2 + u_0\nu_0^2 k^4 + (\boldsymbol{B}_0 \cdot \boldsymbol{k})^2, \tag{96}$$

which encodes damped Alfvén waves in resistive MHD. In addition to the exponential damping, the exotic term (already present at the one-loop level), together with drift and bizarre terms (appearing starting from the two-loop level), induces long-lived polynomial prefactors in time. Specifically, for the polarization orthogonal to the $\boldsymbol{B}_0$–$\boldsymbol{k}$ plane, the solution of the linearized equations of motion in the dynamo regime contains pulses of the form

$$\psi(t) \sim A_1 \mathrm{e}^{-\kappa_0 t} \left[(A_2 + tA_3) \sin(\omega_A t) + (A_3 + tA_4) \cos(\omega_A t) \right], \tag{97}$$

superimposed on the exponentially decaying Alfvén oscillations. Here $\psi(t)$ denotes any transverse mode from the set $\{v_2(t), v_3(t), b_2(t), b_3(t)\}$; choosing coordinates with $\boldsymbol{k} \parallel \boldsymbol{e}_1$ implies $v_1(t) = b_1(t) = 0$ by solenoidality. Furthermore, $\kappa_0 := (1+u_0)\nu_0 k^2/2$ and $\omega_A := \sqrt{D(k)}/2$, $D(k) := 4(\boldsymbol{B}_0 \cdot \boldsymbol{k})^2 - (u_0 - 1)^2 \nu_0^2 k^4$ while the (generally complex) amplitudes A_i depend on the remaining parameters of the model; explicit formulas are given in the Appendix [294]. These pulses, $\sim t\,\mathrm{e}^{-\kappa_0 t}$, can be viewed as soft (Goldstone-type) contributions associated with the broken rotational symmetry: they reflect the slow relaxation of transverse fluctuations in the anisotropic vacuum selected by $\boldsymbol{B}_0$. A technically important point is that in the ideal-MHD limit, the corresponding linearized solution contains an unavoidable weak polynomial growth, whereas finite viscosity and resistivity generate exponential damping and render the dynamo vacuum locally stable.

The turbulent dynamo regime required several genuinely new technical ingredients in the diagrammatic analysis. Compared to the kinematic regime, the number of contributing diagrams grows by orders of magnitude, and the shifted propagators lead to denominators built from functions $\xi(\boldsymbol{k}, \omega)$ in (96). These $\xi(\boldsymbol{k}, \omega)$ are stable polynomials whose roots in ω lie in the appropriate half-planes for all physically admissible values of parameters, which enables a strategy for analytic frequency integration based on stability criteria (invoking the Hermite–Biehler theorem [304]) rather than on standard Feynman-parameter tricks. It must be said that Feynman diagrams in this mode do not allow Feynman parameterization, as well as any other (Schwinger, etc.) Also, intermediate frequency integrals generate square-root structures and pole locations that depend nontrivially on loop momenta; a key check is that these 'moving poles' cancel after summing diagrams into physical combinations such as self-energies. Moreover, the appearance of $\boldsymbol{B}_0$ significantly enlarges the tensor algebra: tensor integrals must be

decomposed in a basis built from δ_{ij} and $\hat{B}_{0i}\hat{B}_{0j}$. In particular, this analysis shows that curl-type (parity-odd, linear-in-k) contributions cannot be generated in $\Gamma^{v'v}$ and $\Gamma^{v'b}$ and, more generally, do not arise in the velocity and Lorentz-force sectors of the model.

As discussed in the previous section, in the kinematic approximation, the magnetic field is passive, and the equipartition-like scaling between kinetic and magnetic energies occurs in the inertial range. The dynamo regime violates this expectation due to the appearance of an additional dimensional parameter $\boldsymbol{B}_0$. The velocity field retains its exact Kolmogorov scaling (as a consequence of the exact relation $Z_{g_1} = Z_\nu^{-3}$), while the magnetic field acquires an additional anomalous contribution from its nontrivial renormalization. The anisotropic three-dimensional energy spectra are obtained analogously to Eqs. (89) and (90).

$$E^v(\boldsymbol{k}) = \frac{1}{2}k^{-\frac{11}{3}}\, E_{\rm in}^{\frac{2}{3}}\, R^v_{ii}\left(\boldsymbol{B}\frac{k^{1/3}\mu^{\gamma_{b\star}}}{E_{\rm in}^{1/3}k^{\gamma_{b\star}}}\right), \quad E^b(\boldsymbol{k}) = \frac{1}{2}k^{-\frac{11}{3}+2\gamma_{b\star}}\, E_{\rm in}^{\frac{2}{3}}\mu^{-2\gamma_{b\star}}\, R^b_{ii}\left(\boldsymbol{B}\frac{k^{1/3}\mu^{\gamma_{b\star}}}{E_{\rm in}^{1/3}k^{\gamma_{b\star}}}\right), \quad (98)$$

where $R^{v,b}$ are nontrivial scaling functions depending also on helicity parameter ρ_1 and may also depend on the ratio k/m, where $m \sim L^{-1}$ is the inverse integral scale (IR cutoff). In the inertial range $k \gg m$, one typically finds that the dependence on k/m saturates rapidly and can be neglected to leading order; we will often suppress this argument in what follows.

From these scaling relations it is evident that the magnetic spectrum is systematically steeper than the Kolmogorov velocity spectrum. The decisive conceptual consequence is that in the dynamo regime, the velocity and magnetic sectors acquire different critical dimensions and thus equipartition between kinetic and magnetic energies is violated in a fundamental way. Note, however, that these RG predictions refer to the leading inertial-range behaviour of two-point functions. In fully developed MHD turbulence, the magnetic field is often strongly intermittent (e.g., due to sheet-like structures), and intermittency manifests itself primarily in anomalous scaling of higher-order correlators/structure functions; in finite inertial ranges this may also affect the 'effective' spectral slopes inferred from data (see, e.g., [232, 303]).

In general, the 'zeros in R-functions' issue mentioned in Sec. 4.5 is absent in the dynamo regime. The reason is that the shifted theory contains a nonvanishing magnetic correlator Δ^{bb} already at the level of the propagator matrix (see Eq. (59)), with the mean field B entering the bare propagators as an additional dimensional parameter. This differs qualitatively from the kinematic regime, where scaling functions become critically dimensional only in the special case $g^{\rm k}_{2\star} = 0$. As a result, the critical dimensions in the dynamo regime are obtained by the standard rule (83) and take the form

$$\Delta^{\rm d}_\omega = -\Delta^{\rm d}_t = 2 - \gamma^{\rm k}_{1\star}, \quad \Delta^{\rm d}_{\boldsymbol{b}} = \Delta^{\rm d}_{\boldsymbol{v}} + \gamma^{\rm k}_{3\star}/2, \quad \Delta^{\rm d}_{\boldsymbol{v}} = 1 - \gamma^{\rm k}_{1\star}, \quad \Delta^{\rm d}_{\boldsymbol{v}} + \Delta^{\rm d}_{\boldsymbol{v}'} = \Delta^{\rm d}_{\boldsymbol{b}} + \Delta^{\rm d}_{\boldsymbol{b}'} = 3. \quad (99)$$

The turbulent dynamo regime also exposes a set of open conceptual and modelling questions. In the present construction, helicity is essential to produce the curl instability in the first place. Yet, once the system is in the dynamo regime, the amplitude B appears only weakly dependent on ρ_1 (at least up to two-loop order). This motivates a sharpened question [251]: is parity breaking strictly necessary for the existence of a stable $\langle \boldsymbol{b}\rangle \neq \boldsymbol{0}$ phase, or only for selecting it dynamically from the isotropic vacuum $\langle \boldsymbol{b}\rangle = \boldsymbol{0}$? From a field-theoretic standpoint, this is naturally phrased in the language of Bogoliubov quasiaverages (see, e.g., [305]): one introduces an infinitesimal symmetry-breaking source coupled to $\boldsymbol{b}$, and considers sending this source to zero, thereby selecting a definite broken-symmetry vacuum. This problem remains open. The point is that in a strictly mirror-symmetric MHD system, curl-type (parity-odd) terms are forbidden by symmetry. In that case, both states $\langle \boldsymbol{b}\rangle = \boldsymbol{0}$ and $\langle \boldsymbol{b}\rangle = \boldsymbol{B}_0$ may be stationary with respect to small perturbations, and an additional selection criterion (analogous to minimizing

a free-energy functional in equilibrium systems) would be needed to decide which state is physically realized. As far as we know, the present class of stochastic dynamical models does not provide such a functional.

The SFT perspective also aligns the dynamo regime with broader notions of self-organization and relaxation: the spontaneous $\boldsymbol{B}$ can be viewed as a helicity-driven large-scale condensate, i.e., a relaxation of an unstable isotropic state into an ordered anisotropic state, where magnetic helicity (approximately conserved at high magnetic Reynolds number) supports an inverse transfer that builds magnetic structures at progressively larger scales and provides, in energetic terms, the possibility for a macroscopic field to emerge. In that sense, the turbulent dynamo becomes a prototypical nonequilibrium 'phase transition' with an order parameter (B), broken symmetry, and a Goldstone sector (the power-law corrections to Alfvén waves).

Closely related is the issue of how to formalize the selection of the mean-field direction. The dynamo regime fixes only B_0 via (93); its direction is arbitrary. In practice, a direction is selected by boundary conditions, rotation, weak imposed fields, or initial seeds. Here we mention the conclusion made in Ref. [306] (although on an incorrect one-loop calculation) that the presence of a small anisotropy of energy forcing into the helical turbulent system leads to the determined direction of $\boldsymbol{B}_0$.

Finally, for astrophysical applications, especially in the context of stellar magnetism, the present incompressible setup is deliberately minimal and has no explicit temperature (or entropy) dynamics, hence it cannot address how the emergent $\boldsymbol{B}$ modifies thermal transport, stratification, or buoyancy—key ingredients in stellar and planetary dynamos. A minimal extension would couple the MHD sector to an advection–diffusion equation for temperature (or entropy), together with an equation of state and a buoyancy closure (Boussinesq or anelastic approximations). In such a framework, the spontaneously generated mean field would naturally induce anisotropic turbulent transport (distinct parallel/perpendicular diffusivities) and additional cross-effects (magnetothermal couplings), potentially affecting heat flux and thus the global energetics of the object; from the RG viewpoint, this would introduce additional running couplings and new candidates for anomalous scaling in mixed correlators. These directions, together with the systematic inclusion of additional slow fields (rotation, stratification, boundaries) that can lift the degeneracy of the mean-field direction and produce structured large-scale configurations (dipolar, multipolar), constitute a natural next step toward connecting the homogeneous order-parameter realization of the dynamo regime to realistic astrophysical and geophysical settings.

5. Conclusion and outlook

Statistical field theory provides an important combination of systematicity and predictive power in turbulence research: it translates (stochastic) nonlinear evolution equations into a renormalizable functional integral, and it equips us with RG and OPE tools to organize scaling regimes, identify universality classes, and calculate anomalous dimensions and universal amplitude ratios in a controlled expansion (see, e.g., [2, 3]). In helical magnetohydrodynamics, where mirror-symmetry breaking and coupled velocity–magnetic dynamics produce an unusually rich landscape of regimes, this framework is especially appealing; at the same time, it brings into sharp focus a set of fundamental questions that remain unresolved and that, in our view, define a natural agenda for the next stage of research.

A first conceptual difficulty concerns the interpretation of the magnetic spectrum associated with the putative turbulent dynamo regime. Even if the RG analysis yields a well-defined inertial-range scaling form (and, in the presence of a mean field $\boldsymbol{B}_0$, a corresponding anisotropic

scaling function), it is not obvious to what extent this spectrum corresponds to a uniquely defined and directly measurable object in laboratory experiments or in numerical simulations with realistic forcing and unavoidable finite-size effects. Closely related is the question of whether a dynamo can exist in the limit $\rho_1 \to 0$, particularly in formulations where magnetic noise is absent. Resolving this appears to require a genuinely global selection criterion for the energetically most favourable stable state in stochastic dynamics, going beyond purely local stability considerations. In realistic settings, the answer to this formal question is most likely negative. We emphasize that we are interested in the existence of a large-scale, not a small-scale (fluctuation) dynamo, which can exist in a mirror-symmetric medium (see, e.g., [307]).

Experimental confirmation of the subtle effect associated with perturbations of Alfvén waves that may grow polynomially in time on top of an overall exponentially decaying background remains, generally speaking, an open question. However, in this regard, we note the measurements reported in [308] for torsional Alfvén waves [309] in liquid sodium, which appear qualitatively close to our predictions.

Among the most important directions for further development is to clarify the status of mean-field effects — in particular, to put the α-effect on the same field-theoretic footing as inertial-range scaling. In mean-field dynamo theory, the turbulent electromotive force, $\mathcal{E}(\boldsymbol{x},t) := \langle \boldsymbol{v}(\boldsymbol{x},t) \times \boldsymbol{b}(\boldsymbol{x},t) \rangle$, is often parameterized, in the simplest closure, as $\mathcal{E} = \alpha_0 \boldsymbol{B}_0$ for a prescribed mean field $\boldsymbol{B}_0$. In the SFT approach adopted here, the diagrammatic expansion provides a direct route to a representation of this type and, crucially, allows one to compute the RG scaling of both the prefactor and the composite operator itself. Technically, this requires a systematic renormalization of the operator family with canonical dimension 2, and thus a dedicated OPE/RG analysis of this family. At the same time, going beyond the α-effect ultimately calls for a space- and time-dependent mean field $\boldsymbol{B}_0(\boldsymbol{x},t)$; implementing this goes beyond the present constant-$\boldsymbol{B}_0$ setup and suggests extensions in the spirit of Kraichnan-type constructions with additional large-scale randomness [135, 255] or multi-scale mean-field formulations. From the empirical perspective, a targeted measurement of $\boldsymbol{v}(\boldsymbol{x},t) \times \boldsymbol{b}(\boldsymbol{x},t)$ together with the emerging large-scale field $\boldsymbol{B}_0$ in [222] provides a relatively direct estimate of α_0, whereas measurements aimed at the critical dimension of $\boldsymbol{v}(\boldsymbol{x},t) \times \boldsymbol{b}(\boldsymbol{x},t)$ (or related composite operators) appear, to the best of our knowledge, to be essentially unexplored.

Beyond critical exponents, a major physical challenge is to understand the turbulent cascade in MHD — including the constraints imposed by helicity, the coexistence of direct and inverse transfers, and the partition of injected power between kinetic and magnetic channels — since these issues are central to any dynamo scenario in which magnetic energy is reorganized across scales. Addressing this within the field-theoretic framework likely requires a generalization to a model with a full matrix of forcing correlators specified by an essentially arbitrary kernel, rather than by a restricted ansatz. In particular, for purely kinetic forcing (with no magnetic noise), it should be possible to derive self-consistency relations analogous to those obtained in [250] for the stochastic hydrodynamic turbulence model and thereby reconstruct, at least partially, the effective pumping profile in the energy-containing and inertial ranges.

In parallel, the computation of universal amplitude factors for paired correlators — MHD analogues of the Kolmogorov constant — is important in its own right. A promising strategy is to extract such constants from universal ratios (for example, via inertial-range skewness) rather than to attempt a direct perturbative calculation of the constants themselves [108]. For MHD, the relevant exact third-order relations are not Kolmogorov's 4/5 law but the Politano–Pouquet exact laws (10); implementing an analogous program therefore requires perturbative control over the remaining composite-operator contributions that enter those exact relations.

A particularly intriguing theoretical issue arises at the physical value $a = 1$ in the extended stochastic MHD theory with magnetic noise. RG analysis admits two infrared-attractive fixed points already in the mirror-symmetric setting, and for $a = 1$, these two fixed points may coexist as admissible scaling regimes. This immediately poses a basic conceptual question that is especially pronounced in the context of dynamo physics: which of these fixed points, if any, corresponds to the dynamo regime? Is the dynamo to be identified with the kinetic fixed point, or is the turbulent dynamo scenario realized at the magnetic one (with a finite magnetic forcing charge), or is the relevant selection principle not captured by the perturbative fixed-point?

Another direction in which structural insight may be gained is the study of the asymptotic limit $d \to \infty$, where, as in ordinary turbulence, many calculations are significantly simplified and where one can probe the robustness of perturbative conclusions. In particular, such an analysis may shed light on the long-standing problem of renormalization of the interaction parameter A in the paradigmatic A-model of generalized coupling to an active vector admixture introduced in [310]: one-loop estimates suggest an absence of A renormalization, yet this feature does not appear to be protected by any known symmetry and thus calls for a deeper explanation.

Finally, there are clear gaps in the existing SFT literature that are directly relevant to helical MHD. A full field-theoretic analysis of two-dimensional helical MHD, parallel to what has been developed for the mirror-symmetric case [296], appears to be missing; in this setting, additional ultraviolet subtleties arise, including the renormalization of operators of the schematic form $\langle \boldsymbol{v}' \otimes \boldsymbol{v}' \rangle$ and $\langle \boldsymbol{b}' \otimes \boldsymbol{b}' \rangle$. Moreover, the present model (12)–(14) employs an effectively trivial equation of state: density and temperature dynamics are absent (or frozen), and transport coefficients are treated as prescribed. For many astrophysical dynamos, however, the coupling between turbulence, temperature/entropy fluctuations, and magnetic fields is widely regarded as crucial — for instance, through convection, stratification, and temperature-dependent transport — with stellar magnetism providing a particularly compelling motivation [215]. A natural and important extension is therefore to enrich the model by adding an explicit temperature or entropy field (as an active scalar), together with an energy equation and, depending on the regime of interest, Boussinesq or anelastic constraints, buoyancy forcing, and possibly rotation. Such a generalization would facilitate addressing SFT questions that are currently out of reach, including how thermal fluctuations renormalize turbulent transport coefficients, how they modify the EMF and large-scale dynamo thresholds, and how temperature-dependent microphysics feeds back into inertial-range magnetic spectra.

Acknowledgements

The authors have greatly benefited from mutual collaborations and many valuable discussions with Loran Ts. Adzhemyan and Juha Honkonen.

Funding

The work was supported by VEGA Grant No. 1/0297/25 of the Ministry of Education, Science, Research and Sport of the Slovak Republic.

Conflicts of Interest

The authors declare no conflicts of interest.

6. Abbreviations

The following abbreviations are used in this manuscript:

BBGKY	Bogoliubov–Born–Green–Kirkwood–Yvon (chain)
BRST	Becchi-Rouet-Stora-Tyutin (symmetry)
DES	Detached eddy simulation
DIA	Direct interaction approximation
DNS	Direct numerical simulation
DPD	Dissipative particle dynamics
DSMC	Direct simulation Monte Carlo (method)
EDQNM	Eddy-damped quasi-normal Markovian (approximation)
EMF	Electromotive force
FRG	Functional (nonperturbative) renormalization group
GS95	Golderich–Shridar 1995 theory of MHD turbulence
ICM	Intracluster medium
IR	Infrared
ISM	Interstellar medium
K41	Kolmogorov's 1941 theory of turbulence
LBM	Lattice Boltzmann method
LES	Large eddy simulation
MHD	Magnetohydrodynamics
MS	Minimal subtraction (scheme)
MSRJD	Martin–Siggia–Rose–Janssen–De Dominicis (formalism)
MRI	Magnetorotational instability
NS	Navier–Stokes (equation)
OPE	Operator product expansion
1PI	One-particle irreducible (Green's function)
PDF	Probability density function
POD	Proper orthogonal decomposition
QFT	Quantum field theory
RANS	Reynolds-averaged Navier–Stokes (models)
RG	Renormalization group
RSM	Reynolds stress model
SFT	Statistical field theory
SPDE	Stochastic partial differential equation
SRS	Scale-resolving simulation
TSDIA	Two-scale direct interaction approximation
UV	Ultraviolet

Appendix A. Order-of-magnitude estimates for the typical plasma parameters

Table A.1 summarises order-of-magnitude estimates for a set of MHD plasmas that can reasonably be regarded as measurable. For each class of conducting media, we select a representative example and quote parameter values commonly used in the literature and in numerical modelling. The underlying literature is vast; accordingly, we do not aim for precision and report only indicative magnitudes compiled from accessible published sources. These numbers should be interpreted as rough benchmarks: even for a given astrophysical object, the relevant parameters may vary by one–two orders of magnitude depending on location, epoch, and modelling assumptions. When a plausible range is available, we report the typical value. The 'Ion' column lists the predominant ion species; minor constituents, impurities, and dust are neglected. For the magnetic field, we provide both a characteristic flow-scale value δB (representing typical fluctuations) and an estimate of the largest-scale mean field $\langle B_0\rangle$. A substantial separation between these two amplitudes is usually indicative of large-scale field generation by dynamo action (see Table 1).

Section 2 summarises the applicability conditions for a single-fluid, non-relativistic, resistive-MHD description with scalar (isotropic) kinematic viscosity ν_0 and magnetic diffusivity $\nu_{\mathrm{m}0}$, governed by Eqs. (4)–(5). Collecting the requirements, one may express them as the following strong inequalities

$$\begin{aligned} &\ell \gg \{\lambda_{\mathrm{mfp}}, \lambda_D\,(\text{or } \lambda_{TF}), \lambda_{Li}, d_e, d_i\} \quad \text{and} \quad \tau \gg 2\pi/\{\omega_{\mathrm{col}}, \omega_{pe}, \omega_{pi}, \Omega_{ce}, \Omega_{ci}\} \\ &\text{for} \qquad \max(u, u_A, c_s) \ll c \qquad \text{together with} \qquad \{\Omega_{ce}/2\pi\nu_e,\ \Omega_{ci}/2\pi\nu_i\} \ll 1. \end{aligned} \tag{A.1}$$

The key here is the last two inequalities representing the weak magnetization criterion, separating simple isotropic resistive-MHD from the much more cumbersome anisotropic science. Although many media listed in Table 1 violate this criterion, several important classes listed in Table A.2 are described by Eqs. (4)–(5) with good accuracy. Moreover, as noted in Sec. 2, even when the scalar closure is not strictly justified, the same equations often remain a useful model for the inertial-range turbulent cascade at sufficiently large scales. For the systems considered below we assume full ionisation and estimate the remaining characteristic parameters either from standard kinetic (Spitzer-type) formulae for dilute plasmas [343] (see also [160, 161]) or from experimentally measured transport coefficients (liquid metals).

Let T_α and n_α denote typical temperatures and number densities of species $\alpha = e, i$, and let u and B_0 be characteristic flow and magnetic-field amplitudes (e.g., one may take $u = u_{\mathrm{th},e}$ in a classical plasma or $u = u_F$ for a degenerate electron liquid). Given these inputs, one can estimate the microscopic scales entering (A.1), as well as the transport coefficients $\nu_0 = \mu_0/\rho_0$ and $\nu_{\mathrm{m}0} = c^2/(4\pi\sigma_0)$. For length scales,

$$\begin{gathered} \lambda_{\mathrm{mfp}} = \max_\alpha(\lambda_{\mathrm{mfp},\alpha}), \qquad \lambda_{\mathrm{mfp},\alpha} = u/\nu_\alpha, \qquad r_{L\alpha} = u/\Omega_{c\alpha}, \qquad d_\alpha = c/\omega_{p\alpha}, \\ \lambda_D = \sqrt{\frac{k_{\mathrm{B}}}{4\pi e^2}\frac{T_i T_e}{(n_e T_i + n_i T_e)}}, \qquad \lambda_{TF} = \sqrt{\frac{1}{4\pi e^2}\left(\frac{\partial n_e}{\partial \mu_e}\right)_T}, \end{gathered} \tag{A.2}$$

where μ_e is the electron chemical potential and k_{B} is the Boltzmann constant. For simple metals (e.g., Na) the free-electron approximation is often adequate, yielding $\lambda_{TF} = \sqrt{E_F/(6\pi n_e e^2)}$ in terms of the Fermi energy E_F. For speed scales we take

$$u_{\mathrm{th},\alpha} = \sqrt{\frac{2k_{\mathrm{B}}T_\alpha}{m_\alpha}}, \qquad u_F = \left\langle \frac{1}{\hbar}\boldsymbol{\nabla}_{\boldsymbol{k}}\varepsilon(\boldsymbol{k})\Big|_{\mathrm{FS}} \right\rangle_{\mathrm{FS}}, \quad u_A = \frac{B_0}{\sqrt{4\pi\rho_0}}, \qquad c_s = \sqrt{\left(\frac{\partial p_0}{\partial \rho_0}\right)_S}, \tag{A.3}$$

Table A.1. Order-of-magnitude parameters for representative MHD plasmas. Values are indicative and compiled from the literature cited in the notes. The mass number $A_{\rm Ion} \approx m_i/m_p$ represents the ion mass in units of proton mass m_p.

	Conducting medium	Specific example	Ion	$A_{\rm Ion}$	n_e [cm^{-3}]	$k_{\rm B}T_e$ [eV]	δB [G]	$\langle B_0\rangle$ [G]
Astrophysical and cosmic plasmas	Interstellar medium	Dense molecular cloud core[a]	HCO^+	29	1×10^{-3}	9×10^{-4}	2×10^{-4}	8×10^{-6}
	Accretion disks	Cyg X-1 corona[b]	H^+	1	1×10^{17}	7×10^{4}	1×10^{5}	1×10^{5}
	Stellar convective zones	Half Sun's convective zone[c]	H^+	1	3×10^{22}	8×10	4×10^{3}	10
	Jets & supernova remnants	Supernova remnant W51C[d]	H^+	1	1×10^{-1}	1×10^{3}	1×10^{-4}	1×10^{-5}
	Intracluster medium	Hot plasma in ICM[e]	H^+	1	1×10^{-3}	6×10^{3}	1×10^{-5}	1×10^{-6}
	Solar corona	Coronal loop[f]	H^+	1	5×10^{9}	1×10^{2}	3×10	3
	Solar wind	Slow wind at 1 AU[g]	H^+	1	1	10	3×10^{-5}	3×10^{-5}
	Magnetospheric magnetosheath	Earth magnetosheath[h]	H^+	1	2×10	2×10	2×10^{-4}	2×10^{-4}
	Large-scale reconnection region	Central plasma sheet[i]	H^+	1	3×10^{-1}	5×10^{2}	2×10^{-4}	2×10^{-4}
Planetary bowels	Liquid outer core of a planet	Earth[j]	Fe^+	56	1×10^{23}	4×10^{-1}	2×10	3
	Ionospheric-magnetospheric current systems on planets	Earth F region[k]	O^+	16	1×10^{5}	1×10^{-1}	1×10^{-3}	5×10^{-1}
Laboratory systems	Liquid metal flows	Liquid Na[l]	Na^+	23	2×10^{22}	3×10^{-2}	4×10	4×10
	Tokamaks & spheromaks	ITER-like tokamak core[m]	D^+	2	1×10^{14}	2×10^{4}	2×10	5×10^{4}
	MHD pumps & electromagnetic braking	Liquid Na[n]	Na^+	23	2×10^{22}	4×10^{-2}	6×10	6×10^{3}
	Liquid metal batteries	Liquid Na[o]	Na^+	23	2×10^{22}	6×10^{-2}	1	10

Notes. In all particular examples listed, $Z = 1$, the assumptions of electroneutrality $n_e \simeq n_i$ and and temperature equilibration $T_e \simeq T_i$ hold to order of magnitude.

[a] Dense/dark molecular clouds are predominantly neutral (70% of cloud mass is H_2); the weakly ionised component is mainly HCO^+ produced by cosmic-ray ionisation [311]. We take $T_e \approx T_{\rm kin} \sim 10\,{\rm K}$ and estimate n_e from $n({\rm H_2}) \sim 10^4$–$10^5\,{\rm cm^{-3}}$ (cloud density) and an electron fraction in nuclei for low mass cores $x(e) \sim 10^{-8}$–10^{-6} [311]. The characteristic field strength is consistent with the empirical scaling $B \propto n_H^{0.65}$ at $n_H \sim 2\,n({\rm H_2})$, giving $\delta B \sim 10^2\,\mu{\rm G}$ [312]. As a representative large-scale mean field we adopt $\langle B_0\rangle \sim 5$–$15\,\mu{\rm G}$ from *Planck* polarisation analyses [313].

[b] Electron temperature T_e and Thomson optical depth τ_T for a one-zone corona are taken from [314]; δB corresponds to the same one-zone estimate, there is an alternative, higher-field scenario with $\delta B \sim 10^7$ [315]. In this simplified corona model, we cannot distinguish a separate mean and fluctuating field component. The electron density is inferred from $\tau_T \simeq 2.5$ via $\tau_T = n_e\sigma_T H$ with $\sigma_T = 8\pi e^2/3m_ec^2$ the Thomson cross section and a characteristic scale height $H \sim 10r_g$, where $r_g = GM_{\rm BH}/c^2$ and $M_{\rm BH} \simeq 21\,M_\odot$ is the approximate Cyg X-1 black hole mass [316] (with $M_\odot$ is the solar mass).

[c] At $r = 0.85\,R_\odot$, the electron density n_e is taken from [317], and the temperature is estimated using the local sound speed c_s from [317] with an ideal-gas relation (taking a mean molecular weight and $\gamma = 5/3$), yielding $T_e \simeq T_{\rm kin} \approx m_ic_s^2/\gamma k_{\rm B} \sim 10^6\,{\rm K}$. A characteristic small-scale field is estimated from equipartition, giving $\delta B \sim 10^3$–$10^4\,{\rm G}$ for $\rho \simeq 5.4\times10^{-2}\,{\rm g\,cm^{-3}}$ and convective speeds $v_c \sim 10$–$100\,{\rm m\,s^{-1}}$ [318], while the large-scale mean field is taken as $\langle B_0\rangle \sim 10$–$30\,{\rm G}$ [319].

[d] Electron density and temperature are adopted from [320]; the magnetic field estimates are taken from [321], with a characteristic fluctuation level $\delta B \sim 150\,\mu{\rm G}$ and a large-scale mean field $\langle B_0\rangle \sim 15\,\mu{\rm G}$.

[e] For the intracluster medium we adopt n_e and T from [322] (with $T \sim 10^7$–$10^8\,{\rm K}$); a characteristic small-scale field in cool-core regions is taken as $\delta B \sim 10$–$40\,\mu{\rm G}$ [323], while the large-scale mean field is $\langle B_0\rangle \sim 1\,\mu{\rm G}$ [324].

[f] For a representative coronal loop we take $n_e \sim 10^9$–$10^{10}\,{\rm cm^{-3}}$ and T from [325]; the flow-scale field is estimated at the order-of-magnitude level from equipartition using typical loop densities $\rho \sim 10^{-15}$–$10^{-14}\,{\rm g\,cm^{-3}}$ and velocities $v \sim 20\,{\rm km\,s^{-1}}$ [325], and the large-scale mean field is adopted from [326].

[g] Solar-wind parameters at 1 AU are taken from [244].

[h] The values of the typical electron density and electron temperature ($T_e \sim 10 - 30\,{\rm eV}$) are taken from [327]. Note that $T_e \simeq T_i$ is not satisfied here; on the contrary, $T_i/T_e \simeq 6 - 7$ [328]. The small- and large-scale field strengths are comparable [328].

[i] Central plasma sheet parameters (n_e and T_e) are taken from [329]; the region is ion-dominated with $T_i/T_e \sim 7$–8 and $T_e \simeq T_i$ is not satisfied here. The characteristic fluctuation field is taken to be comparable (in order of magnitude) to the large-scale field [330].

[j] For the Earth's liquid outer core we estimate $n_e \simeq n_i = \rho N_A/A_{\rm Fe}$, where N_A is the Avogadro constant, the mass density of liquid core $\rho \simeq 12.5\,{\rm g\,cm^{-3}}$ and $A_{\rm Fe} = 56$ [331]; the temperature estimate is adopted from [332], and magnetic-field magnitudes from [333].

[k] Representative F-region values of n_e and T_e are taken from [334]; the small-scale magnetic perturbation level is adopted from [335], while the large-scale mean field is taken as the typical surface geomagnetic field, $\langle B_0\rangle \simeq 0.5\,{\rm G}$.

[l] For liquid sodium at the operating temperature $T \simeq 393\,{\rm K}$ (slightly above the melting point) we take $T_e \approx T$ and estimate $n_e \simeq n_i = \rho N_A/A_{\rm Na}$, where N_A is the Avogadro constant, $\rho \simeq 0.93\,{\rm g\,m^{-3}}$ is the mass density of ionic liquid at $T = 393\,{\rm K}$ and $A_{\rm Na} = 23$ [336]; magnetic-field magnitudes are adopted from [219].

[m] ITER-like core parameters are taken from [337] (n_e and $\langle B_0\rangle$) and [338] (T_e); a typical level of magnetic fluctuations in tokamaks is $\delta B/\langle B_0\rangle \sim 10^{-4}$–$10^{-3}$ (see, e.g., [339]).

[n] For liquid sodium at $T = 473\,{\rm K}$ (operating temperature) we take $T_e \approx T$ and estimate $n_e \simeq n_i = \rho N_A/A_{\rm Na}$, where the liquid sodium density at $T = 473\,{\rm K}$ is $\rho \simeq 0.90\,{\rm g\,cm^{-3}}$ and $A_{\rm Na} = 23$; the characteristic and mean magnetic fields are taken to be comparable in order of magnitude [340].

[o] For liquid sodium at $T \simeq 748\,{\rm K}$ (operating temperature) we take $T_e \approx T$ and estimate $n_e \simeq n_i = \rho N_A/A_{\rm Na}$, where $\rho \simeq 0.83\,{\rm g\,cm^{-3}}$ at $T = 748\,{\rm K}$ and $A_{\rm Na} = 23$ [341]; a representative fluctuation level is $\delta B \sim 0.1\,\langle B_0\rangle$ [342], and the mean field is commonly set by the self-generated azimuthal current field (order 1–10 G for typical current densities and cell radii) [341].

Table A.2. Kinetic length, time scales, and scalar transport coefficients for systems in Table 1 where simple resistive MHD applies

Conducting medium	$\lambda_{\rm mfp}$ [cm]	$\lambda_D\,(\lambda_{TF})$ [cm]	λ_{Li} [cm]	d_e [cm]	$\omega_{\rm col}$ [$\rm s^{-1}$]	ω_{pe} [$\rm s^{-1}$]	Ω_{ce} [$\rm s^{-1}$]	ν_i [$\rm s^{-1}$]	ν_e [$\rm s^{-1}$]	$u_{{\rm th},e}\,(u_F)$ [$\rm cm\,s^{-1}$]	u_A [$\rm cm\,s^{-1}$]	c_s [$\rm cm\,s^{-1}$]	$\frac{\Omega_{ce}}{2\pi\nu_e}$	ν_0 [$\rm cm^2\,s^{-1}$]	$\nu_{\rm m0}$ [$\rm cm^2\,s^{-1}$]	$l_{\rm min}$ [cm]	$\tau_{\rm min}$ [s]
Half Sun's convective zone	9×10^{-7}	3×10^{-8}	1×10^{2}	3×10^{-6}	1×10^{16}	1×10^{16}	2×10^{8}	1×10^{13}	2×10^{15}	5×10^{8}	1×10^{1}	2×10^{7}	2×10^{-8}	5×10^{0}	2×10^{4}	1×10^{3}	5×10^{-15}
Earth's liquid core	2×10^{-8}	5×10^{-9}	2×10^{2}	2×10^{-6}	5×10^{16}	2×10^{16}	5×10^{7}	5×10^{12}	8×10^{15}	2×10^{8}	3×10^{-1}	3×10^{5}	1×10^{-9}	1×10^{-3}	2×10^{4}	2×10^{3}	1×10^{-15}
Liquid Na flow	2×10^{-7}	8×10^{-9}	3×10^{0}	4×10^{-6}	3×10^{14}	8×10^{15}	7×10^{8}	1×10^{12}	5×10^{13}	1×10^{8}	1×10^{1}	3×10^{5}	2×10^{-6}	1×10^{-2}	7×10^{2}	3×10^{1}	8×10^{-15}
MHD pump (liquid Na)	2×10^{-7}	8×10^{-9}	2×10^{-2}	4×10^{-6}	5×10^{14}	8×10^{15}	1×10^{11}	2×10^{12}	7×10^{13}	1×10^{8}	2×10^{3}	3×10^{5}	2×10^{-4}	6×10^{-3}	1×10^{3}	2×10^{-1}	6×10^{-15}
Liquid Na battery	1×10^{-7}	8×10^{-9}	2×10^{1}	4×10^{-6}	8×10^{14}	8×10^{15}	2×10^{8}	2×10^{12}	1×10^{14}	1×10^{8}	3×10^{0}	3×10^{5}	2×10^{-7}	3×10^{-3}	2×10^{3}	2×10^{2}	8×10^{-15}

where $\langle\bullet\rangle_{\rm FS}$ denotes an average over the Fermi surface (FS), $\varepsilon(\boldsymbol{k})$ is the electronic dispersion relation, and $\hbar$ is the reduced Planck constant. For fully ionised media we take $\rho_0 \simeq n_i m_i$.[36] In the free-electron approximation $u_F = \sqrt{2E_F/m_e}$. As a rough equation of state we use either the classical ideal-gas form $p_0 \simeq n_e k_{\rm B}(T_e + T_i)$ or, for a degenerate electron liquid, $p_0 \simeq n_i k_{\rm B} T_i + (2/5)\, n_e E_F$ (for Na we take $E_F \simeq 3.24\,\rm eV$). Accordingly, for order-of-magnitude purposes we approximate $c_s \simeq \sqrt{\gamma p_0/\rho_0}$ with $\gamma = 5/3$. For characteristic frequencies,

$$\omega_{\rm col} = 2\pi \max_{\alpha}(\nu_\alpha), \quad \omega_{pe} = \sqrt{\frac{4\pi n_e e^2}{m_e}}, \quad \omega_{pi} = \sqrt{\frac{4\pi n_i Z^2 e^2}{m_i}}, \quad \Omega_{ce} = \frac{eB_0}{m_e}, \quad \Omega_{ci} = \frac{ZeB_0}{m_i}. \tag{A.4}$$

In the environments considered in Table A.1, T_e and T_i typically differ by at most an order of magnitude, implying $u_{{\rm th},e} \gg u_{{\rm th},i}$ because $m_e/m_i \ll 1$. Consequently, one usually has $d_e \gg d_i$, $\omega_{pe} \gg \omega_{pi}$, $\Omega_{ce} \gg \Omega_{ci}$, and $\Omega_{ce}/(2\pi\nu_e) \gg \Omega_{ci}/(2\pi\nu_i)$.

For dilute classical plasmas we employ standard Spitzer-type estimates,

$$\mu_0 = 0.96\frac{n_i k_{\rm B} T_i}{\nu_i}, \quad \sigma_0 = \frac{e^2 n_e}{m_e \nu_e}, \quad \nu_i = \frac{2\sqrt{2\pi}}{3}\frac{n_i e^4 \ln\Lambda_{\rm C}}{m_i^{1/2}(k_{\rm B}T_i)^{3/2}}, \quad \nu_e = \frac{2\sqrt{2\pi}}{3}\frac{(2Z+1) n_e e^4 \ln\Lambda_{\rm C}}{m_e^{1/2}(k_{\rm B}T_e)^{3/2}}, \tag{A.5}$$

where $\ln\Lambda_{\rm C}$ is the Coulomb logarithm, often estimated as $\ln\Lambda_{\rm C} \simeq \ln N_D$ with $N_D \coloneqq (4\pi/3)\, n_e\, \lambda_D^3$; for order-of-magnitude estimates it is customary to take $\ln\Lambda_{\rm C} \sim 10$–$20$.

For liquid metals, μ_0 and σ_0 are typically taken from measurements. For liquid sodium we use the approximated from experiment temperature dependences from [344] for $\mu_{0\,\rm Na}(T)$ and from [345] for $\rho_{\rm Na}(T) \coloneqq \sigma_0^{-1}(T)$. They are valid up to $\gtrsim 1000$ degrees Celsius

$$\begin{aligned} \mu_{0\,\rm Na}\big(T[\rm K]\big) &= 3.65\times10^{-5} + 0.17\,T[\rm K]^{-1} - 4.57\times10^{1}\,T[\rm K]^{-2} + 2.87\times10^{4}\,T[\rm K]^{-3}, \\ \rho_{\rm Na}\big(T[^\circ\rm C]\big) &= 6.37 + 2.87\times10^{-2}\,T[^\circ\rm C] + 1.84\times10^{-5}\,T[^\circ\rm C]^2 + 5.16\times10^{-9}\,T[^\circ\rm C]^3, \end{aligned} \tag{A.6}$$

where $\mu_{0,\rm Na}$ is in $\rm Pa\,s$ and $\rho_{\rm Na}$ is in $\mu\Omega\,\rm cm$.

In liquid metals, the momentum-relaxation frequencies ν_e and ν_i were estimated as follows: ν_e was obtained in the spirit of the Drude theory (the second formula in (A.5)) from the measured σ_0, while for ions we adopted the rough estimate $\nu_i \sim u_{{\rm th},i}/a$ with $a \sim n_i^{-1/3}$. For the liquid-metal systems considered here one typically has $\nu_e \gg \nu_i$ and $\Omega_{ce} \gg \Omega_{ci}$, so these approximations suffice for order-of-magnitude purposes.

Finally, we define conservative minimal scales of simple resistive MHD applicability as

$$l_{\rm min} = \max(\lambda_{\rm mfp}, \lambda_D\,(\text{or } \lambda_{TF}), \lambda_{Li}, d_e, d_i), \quad \tau_{\rm min} = \max\left(2\pi/\{\omega_{\rm col}, \omega_{pe}, \omega_{pi}, \Omega_{ce}, \Omega_{ci}\}\right). \tag{A.7}$$

[36] In weakly ionised media one should instead use $\rho_0 \simeq nm$, where n and m refer to the predominant neutral component.

References

[1] L. T. Adzhemyan, N. V. Antonov, A. N. Vasil'ev, Quantum field renormalization group in the theory of fully developed turbulence, Physics-Uspekhi 39 (1996) 1193–1219, https://ufn.ru/en/articles/1996/12/a/. doi:10.1070/PU1996v039n12ABEH000183.

[2] L. Adzhemyan, A. N. Vasiliev, N. V. Antonov, The field theoretic renormalization group in fully developed turbulence, Gordon & Breach, 1999.

[3] A. N. Vasil'ev, The field theoretic renormalization group in critical behavior theory and stochastic dynamics, Chapman & Hall/CRC, 2004.

[4] W. D. McComb, Theory of turbulence, Reports on Progress in Physics 58 (10) (1995) 1117, https://dx.doi.org/10.1088/0034-4885/58/10/001. doi:10.1088/0034-4885/58/10/001.

[5] W. D. McComb, The physics of fluid turbulence, Oxford University Press, 1990.

[6] V. Yakhot, S. A. Orszag, Renormalization-group analysis of turbulence, Physical Review Letters 57 (1986) 1722–1724, https://link.aps.org/doi/10.1103/PhysRevLett.57.1722. doi:10.1103/PhysRevLett.57.1722.

[7] V. Yakhot, S. Orszag, Renormalization group analysis of turbulence. I. Basic theory, Journal of Scientific Computing 1 (1986) 3–51, https://doi.org/10.1007/BF01061452. doi:10.1007/BF01061452.

[8] R. H. Kraichnan, An interpretation of the Yakhot-Orszag turbulence theory, Physics of Fluids 30 (1987) 2400–2405. doi:10.1063/1.866130.

[9] E. V. Teodorovich, On the Yakhot-Orszag theory of turbulence, Fluid Dynamics 29 (1994) 770–779. doi:10.1007/BF02040784.

[10] G. L. Eyink, The renormalization group method in statistical hydrodynamics, Physics of Fluids 6 (1994) 3063–3078. doi:10.1063/1.868131.

[11] Y. Zhou, Turbulence theories and statistical closure approaches, Physics Reports 935 (2021) 1–117, https://www.sciencedirect.com/science/article/pii/S0370157321002763. doi:https://doi.org/10.1016/j.physrep.2021.07.001.

[12] L. Canet, Functional renormalisation group for turbulence, Journal of Fluid Mechanics 950 (2022) P1. doi:10.1017/jfm.2022.808.

[13] D. Biskamp, Magnetohydrodynamic turbulence, Cambridge University Press, 2003.

[14] A. Beresnyak, A. Lazarian, Turbulence in magnetohydrodynamics, De Gruyter, 2019.

[15] G. Parisi, Statistical field theory, Addison-Wesley, 1988.

[16] J. Zinn-Justin, Quantum Field Theory and Critical Phenomena, 5th Edition, Oxford University Press, 2021.

[17] J. Zinn-Justin, Phase transitions and renormalization group, Oxford University Press, 2007.

[18] D. J. Amit, V. Martín-Mayor, Field theory, the renormalization group, and critical phenomena, 3rd Edition, WSP, 2005.

[19] U. C. Täuber, Critical dynamics: a field theory approach to equilibrium and non-equilibrium scaling behavior, Cambridge University Press, 2014.

[20] A. Kamenev, Field theory of non-equilibrium systems, Cambridge University Press, 2011.

[21] G. Eyink, Turbulence noise, Journal of Statistical Physics 83 (1996) 955–1019. doi:10.1007/BF02179551.

[22] M. Hnatič, J. Honkonen, T. Lučivjanský, Advanced field-theoretical methods in stochastic dynamics and theory of developed turbulence, Acta Physica Slovaca 66 (2016) 69. arXiv:1611.06741.

[23] C. Aron, D. G. Barci, L. F. Cugliandolo, Z. G. Arenas, G. S. Lozano, Dynamical symmetries of Markov processes with multiplicative white noise, Journal of Statistical Mechanics: Theory and Experiment 2016 (5) (2016) 053207, https://doi.org/10.1088%2F1742-5468%2F2016%2F05%2F053207. doi:10.1088/1742-5468/2016/05/053207.

[24] P. C. Martin, E. D. Siggia, H. A. Rose, Statistical dynamics of classical systems, Physical Review A 8 (1973) 423–437, https://link.aps.org/doi/10.1103/PhysRevA.8.423. doi:10.1103/PhysRevA.8.423.

[25] H. Janssen, On a lagrangian for classical field dynamics and renormalization group calculations of dynamical critical properties, Journal of Physics B 23 (1976) 377, https://doi.org/10.1007/BF01316547. doi:10.1007/BF01316547.

[26] C. De Dominicis, Techniques de renormalisation de la théorie des champs et dynamique des phénomènes critiques, Le Journal de Physique Colloques 37 (1976) 247–253. doi:10.1051/jphyscol:1976138.

[27] A. Vasil'ev, Functional methods in quantum field theory and statistical physics, Gordon and Breach, 1998.

[28] I. Montvay, G. Münster, Quantum fields on a lattice, Cambridge University Press, 1994.

[29] J. Smit, Introduction to quantum fields on a lattice, Vol. 15 of Cambridge Lecture Notes in Physics, Cambridge University Press, 2002.

[30] A. L. Kataev, K. V. Stepanyantz, Algebraic structure of the renormalization group in the renormalizable QFT theories, International Journal of Modern Physics A 39 (2024) 2445001. doi:10.1142/S0217751X24450015.

[31] M. Mariño, Instantons and large N: An introduction to non-perturbative methods in quantum field theory, Cambridge University Press, 2015.

[32] L. T. Adzhemyan, J. Honkonen, M. V. Kompaniets, A. N. Vasil'ev, Improved ϵ expansion for three-dimensional turbulence: Two-loop renormalization near two dimensions, Physical Review E 71 (2005) 036305, https://link.aps.org/doi/10.1103/PhysRevE.71.036305. doi:10.1103/PhysRevE.71.036305.

[33] J. Henriksson, The critical O(N) CFT: Methods and conformal data, Physics Reports 1002 (2023) 1–72, https://doi.org/10.1016/j.physrep.2022.12.002. doi:10.1016/j.physrep.2022.12.002.

[34] C. De Dominicis, I. Giardina, Random fields and spin glasses: A field theory approach, Cambridge University Press, 2006.

[35] M. C. Angelini, Real-space renormalization group for spin glasses, arXiv preprint (Feb. 2023). arXiv:2302.05292.

[36] N. V. Antonov, A. A. Ignatieva, Critical behaviour of a fluid in a random shear flow: Renormalization group analysis of a simplified model, Journal of Physics A 39 (44) (2006) 13593–13620, https://doi.org/10.1088/0305-4470/39/44/001. doi:10.1088/0305-4470/39/44/001.

[37] N. V. Antonov, A. V. Malyshev, Inertial-range behavior of a passive scalar field in a random shear flow: Renormalization group analysis of a simple model, Journal of Statistical Physics 146 (2012) 33–55, https://doi.org/10.1007/s10955-011-0399-0. doi:10.1007/s10955-011-0399-0.

[38] L. Schäfer, Excluded volume effects in polymer solutions: As explained by the renormalization group, Springer, 1999. doi:10.1007/978-3-642-60093-7.

[39] T. A. Vilgis, Polymer theory: Path integrals and scaling, Physics Reports 336 (3) (2000) 167–254, https://doi.org/10.1016/S0370-1573(99)00122-2. doi:10.1016/S0370-1573(99)00122-2.

[40] J. Qin, D. C. Morse, Renormalized one-loop theory of correlations in disperse polymer blends, The Journal of Chemical Physics 130 (22) (2009) 224902, https://doi.org/10.1063/1.3124799. doi:10.1063/1.3124799.

[41] S. Metayer, S. Teber, Field-theory approach to flat polymerized membranes, Journal of Statistical Mechanics: Theory and Experiment (2025) 092001, https://doi.org/10.1088/1742-5468/add516. arXiv:2412.18490, doi:10.1088/1742-5468/add516.

[42] M. W. Matsen, Field theoretic approach for block polymer melts: SCFT and FTS, The Journal of Chemical Physics 152 (11) (2020) 110901, https://doi.org/10.1063/1.5145098. doi:10.1063/1.5145098.

[43] E. Medina, T. Hwa, M. Kardar, Y.-C. Zhang, Burgers equation with correlated noise: Renormalization-group analysis and applications to directed polymers and interface growth, Physical Review A 39 (1989) 3053–3075, https://link.aps.org/doi/10.1103/PhysRevA.39.3053. doi:10.1103/PhysRevA.39.3053.

[44] T. Halpin-Healy, Y.-C. Zhang, Kinetic roughening phenomena, stochastic growth, directed polymers and all that, Physics Reports 254 (4–6) (1995) 215–414, https://doi.org/10.1016/0370-1573(94)00087-J. doi:10.1016/0370-1573(94)00087-J.

[45] L. Canet, H. Chaté, B. Delamotte, N. Wschebor, Non-perturbative renormalisation group for the Kardar-Parisi-Zhang equation: General framework and first applications, Physical Review E 84 (6) (2011) 061128, https://doi.org/10.1103/PhysRevE.84.061128. doi:10.1103/PhysRevE.84.061128.

[46] N. V. Antonov, N. M. Gulitskiy, P. I. Kakin, N. M. Lebedev, M. M. Tumakova, Field-theoretic renormalization group in models of growth processes, surface roughening and non-linear diffusion in random environment: mobilis in mobili, Symmetry 15 (8) (2023) 1556, https://doi.org/10.3390/sym15081556. doi:10.3390/sym15081556.

[47] B. Lee, Renormalization group calculation for the reaction $kA \to OE$, Journal of Physics A 27 (8) (1994) 2633–2652. doi:10.1088/0305-4470/27/8/004.

[48] B. P. Lee, J. Cardy, Renormalization group study of the A+B→ ∅ diffusion-limited reaction, Journal of Statistical Physics 80 (5) (1995) 971–1007. doi:10.1007/BF02179861.

[49] G. Ódor, Universality classes in nonequilibrium lattice systems, Reviews of Modern Physics 76 (2004) 663–724, https://link.aps.org/doi/10.1103/RevModPhys.76.663. doi:10.1103/RevModPhys.76.663.

[50] U. C. Täuber, M. Howard, B. P. Vollmayr-Lee, Applications of field-theoretic renormalization group methods to reaction–diffusion problems, Journal of Physics A 38 (17) (2005) R79–R131, https://doi.org/10.1088/0305-4470/38/17/R01. doi:10.1088/0305-4470/38/17/R01.

[51] D. Shapoval, V. Blavatska, M. Dudka, Survival in two-species reaction-diffusion system with Lévy flights: Renormalization group treatment and numerical simulations, Journal of Physics A: Mathematical and Theoretical 55 (2022) 455002, https://doi.org/10.1088/1751-8121/ac9c39. doi:10.1088/1751-8121/ac9c39.

[52] M. Hnatič, J. Honkonen, Velocity-fluctuation-induced anomalous kinetics of the reaction $A + A \to \varnothing$, Physical Review E 61 (2000) 3904–3911, https://doi.org/10.1103/PhysRevE.61.3904. doi:10.1103/PhysRevE.61.3904.

[53] N. V. Antonov, A. S. Kapustin, Effects of turbulent mixing on critical behaviour in the presence of compressibility: Renormalization group analysis of two models, Journal of Physics A: Mathematical and Theoretical 43 (2010) 405001, https://doi.org/10.1088/1751-8113/43/40/405001. doi:10.1088/1751-8113/43/40/405001.

[54] M. Hnatič, J. Honkonen, T. Lučivjanský, Study of anomalous kinetics of the annihilation reaction $A + A \to \varnothing$, Theoretical and Mathematical Physics 169 (2011) 1481–1488, https://doi.org/10.1007/s11232-011-0124-9. doi:10.1007/s11232-011-0124-9.

[55] M. Hnatič, J. Honkonen, T. Lučivjanský, Two-loop calculation of anomalous kinetics of the reaction $A + A \to \varnothing$ in randomly stirred fluid, The European Physical Journal B 86 (2013) 214, https://doi.org/10.1140/epjb/e2013-30982-9. doi:10.1140/epjb/e2013-30982-9.

[56] A. S. Il'yn, V. A. Sirota, K. P. Zybin, Turbulent transport in reaction–diffusion systems, Physical Review E 99 (2019) 052220, https://doi.org/10.1103/PhysRevE.99.052220. doi:10.1103/PhysRevE.99.052220.

[57] M. Hnatič, M. Kecer, T. Lučivjanský, Anomalous kinetics of a multi-species reaction-diffusion system: Effect of random velocity fluctuations, Physics of Particles and Nuclei Letters 20 (2023) 1081–1083, https://doi.org/10.1134/S1547477123050370. doi:10.1134/S1547477123050370.

[58] M. Hnatič, M. Kecer, T. Lučivjanský, Two-species reaction–diffusion system in the presence of random velocity fluctuations, Theoretical and Mathematical Physics 217 (2023) 1437–1445, https://doi.org/10.1134/S0040577923100021. doi:10.1134/S0040577923100021.

[59] M. Hnatič, M. Kecer, T. Lučivjanský, Renormalization Group Analysis of Two-Species Reaction-Diffusion System: Crossover between Long-Range and Short-Range Spreading, Physics of Particles and Nuclei Letters 22 (2025) 522–524, https://doi.org/10.1134/S1547477125700086. doi:10.1134/S1547477125700086.

[60] H. Hinrichsen, Non-equilibrium critical phenomena and phase transitions into absorbing states, Advances in Physics 49 (2000) 815.

[61] H.-K. Janssen, U. C. Täuber, The field theory approach to percolation processes, Annals of Physics 315 (1) (2005) 147–192, special Issue, https://www.sciencedirect.com/science/article/pii/S0003491604001769. doi:https://doi.org/10.1016/j.aop.2004.09.011.

[62] M. Henkel, H. Hinrichsen, S. Lübeck, Non-Equilibrium Phase Transitions, Vol. I: Absorbing Phase Transitions, Springer, 2008.

[63] M. Hnatič, J. Honkonen, T. Lučivjanský, L. Mižišin, Universality classes of percolation processes: Renormalization group approach, Symmetry 15 (9) (2023) 1696, https://doi.org/10.3390/sym15091696. doi:10.3390/sym15091696.

[64] L. T. Adzhemyan, M. Hnatič, E. V. Ivanova, M. V. Kompaniets, T. Lučivjanský, L. Mižišin, Field-theoretic analysis of directed percolation: Three-loop approximation, Physical Review E 107 (2023) 064138, https://doi.org/10.1103/PhysRevE.107.064138. doi:10.1103/PhysRevE.107.064138.

[65] M. Hnatič, M. Kecer, M. V. Kompaniets, T. Lučivjanský, L. Mižišin, Y. G. Molotkov, Field-theoretic analysis of dynamic isotropic percolation: Three-loop approximation, Physical Review E 112 (2025) 014113, https://doi.org/10.1103/87m5-mt2b. doi:10.1103/87m5-mt2b.

[66] L. Adzhemyan, N. Antonov, M. Hnatič, J. Honkonen, P. Kakin, D. Kazakov, M. Komarova, M. Kompaniets, A. Kudlis, T. Lučivjanský, M. Nalimov, Field-Theoretic Renormalization Group in Models of Critical Behavior, Turbulence and Non-equilibrium Dynamics, World Scientific, 2024, Ch. Chapter 35, pp. 631–674, https://www.worldscientific.com/doi/abs/10.1142/9789811282386_0035. doi:10.1142/9789811282386_0035.

[67] N. V. Antonov, M. Hnatič, J. Honkonen, P. I. Kakin, T. Lučivjanský, L. Mižišin, Renormalized Field Theory for Non-equilibrium Systems, La Rivista del Nuovo Cimento 47 (2024) 653–728, https://doi.org/10.1007/s40766-025-00064-5. doi:10.1007/s40766-025-00064-5.

[68] A. van Kan, Phase transitions in anisotropic turbulence, Chaos 34 (2024) 122103, https://doi.org/10.1063/5.0232179. doi:10.1063/5.0232179.

[69] E. Knowles (Ed.), Oxford Dictionary of Quotations, 8th Edition, Oxford University Press, 2014.

[70] G. Lyttelton, The History of the Life of King Henry the Second, J. Dodsley, 1769, 3rd ed., 6 vols.

[71] J. Carlson, A. Jaffe, A. Wiles, The Millennium Prize Problems, AMS, 2006.

[72] L. Keller, A. Fridman, Differentialgleichung für die turbulente Bewegung einer kompressiblen Flüssigkeit, in: Proc. 1st Int. Congr. Appl. Mech., 1924, pp. 395–405.

[73] N. N. Bogoliubov, Problems of a Dynamical Theory in Statistical Physics, in: J. de Boer, G. E. Uhlenbeck (Eds.), Studies in Statistical Mechanics, Vol. 1, North-Holland Publishing Company, Amsterdam, 1962, english translation of the 1946 Russian monograph *Problemy dinamicheskoi teorii v statisticheskoi fizike*.

[74] C. G. Speziale, Analytical methods for the development of Reynolds-stress closures in turbulence, Annual Review of Fluid Mechanics 23 (1991) 107–157, https://www.annualreviews.org/content/journals/10.1146/annurev.fl.23.010191.000543. doi:https://doi.org/10.1146/annurev.fl.23.010191.000543.

[75] K. Hanjalić, Advanced turbulence closure models: a view of current status and future prospects, International Journal of Heat and Fluid Flow 15 (1994) 178–203, https://

www.sciencedirect.com/science/article/pii/0142727X94900388. doi:https://doi.org/10.1016/0142-727X(94)90038-8.

[76] H. W. Wyld, Formulation of the theory of turbulence in an incompressible fluid, Annals of Physics 14 (1961) 143–165, https://doi.org/10.1016/0003-4916(61)90056-2. doi:10.1016/0003-4916(61)90056-2.

[77] R. H. Kraichnan, The structure of isotropic turbulence at very high Reynolds numbers, Journal of Fluid Mechanics (1959) 497–543. doi:10.1017/S0022112059000362.

[78] R. H. Kraichnan, Dynamics of nonlinear stochastic systems, Journal of Mathematical Physics 2 (1) (1961) 124–148. doi:10.1063/1.1724206.

[79] R. H. Kraichnan, Lagrangian history closure approximation for turbulence, Physics of Fluids 8 (1965) 575–598. doi:10.1063/1.1761271.

[80] R. H. Kraichnan, Stochastic Modeling of Isotropic Turbulence, in: L. Sirovich (Ed.), New Perspectives in Turbulence, Springer New York, New York, NY, 1991, pp. 1–54.

[81] A. Yoshizawa, Statistical modelling of passive-scalar diffusion in turbulent shear flows, Journal of Fluid Mechanics 195 (1988) 541–555. doi:10.1017/S0022112088002514.

[82] S. A. Orszag, Analytical theories of turbulence, Journal of Fluid Mechanics 41 (1970) 363–386, https://doi.org/10.1017/S0022112070000642. doi:10.1017/S0022112070000642.

[83] C. G. Speziale, Turbulence modeling for time-dependent RANS and VLES: A review, AIAA Journal 36 (1998) 173–184, https://doi.org/10.2514/2.7499. doi:10.2514/2.7499.

[84] P. Spalart, W.-H. Jou, M. Strelets, S. Allmaras, Comments on the Feasibility of LES for Wings, and on a Hybrid RANS/LES Approach, Conference: Advances in DNS/LES, 1997.

[85] Y. Zhiyin, Large-eddy simulation: Past, present and the future, Chinese Journal of Aeronautics 28 (2015) 11–24, https://www.sciencedirect.com/science/article/pii/S1000936114002064. doi:https://doi.org/10.1016/j.cja.2014.12.007.

[86] P. Moin, K. Mahesh, Direct numerical simulation: A tool in turbulence research, Annual Review of Fluid Mechanics 30 (1998) 539–578, https://doi.org/10.1146/annurev.fluid.30.1.539. doi:10.1146/annurev.fluid.30.1.539.

[87] S. B. Pope, PDF methods for turbulent reactive flows, Progress in Energy and Combustion Science 11 (1985) 119–192, https://doi.org/10.1016/0360-1285(85)90002-4. doi:10.1016/0360-1285(85)90002-4.

[88] L. Jahanshaloo, E. Pouryazdanpanah, N. A. Che Sidik, A review on the application of the lattice boltzmann method for turbulent flow simulation, Numerical Heat Transfer; Part A: Applications 64 (2013) 938–953, https://doi.org/10.1080/10407782.2013.807690. doi:10.1080/10407782.2013.807690.

[89] K. Taira, S. L. Brunton, S. T. M. Dawson, S. W. Rowley, T. Colonius, B. J. McKeon, O. T. Schmidt, S. Gordeyev, V. Theofilis, L. S. Ukeiley, Modal analysis of fluid flows: An overview, AIAA Journal 55 (2017) 4013–4041. doi:10.2514/1.J056060.

[90] M. B. Liu, G. R. Liu, L. W. Zhou, J. Z. Chang, Dissipative Particle Dynamics (DPD): An overview and recent developments, Archives of Computational Methods in Engineering 22 (2015) 529–556, https://doi.org/10.1007/s11831-014-9124-x. doi:10.1007/s11831-014-9124-x.

[91] M. A. Gallis, N. P. Bitter, T. P. Koehler, J. R. Torczynski, S. J. Plimpton, G. Papadakis, Molecular-level simulations of turbulence and its decay, Physical Review Letters 118 (2017) 064501, https://link.aps.org/doi/10.1103/PhysRevLett.118.064501. doi:10.1103/PhysRevLett.118.064501.

[92] A. S. Monin, A. Yaglom, Statistical fluid mechanics: The mechanics of turbulence, Vol. 1, 2, MIT Press, 1975.

[93] U. Frisch, Turbulence: The Legacy of A. N. Kolmogorov, Cambridge University Press, 1995.

[94] P. Bradshaw, An introduction to turbulence and its measurement: thermodynamics and fluid mechanics series, Elsevier, 2013. doi:10.1016/C2013-0-02451-6.

[95] S. B. Pope, Turbulent Flows, Cambridge University Press, 2000.

[96] A. N. Kolmogorov, The local structure of turbulence in incompressible viscous fluid for very large Reynolds number, Doklady Akademii Nauk SSSR 30 (1941) 9–13, reprinted in Proc. Roy. Soc. Lond., 434, 1991, pp. 9–13.

[97] A. N. Kolmogorov, On degeneration (decay) of isotropic turbulence in an incompressible viscous liquid, Doklady Akademii Nauk SSSR 31 (1941) 538–540.

[98] A. N. Kolmogorov, Dissipation of energy in locally isotropic turbulence, Doklady Akademii Nauk SSSR 32 (1941) 16–18, reprinted in Proc. Roy. Soc. Lond., 434, 1991, pp. 15–17.

[99] A. Obukhov, Spectral energy distribution in a turbulent flow, Izvestiya Akademii Nauk, Seriya Geograficheskaya i Geofizicheskaya 5 (1941) 453–466.

[100] H. L. Grant, R. W. Stewart, A. Moilliet, Turbulence spectra from a tidal channel, Journal of Fluid Mechanics 12 (1962) 241–268. doi:10.1017/S002211206200018X.

[101] D. Forster, D. R. Nelson, M. J. Stephen, Long-time tails and the large-eddy behavior of a randomly stirred fluid, Physical Review Letters 36 (1976) 867–870. doi:10.1103/PhysRevLett.36.867.

[102] C. DeDominicis, P. C. Martin, Energy spectra of certain randomly-stirred fluids, Physical Review A 19 (1979) 419–422, https://link.aps.org/doi/10.1103/PhysRevA.19.419. doi:10.1103/PhysRevA.19.419.

[103] L. Adzhemyan, A. N. Vasil'ev, Y. Pis'mak, Renormalization-group approach in the theory of turbulence: The dimensions of composite operators, Theoretical and Mathematical Physics 57 (1983) 1131–1141. doi:10.1007/BF01018658.

[104] L. T. Adzhemyan, N. V. Antonov, A. N. Vasilev, Infrared divergences and the renormalization group in the theory of fully developed turbulence, Journal of Experimental and Theoretical Physics 68 (4) (1989) 733–742.

[105] N. Antonov, Renormalizing approach to the theory of developed turbulence: Infrared asymptotic of scaling functions, Journal of Mathematical Sciences 54 (1991) 873–879, https://doi.org/10.1007/BF01101114. doi:10.1007/BF01101114.

[106] L. Adzhemyan, N. Antonov, T. Kim, Composite operators, operator expansion, and Galilean invariance in the theory of fully developed turbulence. Infrared corrections to Kolmogorov scaling, Theoretical and Mathematical Physics 100 (1994) 1086–1099, https://doi.org/10.1007/BF01018574. doi:10.1007/BF01018574.

[107] L. T. Adzhemyan, N. V. Antonov, A. N. Vasil'ev, Infrared divergences and the renormalization group in the theory of fully developed turbulence, Journal of Experimental and Theoretical Physics 95 (1989) 1272–1288.

[108] L. T. Adzhemyan, N. V. Antonov, M. V. Kompaniets, A. N. Vasil'ev, Renormalization-group approach to the stochastic Navier-Stokes equation: Two-loop approximation, International Journal of Modern Physics B 17 (10) (2003) 2137–2170, https://doi.org/10.1142/S0217979203018193. doi:10.1142/S0217979203018193.

[109] L. T. Adzhemyan, J. Honkonen, M. V. Kompaniets, A. N. Vasil'ev, Improved ε expansion for three-dimensional turbulence: Summation of nearest dimensional singularities, Physical Review E 68 (2003) 055302, https://link.aps.org/doi/10.1103/PhysRevE.68.055302. doi:10.1103/PhysRevE.68.055302.

[110] L. Adzhemyan, M. Hnatich, J. Honkonen, Improved ε expansion in the theory of turbulence: summation of nearest singularities by inclusion of an infrared irrelevant operator, The European Physical Journal B 73 (2010) 275–285, https://doi.org/10.1140/epjb/e2009-00432-8. doi:10.1140/epjb/e2009-00432-8.

[111] L. T. Adzhemyan, N. V. Antonov, P. B. Gol'din, T. L. Kim, M. V. Kompaniets, Renormalization group in the infinite-dimensional turbulence: third-order results, Journal of Physics A 41 (2008) 495002. doi:10.1088/1751-8113/41/49/495002.

[112] R. Ni, K.-Q. Xia, Kolmogorov constants for the second-order structure function and the energy spectrum, Physical Review E 87 (2013) 023002, https://link.aps.org/doi/10.1103/PhysRevE.87.023002. doi:10.1103/PhysRevE.87.023002.

[113] N. V. Antonov, M. Hnatič, J. Honkonen, P. I. Kakin, T. Lučivjanský, L. Mižišin, Renormalized field theory for non-equilibrium systems, La Rivista del Nuovo Cimento 47 (2024) 653–728, https://doi.org/10.1007/s40766-025-00064-5. doi:10.1007/s40766-025-00064-5.

[114] N. V. Antonov, M. Gnatich, M. Y. Nalimov, The influence of compressibility on the spectra of highly anisotropic developed turbulence [in russian], JINR Letters, 1997.

[115] E. Jurčišinová, M. Jurčišin, R. Remecký, Influence of helicity on the Kolmogorov regime in fully developed turbulence, Physical Review E 79 (2009) 046319, [Erratum: in Physical Review E, 86, (2012) 049902]. doi:10.1103/PhysRevE.79.046319.

[116] C.-Y. Mou, P. B. Weichman, Multicomponent turbulence, the spherical limit, and non-Kolmogorov spectra, Physical Review E 52 (1995) 3738–3796, https://link.aps.org/doi/10.1103/PhysRevE.52.3738. doi:10.1103/PhysRevE.52.3738.

[117] R. H. Kraichnan, Convection of a passive scalar by a quasi-uniform random straining field, Journal of Fluid Mechanics 64 (1974) 737–762, https://doi.org/10.1017/S0022112074001881. doi:10.1017/S0022112074001881.

[118] J.-D. Fournier, U. Frisch, J. H. A. Rose, Infinite-dimensional turbulence, Journal of Physics A: Mathematical and Theoretical 11 (1978) 187–198, https://doi.org/10.1088/0305-4470/11/1/020. doi:10.1088/0305-4470/11/1/020.

[119] H. L. Frisch, M. Schulz, Turbulence effects in the high dimensionality limit, Journal of Physics A: Mathematical and Theoretical 211 (1994) 37–42, https://doi.org/10.1016/0378-4371(94)90066-3. doi:10.1016/0378-4371(94)90066-3.

[120] L. T. Adzhemyan, N. V. Antonov, A. V. Runov, Anomalous scaling, nonlocality, and anisotropy in a model of the passively advected vector field, Physical Review E 64 (2001) 046310, https://link.aps.org/doi/10.1103/PhysRevE.64.046310. doi:10.1103/PhysRevE.64.046310.

[121] L. T. Adzhemyan, N. V. Antonov, P. B. Gol'din, M. V. Kompaniets, Anomalous scaling of a passive vector field in d dimensions: higher order structure functions, Journal of Physics A 46 (2013) 135002. doi:10.1088/1751-8113/46/13/135002.

[122] L. T. Adzhemyan, D. A. Evdokimov, M. V. Kompaniets, Hyperlogarithms in the theory of turbulence of infinite dimension, Nuclear Physics B 1008 (2024) 116716. doi:10.1016/j.nuclphysb.2024.116716.

[123] L. T. Adzhemyan, Y. Kirienko, Theory of turbulence for $d \to \infty$: Four-loop approximation of the renormalization group (2024). arXiv:2406.14575.

[124] M. Moshe, J. Zinn-Justin, Quantum field theory in the large N limit: a review, Physics Reports 385 (3) (2003) 69–228, https://www.sciencedirect.com/science/article/pii/S0370157303002631. doi:https://doi.org/10.1016/S0370-1573(03)00263-1.

[125] C. Wetterich, Exact evolution equation for the effective potential, Physics Letters B 301 (1) (1993) 90–94, https://www.sciencedirect.com/science/article/pii/037026939390726X. doi:https://doi.org/10.1016/0370-2693(93)90726-X.

[126] J. Berges, N. Tetradis, C. Wetterich, Non-perturbative renormalization flow in quantum field theory and statistical physics, Physics Reports 363 (2002) 223–386. doi:10.1016/S0370-1573(01)00098-9.

[127] N. Dupuis, L. Canet, A. Eichhorn, W. Metzner, J. Pawlowski, M. Tissier, N. Wschebor, The nonperturbative functional renormalization group and its applications, Physics Reports 910 (2021) 1–114, https://doi.org/10.1016%2Fj.physrep.2021.01.001. doi:10.1016/j.physrep.2021.01.001.

[128] L. Canet, B. Delamotte, N. Wschebor, Fully developed isotropic turbulence: Symmetries and exact identities, Physical Review E 91 (2015) 053004. doi:10.1103/PhysRevE.91.053004.

[129] L. Canet, B. Delamotte, N. Wschebor, Fully developed isotropic turbulence: Nonperturbative renormalization group formalism and fixed-point solution, Physical Review E 93 (2016) 063101. doi:10.1103/PhysRevE.93.063101.

[130] M. Tarpin, L. Canet, C. Pagani, N. Wschebor, Breaking of scale invariance in the time dependence of correlation functions in isotropic and homogeneous turbulence, Physics of Fluids 30 (2018) 055102. doi:10.1063/1.5020022.

[131] Z.-S. She, E. Leveque, Universal scaling laws in fully developed turbulence, Physical Review Letters 72 (1996) 336–339. doi:10.1103/PhysRevLett.72.336.

[132] A. Gorbunova, G. Balarac, L. Canet, G. Eyink, V. Rossetto, Spatio-temporal correlations in three-dimensional homogeneous and isotropic turbulence, Physics of Fluids 33 (2021) 045114. doi:10.1063/5.0046677.

[133] L. Gosteva, M. Tarpin, N. Wschebor, L. Canet, Inviscid fixed point of the multidimensional Burgers–Kardar-Parisi-Zhang equation, Physical Review E 110 (2024) 054118. doi:10.1103/PhysRevE.110.054118.

[134] G. Falkovich, K. Gawędzki, M. Vergassola, Particles and fields in fluid turbulence, Reviews of Modern Physics 73 (2001) 913–975. doi:10.1103/RevModPhys.73.913.

[135] R. H. Kraichnan, Anomalous scaling of a randomly advected passive scalar, Physical Review Letters 72 (1994) 1016–1019. doi:10.1103/PhysRevLett.72.1016.

[136] K. Gawędzki, A. Kupiainen, Anomalous Scaling of the Passive Scalar, Physical Review Letters 75 (1995) 3834–3837. doi:10.1103/PhysRevLett.75.3834.

[137] L. T. Adzhemyan, N. V. Antonov, A. N. Vasil'ev, Renormalization-group, operator product expansion, and anomalous scaling in a model of advected passive scalar, Physical Review E 58 (1998) 1823. doi:10.1103/PhysRevE.58.1823.

[138] L. T. Adzhemyan, N. V. Antonov, V. A. Barinov, Y. S. Kabrits, A. N. Vasil'ev, Calculation of the anomalous exponents in the rapid-change model of passive scalar advection to order ε^3, Physical Review E 64 (2001) 056306. doi:10.1103/PhysRevE.64.056306.

[139] N. V. Antonov, J. Honkonen, Anomalous scaling in two models of passive scalar advection: Effects of anisotropy and compressibility, Physical Review E 63 (2001) 036302. doi:10.1103/PhysRevE.63.036302.

[140] N. V. Antonov, M. Hnatich, J. Honkonen, M. Jurčišin, Turbulence with pressure: Anomalous scaling of a passive vector field, Physical Review E 68 (2003) 046306. doi:10.1103/PhysRevE.68.046306.

[141] L. T. Adzhemyan, N. V. Antonov, J. Honkonen, Anomalous scaling of a passive scalar advected by the turbulent velocity field with finite correlation time: Two-loop approximation, Physical Review E 66 (2002) 036313. doi:10.1103/PhysRevE.66.036313.

[142] L. T. Adzhemyan, N. V. Antonov, J. Honkonen, T. L. Kim, Anomalous scaling of a passive scalar advected by the Navier–Stokes velocity field: Two-loop approximation, Physical Review E 71 (2005) 016303. doi:10.1103/PhysRevE.71.016303.

[143] D. Carati, Colored stochastic noises in the renormalization group approach of turbulence, Physics of Fluids 2 (1990) 1854–1858. doi:10.1063/1.857659.

[144] A. L. Fairhall, O. Gat, V. L'vov, I. Procaccia, Anomalous scaling in a model of passive scalar advection: Exact results, Physical Review E 53 (1996) 3518–3535. doi:10.1103/PhysRevE.53.3518.

[145] N. V. Antonov, Anomalous scaling regimes of a passive scalar advected by the synthetic velocity field, Physical Review E 60 (1999) 6691–6707. doi:10.1103/PhysRevE.60.6691.

[146] N. Antonov, Anomalous scaling of a passive scalar advected by the synthetic compressible flow, Journal of Physics D: Applied Physics 144 (2000) 370–386. doi:10.1016/S0167-2789(00)00089-0.

[147] L. T. Adzhemyan, N. V. Antonov, J. Honkonen, Anomalous scaling of a passive scalar advected

by the turbulent velocity field with finite correlation time: Two-loop approximation, Physical Review E 66 (2002) 036313. doi:10.1103/PhysRevE.66.036313.

[148] N. V. Antonov, N. M. Gulitskiy, A. V. Malyshev, Stochastic Navier-Stokes equation with colored noise: renormalization-group analysis, EPJ Web of Conferences 126 (2016) 04019. doi:10.1051/epjconf/201612604019.

[149] N. V. Antonov, N. M. Gulitskiy, M. M. Kostenko, A. V. Malyshev, Statistical symmetry restoration in fully developed turbulence: Renormalization group analysis of two models, Physical Review E 97 (2018) 033101. doi:10.1103/PhysRevE.97.033101.

[150] P. C. Hohenberg, B. I. Halperin, Theory of dynamic critical phenomena, Reviews of Modern Physics 49 (1977) 435–479, https://link.aps.org/doi/10.1103/RevModPhys.49.435. doi:10.1103/RevModPhys.49.435.

[151] N. V. Antonov, M. Hnatich, J. Honkonen, Effects of stirring and mixing on the critical behaviour, Journal of Physics A 39 (2006) 7867–7887. doi:10.1088/0305-4470/39/25/S05.

[152] M. Hnatič, T. Lučivjanský, L. Mižišin, Y. Molotkov, A. Ovsiannikov, Renormalization analysis of magnetohydrodynamics: Two-loop approximation, Universe 10 (2024) 240. doi:10.3390/universe10060240.

[153] H. Alfvén, Existence of electromagnetic-hydrodynamic waves, Nature 150 (1942) 405–406. doi:10.1038/150405d0.

[154] K. Hattori, M. Hongo, X.-G. Huang, New developments in relativistic magnetohydrodynamics, Symmetry 14 (2022) 1851. doi:10.3390/sym14091851.

[155] L. D. Landau, E. M. Lifshitz, Fluid mechanics: Landau and Lifshitz: course of theoretical physics, Vol. 6, Elsevier, 2013.

[156] T. G. Cowling, Magnetohydrodynamics, Interscience, 1957.

[157] P. A. Davidson, An introduction to magnetohydrodynamics, Cambridge University Press, 2001.

[158] H. K. Moffatt, Magnetic field generation in electrically conducting fluids, Cambridge University Press, 1978.

[159] F. M. White, Fluid mechanics, 7th Edition, McGraw-Hill, 2011.

[160] A. E. Lifschitz, Magnetohydrodynamics and spectral theory, 1st Edition, no. 4 in Developments in Electromagnetic Theory and Applications, Springer Dordrecht, 1989.

[161] S. I. Braginskii, Transport processes in a plasma, in: M. A. Leontovich (Ed.), Reviews of Plasma Physics, Vol. 1, Consultants Bureau, 1965, pp. 205–311, translated from Russian.

[162] R. Lüst, Über die Ausbreitung von Wellen in einem Plasma, Fortschritte der Physik — Progress of Physics 7 (1959) 503–558, https://doi.org/10.1002/prop.19590070902. doi:10.1002/prop.19590070902.

[163] I. Keramidas Charidakos, M. Lingam, P. J. Morrison, R. L. White, A. Wurm, Action principles for extended magnetohydrodynamic models, Physics of Plasmas 21 (2014) 092118, https://doi.org/10.1063/1.4896336. doi:10.1063/1.4896336.

[164] J. P. Freidberg, Ideal MHD, Cambridge University Press, 2014.

[165] M. A. Sadybekov, B. T. Torebek, B. K. Turmetov, Representation of Green's function of the Neumann problem for a multi-dimensional ball, Complex Variables and Elliptic Equations 61 (2016) 104–123, http://dx.doi.org/10.1080/17476933.2015.1064402. doi:10.1080/17476933.2015.1064402.

[166] F. W. King, Hilbert Transforms, Encyclopedia of Mathematics and its Applications, Cambridge University Press, 2009.

[167] J. Sommeria, R. Moreau, Why, how, and when, MHD turbulence becomes two-dimensional, Journal of Fluid Mechanics 118 (1982) 507–518, http://dx.doi.org/10.1017/S0022112082001177. doi:10.1017/S0022112082001177.

[168] G. P. Zank, W. H. Matthaeus, The equations of reduced magnetohydrodynamics, Journal of Plasma Physics 48 (1992) 85–100, https://doi.org/10.1017/S002237780001638X. doi:10.

1017/S002237780001638X.

[169] S. Galtier, S. Nazarenko, A. C. Newell, A. Pouquet, A weak turbulence theory for incompressible magnetohydrodynamics, Journal of Plasma Physics 63 (2000) 447–488, https://doi.org/10.1017/S0022377899008284. doi:10.1017/S0022377899008284.

[170] P. Goldreich, S. Sridhar, Toward a theory of interstellar turbulence. II. Strong Alfvenic turbulence, The Astrophysical Journal 438 (1995) 763–775. doi:10.1086/175121.

[171] S. Boldyrev, Spectrum of magnetohydrodynamic turbulence, Physical Review Letters 96 (2006) 115002. doi:10.1103/PhysRevLett.96.115002.

[172] A. Lazarian, Theoretical approaches to particle propagation and acceleration in turbulent intergalactic medium, Astronomische Nachrichten 327 (2006) 609–614, https://doi.org/10.1002/asna.200610603. doi:10.1002/asna.200610603.

[173] N. F. Loureiro, S. Boldyrev, Role of magnetic reconnection in magnetohydrodynamic turbulence, Physical Review Letters 118 (2017) 245101, https://link.aps.org/doi/10.1103/PhysRevLett.118.245101. doi:10.1103/PhysRevLett.118.245101.

[174] S. Boldyrev, N. F. Loureiro, Magnetohydrodynamic turbulence mediated by reconnection, The Astrophysical Journal 844 (2017) 125, https://doi.org/10.3847/1538-4357/aa7d02. doi:10.3847/1538-4357/aa7d02.

[175] S. I. Vainshtein, I. B. Zeldovich, A. A. Ruzmaikin, The turbulent dynamo in astrophysics (in Russian), Nauka, 1980.

[176] S. I. Vainshtein, Magnetic fields in space (in Russian), Nauka, Moscow, 1983.

[177] I. B. Zeldovich, A. A. Ruzmaikin, D. D. Sokoloff, Magnetic fields in astrophysics, Gordon and Breach, 1983.

[178] F. Krause, K.-H. Rädler, Mean-field magnetohydrodynamics and dynamo theory, Pergamon, 1980.

[179] G. Ruediger, L. Kitchatinov, R. Hollerbach, Magnetic processes in astrophysics: Theory, simulations, experiments, Wiley-VCH, 2013.

[180] A. Shukurov, K. Subramanian, Astrophysical magnetic fields: from galaxies to the early universe, Cambridge University Press, 2022.

[181] H. Moffatt, E. Dormy, Self-exciting fluid dynamos, Cambridge University Press, 2019.

[182] J. Larmor, How could a rotating body such as the Sun become a magnet? Report of the British Association for the Advancement of Science 113 (1919) 159–160.

[183] M. J. Nye, Temptations of theory, strategies of evidence: P. M. S. Blackett and the earth's magnetism, British Journal for the History of Science 32 (1999) 69–92, https://doi.org/10.1017/S0007087498003495. doi:10.1017/S0007087498003495.

[184] T. G. Cowling, The magnetic field of sunspots, Monthly Notices of the Royal Astronomical Society 94 (1934) 39–48. doi:10.1093/mnras/94.1.39.

[185] Y. B. Zel'dovich, A magnetic field in connection with the two-dimen-sional motion of a conductive turbulent liquid, Journal of Experimental and Theoretical Physics 31 (1956) 154–155.

[186] F. Busse, M. Proctor, Antidynamo and bounding theorems, in: D. Gubbins, E. Herrero-Bervera (Eds.), Encyclopedia of Geomagnetism and Paleomagnetism, Springer Netherlands, Dordrecht, 2007, pp. 21–23, https://doi.org/10.1007/978-1-4020-4423-6_8. doi:10.1007/978-1-4020-4423-6_8.

[187] F. Rincon, Dynamo theories, Journal of Plasma Physics 85 (2019) 205850401, https://doi.org/10.1017/S0022377819000539. doi:10.1017/S0022377819000539.

[188] G. O. Roberts, E. C. Bullard, Dynamo action of fluid motions with two-dimensional periodicity, Philosophical Transactions of the Royal Society A 271 (1972) 411–454. doi:10.1098/rsta.1972.0015.

[189] Y. B. Ponomarenko, Theory of the hydromagnetic generator, Journal of Applied Mechanics and Technical Physics 14 (1973) 775–778. doi:10.1007/BF00853190.

[190] E. Dormy, and A. M. Soward (Eds.), Mathematical aspects of natural dynamos, 1st Edition, Chapman and Hall/CRC, 2007.
[191] E. N. Parker, Hydromagnetic dynamo models, The Astrophysical Journal 122 (1955) 293–314. doi:10.1086/146087.
[192] W. Elsasser, The earth as a dynamo, Scientific American 198 (1958) 44–48. doi:10.1038/scientificamerican0558-44.
[193] S. Braginsky, Self-excitation of a magnetic field during the motion of a highly conducting fluid, Soviet physics, Journal of experimental and theoretical physics 20 (1964) 726–735.
[194] S. Braginsky, Theory of the hydromagnetic dynamo, Soviet physics, Journal of experimental and theoretical physics 20 (1964) 1462–1471.
[195] S. Braginsky, Kinematic models of the Earth's hydrodynamic dynamo, Geomagnetism and Aeronomy 4 (1964) 572–583.
[196] S. Braginsky, Magnetohydrodynamics of the Earth's core, Geomagnetism and Aeronomy 4 (1964) 698–712.
[197] M. Steenbeck, F. Krause, K.-H. Rädler, A calculation of the mean electromotive force in an electrically conducting fluid in turbulent motion, under the influence of coriolis forces, Zeitschrift für Naturforschung 21A (1966) 369–376.
[198] S. Tobias, The turbulent dynamo, Journal of Fluid Mechanics 912 (2021) P1. doi:10.1017/jfm.2020.1055.
[199] H. K. Moffatt, Some topological aspects of fluid dynamics, Journal of Fluid Mechanics 914 (2021) P1, https://doi.org/10.1017/jfm.2020.230. doi:10.1017/jfm.2020.230.
[200] P. J. Morrison, R. D. Hazeltine, Hamiltonian formulation of reduced magnetohydrodynamics, Physics of Fluids 27 (1984) 886–897, https://doi.org/10.1063/1.864718. doi:10.1063/1.864718.
[201] S. Nazarenko, Wave turbulence, 1st Edition, no. 825 in Lecture Notes in Physics, Springer, 2011.
[202] S. L. Musher, A. M. Rubenchik, V. E. Zakharov, Weak Langmuir turbulence, Physics Reports 252 (1995) 177–274, https://doi.org/10.1016/0370-1573(94)00071-A. doi:10.1016/0370-1573(94)00071-A.
[203] G. Pelletier, Langmuir turbulence as a critical phenomenon. Part 1. Destruction of the statistical equilibrium of an interacting-modes ensemble, Journal of Plasma Physics 24 (1980) 287–297, https://doi.org/10.1017/S0022377800022832. doi:10.1017/S0022377800022832.
[204] G. Pelletier, Langmuir turbulence as a critical phenomenon. Part 2. Application of the dynamical renormalization group method, Journal of Plasma Physics 24 (1980) 421–443, https://doi.org/10.1017/S0022377800010382. doi:10.1017/S0022377800010382.
[205] L. T. Adzhemyan, A. N. Vasil'ev, M. Gnatich, Y. M. Pis'mak, Quantum field renormalization group in the theory of stochastic Langmuir turbulence, Theoretical and Mathematical Physics 78 (1989) 260–272, https://doi.org/10.1007/BF01017663. doi:10.1007/BF01017663.
[206] U. Frisch, A. Pouquet, J. Léorat, A. Mazure, Possibility of an inverse cascade of magnetic helicity in magnetohydrodynamic turbulence, Journal of Fluid Mechanics 68 (1975) 769–778. doi:10.1017/S002211207500122X.
[207] A. Pouquet, U. Frisch, J. Léorat, Strong MHD helical turbulence and the nonlinear dynamo effect, Journal of Fluid Mechanics 77 (1976) 321–354. doi:10.1017/S0022112076002140.
[208] E. Priest, T. Forbes, Magnetic reconnection: MHD theory and applications, Cambridge University Press, 2000.
[209] D. Biskamp, Magnetic reconnection in plasmas, Cambridge University Press, 2000.
[210] E. N. Parker, Cosmical magnetic fields, International Series of Monographs on Physics, Clarendon Press, 1979.
[211] S. Childress, A. Gilbert, Stretch, twist, fold: the fast dynamo, Springer-Verlag, 1995.

[212] G. Rüdiger, R. Hollerbach, The magnetic universe, Wiley-VCH, 2004.
[213] A. A. Ruzmaikin, A. M. Shukurov, D. D. Sokoloff, Magnetic fields of galaxies, Vol. 133 of Astrophysics and Space Science Library, Springer, 1988.
[214] S. Tobias, The solar dynamo, Philosophical Transactions of the Royal Society A 43 (2002) 2741–2756. doi:10.1098/rsta.2002.1090.
[215] A. Brandenburg, K. Subramanian, Astrophysical magnetic fields and nonlinear dynamo theory, Physics Reports 417 (2005) 1–209. doi:10.1016/j.physrep.2005.06.005.
[216] F. Rincon, F. Califano, A. A. Schekochihin, V. F., Turbulent dynamo in a collisionless plasma, Proceedings of the National Academy of Sciences of the United States of America 113 (2016) 3950–3953. doi:10.1073/pnas.1525194113.
[217] A. Gailitis, O. Lielausis, E. Platacis, G. Gerbeth, F. Stefani, Colloquium: Laboratory experiments on hydromagnetic dynamos, Reviews of Modern Physics 74 (2002) 973–990. doi:10.1103/RevModPhys.74.973.
[218] M. D. Nornberg, E. J. Spence, R. D. Kendrick, C. M. Jacobson, C. B. Forest, Intermittent magnetic field excitation by a turbulent flow of liquid sodium, Physical Review Letters 97 (2006) 044503. doi:10.1103/PhysRevLett.97.044503.
[219] R. Monchaux, M. Berhanu, M. Bourgoin, M. Moulin, P. Odier, J.-F. Pinton, R. Volk, S. Fauve, N. Mordant, F. Pétrélis, A. Chiffaudel, F. Daviaud, B. Dubrulle, C. Gasquet, L. Marié, F. Ravelet, Generation of a magnetic field by dynamo action in a turbulent flow of liquid sodium, Physical Review Letters 98 (2007) 044502. doi:10.1103/PhysRevLett.98.044502.
[220] F. Stefani, A. Gailitis, G. Gerbeth, Magnetohydrodynamic experiments on cosmic magnetic fields, Journal of Applied Mathematics and Mechanics 88 (2008) 930–954. doi:10.1002/zamm.200800102.
[221] D. Brito, T. Alboussière, P. Cardin, N. Gagnière, D. Jault, P. La Rizza, J.-P. Masson, H.-C. Nataf, D. Schmitt, Zonal shear and super-rotation in a magnetized spherical Couette-flow experiment, Physical Review E 83 (2011) 066310. doi:10.1103/PhysRevE.83.066310.
[222] K. Rahbarnia, B. P. Brown, M. M. Clark, E. J. Kaplan, M. D. Nornberg, A. M. Rasmus, N. Z. Taylor, C. B. Forest, F. Jenko, A. Limone, J.-F. Pinton, N. Plihon, G. Verhille, Direct observation of the turbulent emf and transport of magnetic field in a liquid sodium experiment, The Astrophysical Journal 759 (2012) 80. doi:10.1088/0004-637X/759/2/80.
[223] B. E. Goldstein, E. J. Smith, A. Balogh, T. S. Horbury, M. L. Goldstein, D. A. Roberts, Properties of magnetohydrodynamic turbulence in the solar wind as observed by Ulysses at high heliographic latitudes, Geophysical Research Letters 22 (1995) 3393–3396. doi:10.1029/95GL03183.
[224] J. W. Armstrong, B. J. Rickett, S. R. Spangler, Electron Density Power Spectrum in the Local Interstellar Medium, The Astrophysical Journal 443 (1995) 209–221. doi:10.1086/175515.
[225] A. Chepurnov, A. Lazarian, Extending the big power law in the sky with turbulence spectra from wisconsin Hα mapper data, The Astrophysical Journal 710 (2010) 853–858. doi:10.1088/0004-637X/710/1/853.
[226] C. C. Finlay, et al., International geomagnetic reference field: The eleventh generation, Geophysical Journal International 183 (2010) 1216–1230. doi:10.1111/j.1365-246X.2010.04804.x.
[227] C. L. Johnson, M. E. Purucker, H. Korth, B. J. Anderson, R. M. Winslow, M. M. H. Al Asad, J. A. Slavin, I. I. Alexeev, R. J. Phillips, M. T. Zuber, S. C. Solomon, Messenger observations of Mercury's magnetic field structure, Journal of Geophysical Research E 117 (2012) E00L14. doi:10.1029/2012JE004217.
[228] K. M. Moore, H. Cao, J. Bloxham, D. J. Stevenson, J. E. P. Connerney, S. J. Bolton, Time variation of Jupiter's internal magnetic field consistent with zonal wind advection, Nature Astronomy 3 (2019) 730–735. doi:10.1038/s41550-019-0772-5.
[229] J. E. P. Connerney, S. Kotsiaros, R. J. Oliversen, J. R. Espley, J. L. Joergensen, P. S. Joergensen, J. M. G. Merayo, M. Herceg, J. Bloxham, K. M. Moore, S. J. Bolton, S. M. Levin, A new model

of Jupiter's magnetic field from Juno's first nine orbits, Geophysical Research Letters 45 (2018) 2590–2596. doi:10.1002/2018GL077312.

[230] S. Chandrasekhar, Hydrodynamic and hydromagnetic stability, Clarendon Press, 1961.

[231] A. Favre, Statistical Equations of Turbulent Gases, in: M. A. Lavrentiev (Ed.), Problems of Hydrodynamics and Continuum Mechanics, SIAM, 1969, pp. 37–44.

[232] H. Politano, A. Pouquet, von Kármán–Howarth equation for magnetohydrodynamics and its consequences on third-order longitudinal structure and correlation functions, Physical Review E 57 (1998) R21, https://link.aps.org/doi/10.1103/PhysRevE.57.R21. doi:10.1103/PhysRevE.57.R21.

[233] F. Stefani, Liquid-metal experiments on geophysical and astrophysical phenomena, Nature Reviews Physics 6 (2024) 409–425, https://doi.org/10.1038/s42254-024-00724-1. doi:10.1038/s42254-024-00724-1.

[234] P. D. Mininni, A. G. Pouquet, D. C. Montgomery, Small-scale structures in three-dimensional magnetohydrodynamic turbulence, Physical Review Letters 97 (2006) 244503, https://link.aps.org/doi/10.1103/PhysRevLett.97.244503. doi:10.1103/PhysRevLett.97.244503.

[235] T. D. Lee, Small-scale structures in three-dimensional magnetohydrodynamic turbulence, Quarterly of Applied Mathematics 10 (1952) 69–74, https://doi.org/10.1090/qam/51081. doi:10.1090/qam/51081.

[236] T. Stribling, W. H. Matthaeus, Statistical properties of ideal three-dimensional magnetohydrodynamics, Physics of Fluids B 2 (1990) 1979–1988, https://doi.org/10.1063/1.859419. doi:10.1063/1.859419.

[237] R. Kraichnan, Helical turbulence and absolute equilibrium, Journal of Fluid Mechanics 59 (1973) 745–752, https://doi.org/10.1017/S0022112073001837. doi:10.1017/S0022112073001837.

[238] A. Z. Patashinskii, V. L. Pokrovskii, Fluctuation theory of phase transitions, Pergamon Press, Oxford, 1979.

[239] R. H. Kraichnan, Kolmogorov's hypotheses and Eulerian turbulence theory, Physics of Fluids 7 (1964) 1723–1734, https://doi.org/10.1063/1.2746572. doi:10.1063/1.2746572.

[240] H. Tennekes, Eulerian and Lagrangian time microscales in isotropic turbulence, Journal of Fluid Mechanics 67 (1975) 561–567, https://doi.org/10.1017/S0022112075000468. doi:10.1017/S0022112075000468.

[241] X. He, P. Tong, Kraichnan's random sweeping hypothesis in homogeneous turbulent convection, Physical Review E 83 (2011) 037302, https://link.aps.org/doi/10.1103/PhysRevE.83.037302. doi:10.1103/PhysRevE.83.037302.

[242] P. S. Iroshnikov, Turbulence of a conducting fluid in a strong magnetic field, Astronomicheskii Zhurnal 40 (1963) 742.

[243] C.-Y. Tu, E. Marsch, MHD structures, waves and turbulence in the solar wind: Observations and theories, 1st Edition, Springer Dordrecht, 1995.

[244] R. T. Wicks, T. S. Horbury, C. H. K. Chen, A. A. Schekochihin, Power and spectral index anisotropy of the entire inertial range of turbulence in the fast solar wind, Monthly Notices of the Royal Astronomical Society 407 (2010) L31–L35, https://doi.org/10.1111/j.1745-3933.2010.00898.x. doi:10.1111/j.1745-3933.2010.00898.x.

[245] G. He, G. Jin, Y. Yang, Space-time correlations and dynamic coupling in turbulent flows, Annual Review of Fluid Mechanics 49 (2017) 51–70, https://doi.org/10.1146/annurev-fluid-010816-060309. doi:10.1146/annurev-fluid-010816-060309.

[246] J.-D. Fournier, P.-L. Sulem, P. A, Infrared properties of forced magnetohydrodynamic turbulence, Journal of Physics A 15 (1982) 1393–1420, https://doi.org/10.1088/0305-4470/15/4/037. doi:10.1088/0305-4470/15/4/037.

[247] L. Adzhemyan, A. Vasil'ev, M. Gnatich, Quantum-field renormalization group in the theory of turbulence: Magnetohydrodynamics, Theoretical and Mathematical Physics 64 (1985) 777–785,

https://doi.org/10.1007/BF01017957. doi:10.1007/BF01017957.

[248] K. Furutsu, On the statistical theory of electromagnetic waves in a fluctuating medium (1), Journal of Research of the National Bureau of Standards Sect. D 67 (1963) 303–323.

[249] E. Novikov, Functionals and Random Force Methods for Turbulence Theory, Soviet Physics — Journal of Experimental and Theoretical Physics 47 (5) (1964) p. 1919.

[250] L. T. Adzhemyan, M. Hnatich, D. Horváth, M. Stehlik, Calculation of spectra of turbulence in the energy-containing and inertial ranges, Physical Review E 58 (1998) 4511–4523, https://link.aps.org/doi/10.1103/PhysRevE.58.4511. doi:10.1103/PhysRevE.58.4511.

[251] L. T. Adzhemyan, A. N. Vasil'ev, M. Gnatich, Turbulent dynamo as spontaneous symmetry breaking, Theoretical and Mathematical Physics 72 (1987) 940–950. doi:10.1007/BF01018300.

[252] A. Pouquet, J.-D. Fournier, P. L. Sulem, Is helicity relevant for large scale steady state three-dimensional turbulence? Journal de Physique Lettres 39 (1978) 199–203. doi:10.1051/jphyslet:019780039013019900.

[253] S. Coleman, E. Weinberg, Radiative corrections as the origin of spontaneous symmetry breaking, Physical Review D 7 (1973) 1888–1910. doi:10.1103/PhysRevD.7.1888.

[254] A. P. Kazantsev, Enhancement of a magnetic field by a conducting fluid, Soviet Physics — Journal of Experimental and Theoretical Physics 26 (1968) 1031.

[255] R. H. Kraichnan, Small-scale structure of a scalar field convected by turbulence, Physics of Fluids 11 (1968) 945–953. doi:10.1063/1.1692063.

[256] N. V. Antonov, N. M. Gulitskiy, Two-Loop Calculation of the Anomalous Exponents in the Kazantsev-Kraichnan Model of Magnetic Hydrodynamics, in: G. Adam, J. Buša, M. Hnatič (Eds.), Mathematical Modeling and Computational Science, Vol. 7125 of International Conference, MMCP 2011, Springer Berlin Heidelberg, 2012, pp. 128–135. doi:10.1007/978-3-642-28212-6_11.

[257] N. V. Antonov, N. M. Gulitskiy, Anomalous scaling and large-scale anisotropy in magnetohydrodynamic turbulence: Two-loop renormalization-group analysis of the Kazantsev-Kraichnan kinematic model, Physical Review E 85 (2012) 128–135. doi:10.1103/physreve.85.065301.

[258] N. V. Antonov, N. M. Gulitskiy, [Erratum: Anomalous scaling and large-scale anisotropy in magnetohydrodynamic turbulence: Two-loop renormalization-group analysis of the Kazantsev-Kraichnan kinematic model, Physical Review E 85, 065301(R) (2012)], Physical Review E 87 (2013) 039902, https://link.aps.org/doi/10.1103/PhysRevE.87.039902. doi:10.1103/PhysRevE.87.039902.

[259] E. Jurčišinová, M. Jurčišin, R. Remecký, Turbulent magnetic Prandtl number in kinematic magnetohydrodynamic turbulence: Two-loop approximation, Physical Review E 84 (2011) 046311. doi:10.1103/PhysRevE.84.046311.

[260] N. V. Antonov, M. M. Kostenko, Anomalous scaling in magnetohydrodynamic turbulence: Effects of anisotropy and compressibility in the kinematic approximation, Physical Review E 92 (2015) 053013. doi:10.1103/PhysRevE.92.053013.

[261] E. Jurčišinová, M. Jurčišin, M. Menkyna, R. Remecký, Evidence for enhancement of anisotropy persistence in kinematic magnetohydrodynamic turbulent systems with finite-time correlations, Physical Review E 104 (2021) 015101. doi:10.1103/PhysRevE.104.015101.

[262] N. V. Antonov, M. M. Kostenko, Anomalous scaling of passive scalar fields advected by the Navier-Stokes velocity ensemble: Effects of strong compressibility and large-scale anisotropy, Physical Review E 90 (2014) 063016. doi:10.1103/PhysRevE.90.063016.

[263] N. V. Antonov, M. M. Kostenko, Renormalization Group in the Problem of Active Scalar Advection, Journal of Mathematical Sciences 257 (2021) 425–441. doi:10.1007/s10958-021-05492-2.

[264] M. Hnatič, P. Zalom, Helical turbulent Prandtl number in the A model of passive vector advection, Physical Review E 94 (2016) 053113. doi:10.1103/PhysRevE.94.053113.

[265] N. V. Antonov, N. M. Gulitskiy, Passive advection of a vector field: Anisotropy, finite correlation

time, exact solution, and logarithmic corrections to ordinary scaling, Physical Review E 92 (2015) 043018. doi:10.1103/PhysRevE.92.043018.

[266] E. Jurčišinová, M. Jurčišin, P. Zalom, Turbulent Prandtl number of a passively advected vector field in helical environment: Two-loop renormalization group result, Physical Review E 89 (2014) 043023. doi:10.1103/PhysRevE.89.043023.

[267] E. Jurčišinová, M. Jurčišin, R. Remecký, Turbulent Prandtl number in the A model of passive vector admixture, Physical Review E 93 (2016) 033106. doi:10.1103/PhysRevE.93.033106.

[268] N. V. Antonov, N. M. Gulitskii, M. M. Kostenko, T. Lučivjansky, Renormalization group analysis of models of advection of a vector admixture and a tracer field by a compressible turbulent flow, Theoretical and Mathematical Physics 200 (2019) 1294–1312. doi:10.1134/S0040577919090046.

[269] M. Vergassola, Anomalous scaling for passively advected magnetic fields, Physical Review E 53 (1996) R3021–R3024, https://link.aps.org/doi/10.1103/PhysRevE.53.R3021. doi:10.1103/PhysRevE.53.R3021.

[270] D. Vincenzi, The Kraichnan–Kazantsev dynamo, Journal of Statistical Physics 106 (2002) 1073–1091, https://doi.org/10.1023/A:1014089820881. doi:10.1023/A:1014089820881.

[271] H. Arponen, P. Horvai, Dynamo effect in the Kraichnan magnetohydrodynamic turbulence, Journal of Statistical Physics 129 (2007) 205–239, https://doi.org/10.1007/s10955-007-9399-5. doi:10.1007/s10955-007-9399-5.

[272] H. Arponen, Steady-state existence of passive vector fields under the Kraichnan model, Physical Review E 81 (2010) 036325, https://link.aps.org/doi/10.1103/PhysRevE.81.036325. doi:10.1103/PhysRevE.81.036325.

[273] N. V. Antonov, Renormalization group, operator product expansion and anomalous scaling in models of turbulent advection, Journal of Physics A: Mathematical and General 39 (2006) 7825. doi:10.1088/0305-4470/39/25/S04.

[274] N. G. van Kampen, Stochastic processes in physics and chemistry, North-Holland, Amsterdam, 2007.

[275] C. De Dominicis, Techniques de renormalisation de la théorie des champs et dynamique des phénomenes critiques, in: Journal de Physique, Colloque, Vol. 37, 1976, p. 247.

[276] H. K. Janssen, On the renormalized field theory of nonlinear critical relaxation, From Phase Transitions to Chaos. Eds. G. Györgyi, I. Kondor, L. Sasvári, T. Tél (World Scientific, Singapore, 1992), 1992.

[277] B. Oksendal, Stochastic differential equations: An introduction with applications, Springer, 2010.

[278] G. Da Prato, J. Zabczyk, Stochastic equations in infinite dimensions, 2nd Edition, Cambridge University Press, 2014.

[279] C. C. Chow, M. A. Buice, Path integral methods for stochastic differential equations (2012). arXiv:1009.5966, doi:10.48550/arXiv.1009.5966.

[280] G. Korn, T. Korn, Mathematical handbook for scientists and engineers: Definitions, theorems, and formulas for reference and review, Dover Civil and Mechanical Engineering, Dover Publications, 2013, https://books.google.sk/books?id=A4XCAgAAQBAJ.

[281] M. Hnatič, J. Honkonen, T. Lučivjanský, Advanced field-theoretical methods in stochastic dynamics and theory of developed turbulence, Acta Physica Slovaca 66 (2016) 69–264, https://doi.org/10.48550/arXiv.1611.06741.

[282] J. Honkonen, Reaction models in stochastic field theory, Theoretical and Mathematical Physics 169 (2011) 1460–1469, https://doi.org/10.1007/s11232-011-0122-y. doi:10.1007/s11232-011-0122-y.

[283] L. D. Faddeev, A. A. Slavnov, Gauge fields. Introduction to quantum theory, 2nd Edition, Addison-Wesley, 1991.

[284] E. Gozzi, M. Reuter, W. D. Thacker, Hidden BRS invariance in classical mechanics. II, Physical

Review D 40 (1989) 3363–3377. doi:10.1103/PhysRevD.40.3363.

[285] E. Gozzi, Hidden BRS invariance in classical mechanics, Physics Letters B 201 (1988) 525–528. doi:10.1016/0370-2693(88)90611-9.

[286] J. Honkonen, Ito and Stratonovich calculuses in stochastic field theory, in: The 12th Small Triangle Meeting on Theoretical Physics – Stakčín, September 19–22, 2010, Institute of Experimental Physics, SAS, 2011, pp. 21–30, https://arxiv.org/abs/1102.1581. arXiv:1102.1581.

[287] J. Honkonen, M. Komarova, M. Nalimov, Large-order asymptotes for dynamic models near equilibrium, Nuclear Physics B 707 (3) (2005) 493–508, https://doi.org/10.1016%2Fj.nuclphysb.2004.11.016. doi:10.1016/j.nuclphysb.2004.11.016.

[288] N. N. Bogoliubov, D. V. Shirkov, S. Chomet, Introduction to the theory of quantized fields, Vol. 59, Interscience, 1959.

[289] M. Hnatič, J. Honkonen, T. Lučivjanský, Symmetry breaking in stochastic dynamics and turbulence, Symmetry 11 (2019) 1193. doi:10.3390/sym11101193.

[290] A. M. Polyakov, Turbulence without pressure, Physical Review E 52 (1995) 6183–6188. doi:10.1103/PhysRevE.52.6183.

[291] E. V. Ivashkevich, Symmetries of the stochastic Burgers equation, Journal of Physics A: Mathematical and General 30 (1997) L525. doi:10.1088/0305-4470/30/15/008.

[292] A. Berera, D. Hochberg, Gauge symmetry and Slavnov-Taylor identities for randomly stirred fluids, Physical Review Letters 99 (2007) 254501. doi:10.1103/PhysRevLett.99.254501.

[293] A. Berera, D. Hochberg, Gauge fixing, BRS invariance and Ward identities for randomly stirred flows, Nuclear Physics B 814 (2009) 522–548. doi:10.1016/j.nuclphysb.2009.01.014.

[294] M. Hnatič, T. Lučivjanský, L. Mižišin, Y. Molotkov, A. Ovsiannikov, Two-loop turbulent helical magnetohydrodynamics: Large-scale dynamo and energy spectrum, Physical Review E 112 (2025) 015211, https://link.aps.org/doi/10.1103/xhzb-5hr4. doi:10.1103/xhzb-5hr4.

[295] T.-P. Cheng, L.-F. Li, Gauge theory of elementary particle physics, Oxford University Press, 1984.

[296] M. Hnatich, J. Honkonen, M. Jurcisin, Stochastic magnetohydrodynamic turbulence in space dimensions $d \geqslant 2$, Physical Review E 64 (2001) 056411, https://link.aps.org/doi/10.1103/PhysRevE.64.056411. doi:10.1103/PhysRevE.64.056411.

[297] J. Honkonen, M. Nalimov, Two-parameter expansion in the renormalization-group analysis of turbulence, Journal of Physics B 99 (1995) 297–303, https://doi.org/10.1007/s002570050040. doi:10.1007/s002570050040.

[298] J. Honkonen, Asymptotic behavior of the solution of the two-dimensional stochastic vorticity equation, Physical Review E 58 (1998) 4532–4540, https://link.aps.org/doi/10.1103/PhysRevE.58.4532. doi:10.1103/PhysRevE.58.4532.

[299] J. Honkonen, Renormalization-group analysis of two-dimensional fluid stirred by random force with long-range correlations, International Journal of Modern Physics B 12 (1998) 1291–1300, https://doi.org/10.1142/S0217979298000715. doi:10.1142/S0217979298000715.

[300] E. R. Speer, Generalized Feynman amplitudes, Princeton University Press, 1969.

[301] L. T. Adzhemyan, M. Hnatich, D. Horváth, M. Stehlík, Infrared properties of an anisotropically driven MHD turbulence, International Journal of Modern Physics B 09 (1995) 3401–3419. doi:10.1142/S0217979295001348.

[302] L. T. Adzhemyan, A. N. Vasil'ev, M. Gnatich, Renormalization-group approach to the theory of turbulence. Inclusion of a passive admixture, Theoretical and Mathematical Physics 58 (1984) 47–51, https://doi.org/10.1007/BF01031034. doi:10.1007/BF01031034.

[303] D. Biskamp, W.-Ch. Müller, Scaling properties of three-dimensional isotropic magnetohydrodynamic turbulence, Physics of Plasmas 7 (2000) 4889–4900, https://doi.org/10.1063/1.1322562. doi:10.1063/1.1322562.

[304] P. Langevin, Sur la théorie du mouvement brownien, Comptes-rendus de l'Acad mie des Sciences

de Paris 146 (1908) 530–533.

[305] D. N. Zubarev, Nonequilibrium Statistical Thermodynamics, Springer US, New York, 1974.

[306] B. Shakhov, M. Jurcisin, E. Jurcisinova, M. Stehlik, The spontaneous magnetic field direction in an anisotropic MHD dynamo, Kinematics and Physics of Celestial Bodies 28 (2012) 225–231, https://doi.org/10.3103/S0884591312050066. doi:10.3103/S0884591312050066.

[307] P. Tzeferacos, A. Rigby, A. Bott, et al., Laboratory evidence of dynamo amplification of magnetic fields in a turbulent plasma, Nature Communications 9 (2018) 591, https://doi.org/10.1038/s41467-018-02953-2. doi:10.1038/s41467-018-02953-2.

[308] Z. Tigrine, H.-C. Nataf, N. Schaeffer, P. Cardin, F. Plunian, Torsional Alfvén waves in a dipolar magnetic field: experiments and simulations, Geophysical Journal International 219 (2019) S83–S100, https://doi.org/10.1093/gji/ggz112. doi:10.1093/gji/ggz112.

[309] N. Gillet, D. Jault, E. Canet, A. Fournier, Fast torsional waves and strong magnetic field within the Earth's core, Nature 465 (2010) 74–77, https://doi.org/10.1038/nature09010. doi:10.1038/nature09010.

[310] L. Adzhemyan, N. Antonov, A. Mazzino, P. Muratore-Ginanneschi, A. Runov, Pressure and intermittency in passive vector turbulence, Europhysics Letters 55 (2001) 801. doi:10.1209/epl/i2001-00351-x.

[311] P. Caselli, The fractional ionization in molecular cloud cores, Symposium — International Astronomical Union 197 (2000) 41–50, https://doi.org/10.1017/S0074180900164666. doi:10.1017/S0074180900164666.

[312] P. S. Li, C. F. McKee, R. I. Klein, Magnetized interstellar molecular clouds — I. Comparison between simulations and Zeeman observations, Monthly Notices of the Royal Astronomical Society 452 (2015) 2500–2527, https://doi.org/10.1093/mnras/stv1437. doi:10.1093/mnras/stv1437.

[313] Planck Collaboration, Planck intermediate results — XXXV. Probing the role of the magnetic field in the formation of structure in molecular clouds, Astronomy and Astrophysics 586 (2016) A138, https://doi.org/10.1051/0004-6361/201525896. doi:10.1051/0004-6361/201525896.

[314] J. Malzac, P. Lubiński, A. A. Zdziarski, M. C. Bel, M. Türler, P. Laurent, An intense state of hard X-ray emission of Cyg X-1 observed by INTEGRAL coincident with TeV measurements, Astronomy and Astrophysics 452 (2008) 527–534, https://doi.org/10.1051/0004-6361:200810227. doi:10.1051/0004-6361:200810227.

[315] M. D. Santo, R. B. J. Malzac, L. Bouchet, G. D. Cesare, The magnetic field in the X-ray corona of Cygnus X-1, Monthly Notices of the Royal Astronomical Society 430 (2013) 209–220, https://doi.org/10.1093/mnras/sts574. doi:10.1093/mnras/sts574.

[316] J. C. A. Miller-Jones, et al., Cygnus X-1 contains a 21–solar mass black hole–Implications for massive star winds, Science 371 (2012) 1046–1049, https://doi.org/10.1126/science.abb3363. doi:10.1126/science.abb3363.

[317] J. N. Bahcall, M. H. Pinsonneault, S. Basu, Current epoch and time dependences, neutrinos, and helioseismological properties, The Astrophysical Journal 555 (2001) 990–1012, https://doi.org/10.1086/321493. doi:10.1086/321493.

[318] Y. Fan, Magnetic fields in the solar convection zone, Living Reviews in Solar Physics 18 (2021) 1–96, https://doi.org/10.1007/s41116-021-00031-2. doi:10.1007/s41116-021-00031-2.

[319] P. Charbonneau, Solar dynamo theory, Annual Review of Astronomy and Astrophysics 52 (2014) 251–290, https://doi.org/10.1146/annurev-astro-081913-040012. doi:10.1146/annurev-astro-081913-040012.

[320] J. Reyes-Iturbide, I. Ramírez-Ballinas, M. Rosado, D. Núñez, P. Ambrocio-Cruz, L. Arias, R. Gabbasov, Supernova remnant W51C: optical and X-ray emission analysis, Monthly Notices of the Royal Astronomical Society 516 (2022) 6055–6065, https://doi.org/10.1093/mnras/

stac2568. doi:10.1093/mnras/stac2568.

[321] J. Fang, L. Zhang, On the non-thermal emission from the supernova remnant W51C, Monthly Notices of the Royal Astronomical Society 405 (2010) 462–466, https://doi.org/10.1111/j.1365-2966.2010.16455.x. doi:10.1111/j.1365-2966.2010.16455.x.

[322] C. Sarazin, The Intracluster Medium, in: A. Fabian (Ed.), Clusters and Superclusters of Galaxies, Vol. 366 of NATO ASI Series, Springer, 1992, pp. 1–51, https://doi.org/10.1007/978-94-011-2482-9_9. doi:10.1007/978-94-011-2482-9_9.

[323] F. Govoni, L. Feretti, Magnetic field in clusters of galaxies, International Journal of Modern Physics D 13 (2004) 1549–1594, https://doi.org/10.1142/S0218271804005080. doi:10.1142/S0218271804005080.

[324] K. T. Kim, P. C. Tribble, P. P. Kronberg, Detection of excess rotation measure due to intracluster magnetic fields in clusters of galaxies, The Astrophysical Journal 379 (1991) 80–88, https://doi.org/10.1086/170484. doi:10.1086/170484.

[325] F. Reale, Coronal loops: observations and modeling of confined plasma, Living Reviews in Solar Physics 11 (2014) 1549–1594, https://doi.org/10.12942/lrsp-2014-4. doi:10.12942/lrsp-2014-4.

[326] V. Nakariakov, E. Verwichte, Coronal waves and oscillations, Living Reviews in Solar Physics 2 (2005) 1–65, https://doi.org/10.12942/lrsp-2005-3. doi:10.12942/lrsp-2005-3.

[327] V. Souza, D. Koga, W. Gonzalez, F. R. Cardoso, Observational aspects of magnetic reconnection at the Earth's magnetosphere, Brazilian Journal of Physics 47 (2017) 447–459, https://doi.org/10.1007/s13538-017-0514-z. doi:10.1007/s13538-017-0514-z.

[328] E. Lucek, D. Constantinescu, M. Goldstein, J. L. J. Pickett, F. Pinçon, R. A. Sahraoui, Treumann, S. N. Walker, The magnetosheath, Space Science Reviews 118 (2005) 95–152, https://doi.org/10.1007/s11214-005-3825-2. doi:10.1007/s11214-005-3825-2.

[329] W. Baumjohann, G. Paschmann, C. A. Cattell, Average plasma properties in the central plasma sheet, Journal of Geophysical Research 94 (1989) 6597–6606, https://doi.org/10.1029/JA094iA06p06597. doi:10.1029/JA094iA06p06597.

[330] A. Lui, Dynamics of the magnetotail plasma sheet current, Atmosphere 14 (2023) 222, https://doi.org/10.3390/atmos14020222. doi:10.3390/atmos14020222.

[331] A. M. Dziewonski, D. L. Anderson, Preliminary reference Earth model, Physics of the Earth and Planetary Interiors 25 (1981) 297–356, https://doi.org/10.1016/0031-9201(81)90046-7. doi:10.1016/0031-9201(81)90046-7.

[332] M. Xie, J. Fu, A. B. Belonoshko, Equation of state and thermodynamic properties of liquid Fe-O in the Earth's outer core, Geoscience Frontiers 16 (2025) 101847, https://doi.org/10.1016/j.gsf.2024.101847. doi:10.1016/j.gsf.2024.101847.

[333] B. Buffett, Tidal dissipation and the strength of the Earth's internal magnetic field, Nature 468 (2010) 952–954, https://doi.org/10.1038/nature09643. doi:10.1038/nature09643.

[334] R. W. Schunk, A. F. Nagy, Electron temperatures in the F region of the ionosphere: Theory and observations, Reviews of Geophysics 16 (1978) 355–399, https://doi.org/10.1029/RG016i003p00355. doi:10.1029/RG016i003p00355.

[335] A. Chulliat, P. Vigneron, G. Hulot, First results from the Swarm dedicated ionospheric field inversion chain, Earth, Planets and Space 68 (2016) 104–122, https://doi.org/10.1186/s40623-016-0481-6. doi:10.1186/s40623-016-0481-6.

[336] M. Berhanu, G. Verhille, J. Boisson, B. Gallet, C. Gissinger, S. Fauve, N. Mordant, F. Pétrélis, M. Bourgoin, P. Odier, J.-F. Pinton, N. Plihon, S. Aumaître, A. Chiffaudel, F. Daviaud, B. Dubrulle, C. Pirat, Dynamo regimes and transitions in the VKS experiment, The European Physical Journal B 77 (2010) 459–468, https://doi.org/10.1140/epjb/e2010-00272-5. doi:10.1140/epjb/e2010-00272-5.

[337] A. C. C. Sips, G. Giruzzi, S. Ide, C. Kessel, T. C. Luce, J. A. Snipes, J. K. Stober, the Integrated

Operation Scenario Topical Group of the ITPA, Progress in preparing scenarios for operation of the International Thermonuclear Experimental Reactor, Physics of Plasmas 22 (2015) 021804, https://doi.org/10.1063/1.4904015. doi:10.1063/1.4904015.

[338] A. Sips, J. Schweinzer, T. Luce, S. Wolfe, H. Urano, J. Hobirk, S. Ide, E. Joffrin, C. Kessel, S. Kim, P. Lomas, I. Nunes, T. Pütterich, F. Rimini, W. Solomon, J. Stober, F. Turco, P. de Vries, JET Contributors, The ASDEX Upgrade team, The DIII-D team, The C-Mod team, The JT-60U team, ITPA-IOS TG members and experts, Assessment of the baseline scenario at $q_{95} \sim 3$ for ITER, Nuclear Fusion 58 (2018) 126010, https://doi.org/10.1088/1741-4326/aade57. doi:10.1088/1741-4326/aade57.

[339] R.-H. Lu, G.-S. Pan, Z.-J. Wang, Y.-Z. Wen, C.-X. Yu, S.-D. Wan, W. dong Liu, J. Wang, M. Xu, D.-L. Xiao, Y. Yu, Magnetic fluctuations in the plasma of KT-5C tokamak, Physics Letters A 333 (2004) 298–302, https://doi.org/10.1016/j.physleta.2004.10.052. doi:10.1016/j.physleta.2004.10.052.

[340] H. Araseki, I. R. Kirillov, G. V. Preslitsky, A. P. Ogorodnikov, ICONE15-10081 evaluation of annular linear induction pump efficiency, The Proceedings of the International Conference on Nuclear Engineering (ICONE) 15 (2007) 1–8, https://doi.org/10.1299/jsmeicone.2007.15._ICONE1510_34. doi:10.1299/jsmeicone.2007.15._ICONE1510_34.

[341] D. H. Kelley, T. Weier, Fluid mechanics of liquid metal batteries, Applied Mechanics Reviews 70 (2018) 020801, https://doi.org/10.1115/1.4038699. doi:10.1115/1.4038699.

[342] M. Seilmayer, F. Stefani, T. Gundrum, T. Weier, G. Gerbeth, M. Gellert, G. Rüdiger, Experimental evidence for a transient Tayler instability in a cylindrical liquid-metal column, Physical Review Letters 108 (2012) 244501, https://link.aps.org/doi/10.1103/PhysRevLett.108.244501. doi:10.1103/PhysRevLett.108.244501.

[343] L. Spitzer, Physics of fully ionized gases, 2nd Edition, Interscience Publishers, 1962.

[344] J. Fink, L. Leibowitz, Thermophysical properties of sodium, Tech. Rep. ANL-CEN-RSD-79-1, Argonne National Laboratory (1979).

[345] G. H. Golden, J. V. Tokar, Thermophysical properties of sodium, AEC Research and Development Report ANL-7323, Argonne National Laboratory, Reactor Engineering Division, Argonne, Illinois, chemistry (TID-4500). (1967). doi:10.2172/4511962.